BENTHIC ECOSYSTEM FUNCTIONING OF THE WESTERN CLARION-CLIPPERTON ZONE, PACIFIC OCEAN, AND THE WEST ANTARCTIC PENINSULA

A study to assess the effectiveness of Areas of Particular Environmental Interest (APEIs) in the context of deep-sea mining and the effects of climate change

Marta M Cecchetto

This dissertation is submitted for the degree of

Doctor of Philosophy

The Lyell Centre
Heriot-Watt University
Institute of Life and Earth Sciences
Energy, Geoscience, Infrastructure and Society

May 2022

Research Thesis Submission

Please note this form should be bound into the submitted thesis.

Name:	Marta Maria Cecchetto		
School:	EGIS		
Version: *(i.e. First, Resubmission, Final)*	Final	Degree Sought:	PhD Marine Biology

Declaration

In accordance with the appropriate regulations I hereby submit my thesis and I declare that:

1. The thesis embodies the results of my own work and has been composed by myself
2. Where appropriate, I have made acknowledgement of the work of others
3. The thesis is the correct version for submission and is the same version as any electronic versions submitted*.
4. My thesis for the award referred to, deposited in the Heriot-Watt University Library, should be made available for loan or photocopying and be available via the Institutional Repository, subject to such conditions as the Librarian may require
5. I understand that as a student of the University I am required to abide by the Regulations of the University and to conform to its discipline.
6. I confirm that the thesis has been verified against plagiarism via an approved plagiarism detection application e.g. Turnitin.

ONLY for submissions including published works

Please note you are only required to complete the Inclusion of Published Works Form (page 2) if your thesis contains published works)

7. Where the thesis contains published outputs under Regulation 6 (9.1.2) or Regulation 43 (9) these are accompanied by a critical review which accurately describes my contribution to the research and, for multi-author outputs, a signed declaration indicating the contribution of each author (complete)
8. Inclusion of published outputs under Regulation 6 (9.1.2) or Regulation 43 (9) shall not constitute plagiarism.

*   *Please note that it is the responsibility of the candidate to ensure that the correct version of the thesis is submitted.*

Signature of Candidate:	*Marta M Cecchetto*	Date:	04/05/1993

Submission

Submitted By *(name in capitals)*:	Marta Maria Cecchetto
Signature of Individual Submitting:	*Marta M Cecchetto*
Date Submitted:	04/05/1993

For Completion in the Student Service Centre (SSC)

Limited Access	Requested	Yes		No		Approved	Yes		No	
*E-thesis Submitted (**mandatory for final theses**)*										
Received in the SSC by *(name in capitals)*:					Date:					

Inclusion of Published Works

Declaration

This thesis contains one or more multi-author published works. In accordance with Regulation 6 (9.1.2) I hereby declare that the contributions of each author to these publications is as follows:

Citation details	Marta M Cecchetto, Annabell Moser, Craig R Smith, Dick van Oevelen, Andrew K Sweetman. Abyssal seafloor response to fresh phytodetrital input in three Areas of Particular Environmental Interest (APEIs) in the polymetallic nodule-rich Clarion-Clipperton Zone (CCZ). Deep-Sea Research Part I (submitted & under review)
Marta M Cecchetto	Conducted field work, collected samples and carried out samples analysis. Wrote the manuscript
Annabell Moser	Conducted field work and contributed to manuscript revisions
Craig R Smith	Designed the study and conducted field work. He contributed to manuscript revisions
Dick van Oevelen	Conducted samples analysis and contributed to manuscript revisions
Andrew K Sweetman	Designed the study, conducted field work, helped during data processing and contributed to manuscript revisions
Signature:	*Marta McCcRillo*
Date:	04/05/1993

Please included additional citations as required.

Abstract

The deep sea encompasses the largest ecosystem on Earth and remains largely unexplored. With plans for deep-sea mining and the increasing impacts of climate change on our oceans, there is a growing necessity to understand and safeguard deep-sea biodiversity and ecosystem functioning. The cycling of carbon (C) by deep-sea benthic communities is a key ecosystem function and pulse-chase experiments are aimed to measure this process I conducted pulse-chase experiments in situ at abyssal depths (4800-5300 m) in three no-mining areas, called Areas of Particular Environmental Interest (APEIs), in the Clarion-Clipperton Zone (CCZ) and in ex situ experiments using sediments collected from a bathyal (500-600 m) fjord, Andvord Bay, and the continental shelf of the West Antarctic Peninsula (WAP). My results underline the importance of organic C in driving ecosystem dynamics at the abyssal seafloor and support the notion that Antarctic fjords are hotspots of benthic biomass and ecosystem functions. The microbial community was shown to be a key player in the short term (1.5 d) cycling of C on the abyssal plain of the western equatorial Pacific Ocean, which is consistent with other published studies, while the macrofaunal community (>300 μm) dominated the initial (~1 d) degradation of phytodetritus in Andvord Bay. My study provides important information on benthic ecosystem functioning in the western CCZ, an area targeted for commercial-scale deep-sea mining, and the WAP, a region that is becoming increasingly impacted by climate change.

Acknowledgements

Contents

INTRODUCTION

1 The deep-sea benthos

The deep sea represents the largest ecosystems on Earth, extending from polar to equatorial regions and comprise some of the most diverse, unique and extreme ecosystems (Ramirez-Llodra et al. 2010). Mostly characterised by cold temperatures (<4°C), great hydrostatic pressure and total darkness, the deep sea is defined as the environment that extends beyond ~200 m depth (Ramirez-Llodra et al. 2010). Deep-sea ocean discovery has gone a long way from Edward Forbes' Azoic Theory that limited ocean life to depths shallower than 600 m depth (Anderson and Rice 2006). Now, we know that the deep-sea habitats are teeming with life and play an important role in supporting our current way of life by providing many ecosystem services such as regulating Earth's climate, fisheries and energy (Thurber et al. 2014). In the last century, the challenges that the deep sea have had to face to maintain the correct functioning of the various and valuable ecosystem services have increased. Climate change and the increasing use of deep-sea resources (e.g., fish) will involve significant changes to deep-sea ecological processes and functions along with changes in the environmental properties of the deep ocean such as oxygen, temperature and food supply (Smith et al. 2008a; Sweetman et al. 2017, Levin et al. 2020b).

The vast majority of the ocean seafloor is formed by abyssal ecosystems, an extensive network of seamounts, plains, hills and depression extending between 3000 to 6000 m depth (Smith et al. 2008a) with the potential to harbor a major reservoir of biodiversity (Snelgrove and Smith 2002). Even though the extreme conditions, local diversity is recognized to be quite high (e.g., ~40 species for every 100 macrofaunal individuals and more than 100 macrofaunal species per 0.25 m^2 of soft sediment, Snelgrove and Smith 2002) and more than 80% of the organisms collected are new to science (Danovaro et al. 2008; Smith et al. 2008a).

Generally, faunal abundances and biomass decreases with depth while bacterial density and biomass remains constant and dominates benthic community biomass below 3000 m (Fig. 1)

(Rex et al. 2006; Smith et al. 2008a). This pattern is linked to the ecological characteristic that often defines the deep sea: energy limitation (Smith et al. 2008a). Secondary benthic production and abyssal seafloor communities depend greatly on the input of detrital food from the euphotic zone where for example, shelf and slope habitats such as bathyal environments (200-3000 m) receive a higher energy flux which supports greater energy transfer to higher trophic levels (Smith et al. 2008a).

A

B

C
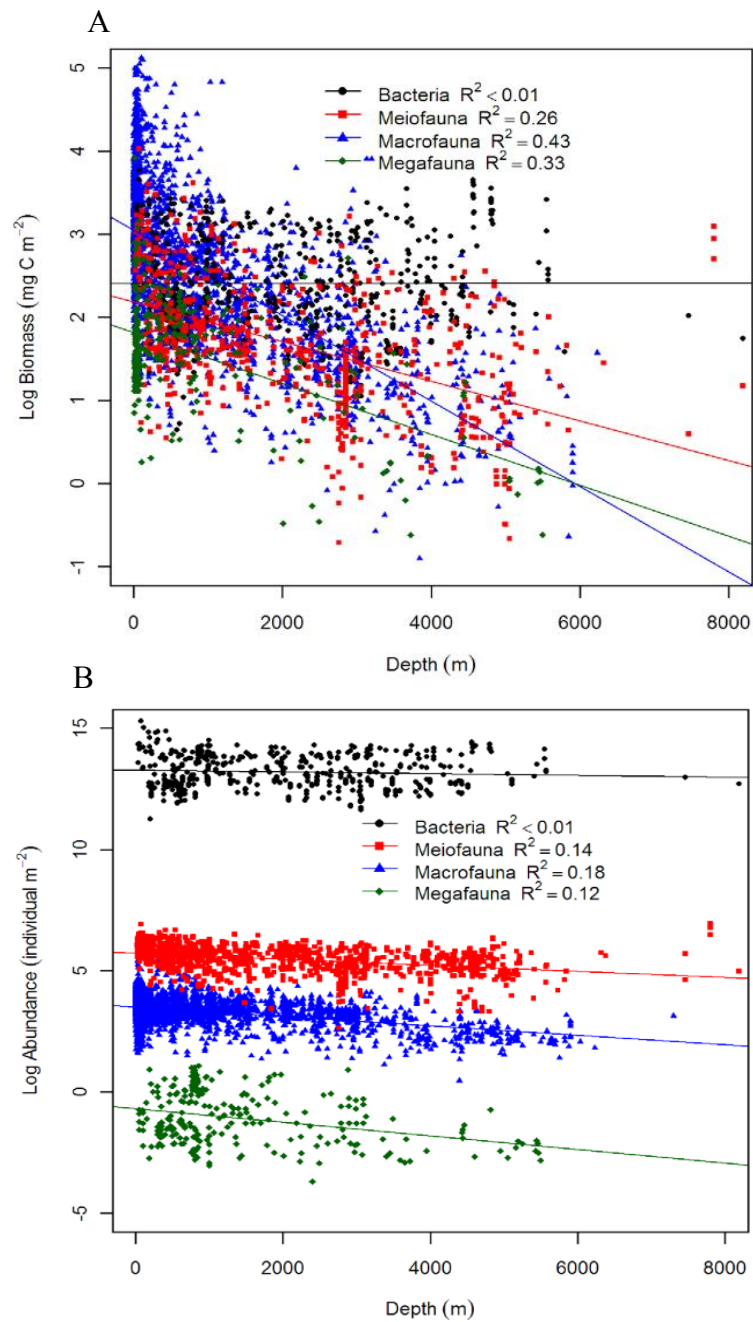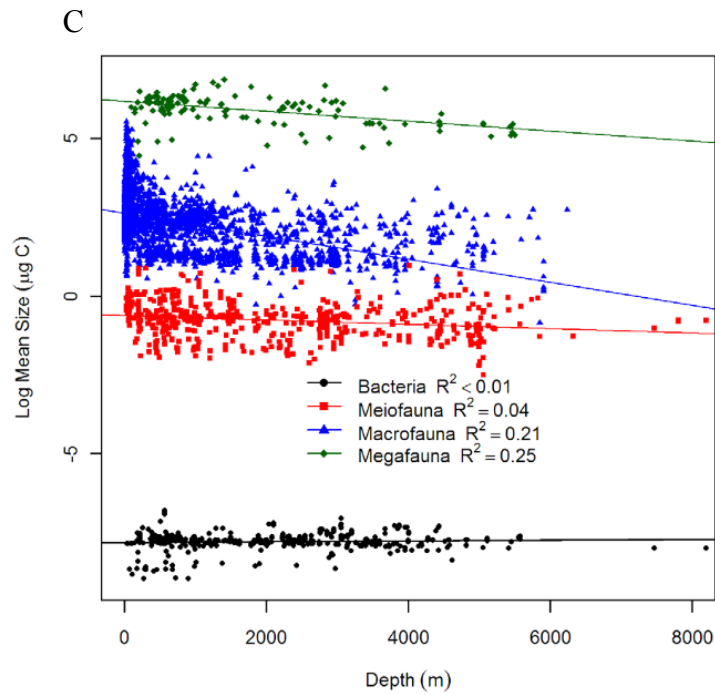
Figure 1: Biomass (A), abundance (B) and average body size (C) as a function of depth for bacteria, meiofauna, macrofauna and megafauna. The effects of latitude and longitude were removed by partial regression. Figures were taken from Wei et al. (2010).

Therefore, the different regions of the deep ocean can support fundamentally different ecosystem functions and are characterized by different benthic community structure (Danovaro et al. 2008; Smith et al. 2008a). At a global scale, the ecological and biogeochemical processes found in the deep sea contribute to provide crucial ecosystem services for the well-being of the planet (e.g., ocean carbon cycling, calcium carbonate dissolution, repository of atmospheric CO_2) (Thurber et al. 2014) and, with large-scale anthropogenic impacts such as deep-sea mining and climate change on the horizon and happening, this will likely change (Ramirez-Llodra et al. 2011; Levin et al. 2016). Given that most deep-sea organisms remain unknown to us (Higgs and Attrill 2015; Sinniger et al. 2016; Shulse et al. 2017), biodiversity loss has been recognized as a critical global environmental problem (Weikard 2002). The ecological effects of biodiversity loss in the deep sea are still poorly understood, however, given the extremely slow recovery rates (Danovaro et al. 2008; Niner et al. 2018) in most deep-sea ecosystems and the existing exponential relationship between deep-sea biodiversity and ecosystem functioning

(Danovaro et al. 2008), loss of biodiversity due to mining and other anthropogenic impacts is inevitable and will likely change ecosystem function and efficiency (Danovaro et al. 2008; Jones et al. 2017; Niner et al. 2018). It is widely recognized that higher biodiversity, such as a high species richness, directly impacts ecological processes promoting bioturbation and faster rates of remineralization by supporting redistribution of food and stimulating detritus processing, digestion and re-working (Danovaro et al. 2008) (Fig. 2).
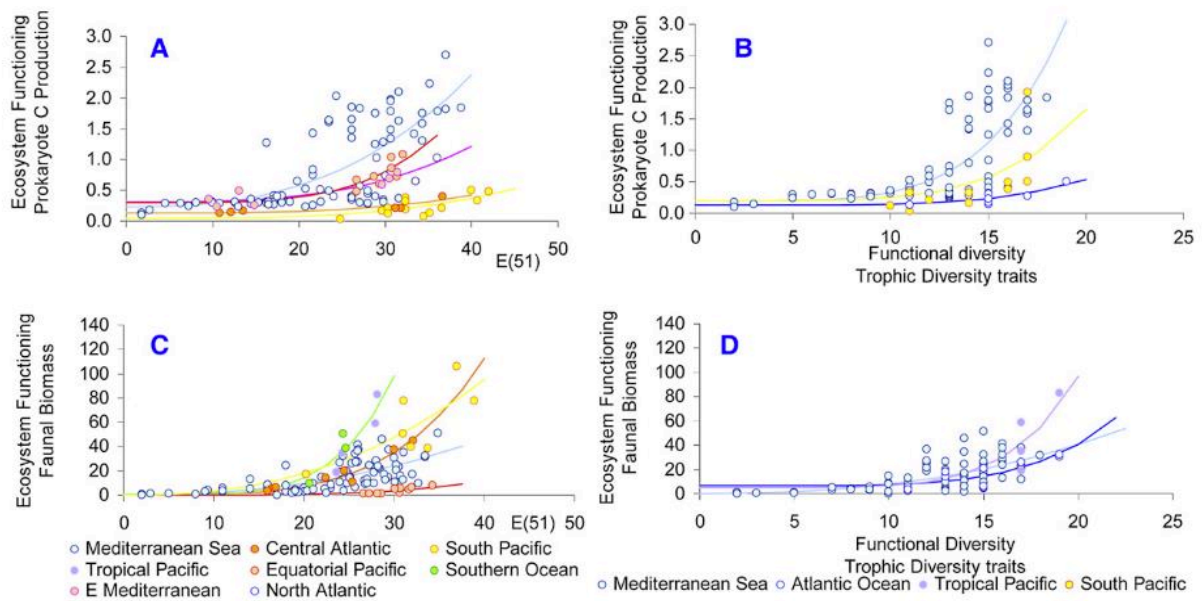
Figure 2: Relationship between biodiversity and ecosystem functioning expressed as (A) expected number of species [E(51)] and prokaryote C production (μg C g^{-1} d^{-1}); (B) functional diversity (number of trophic traits) and prokaryote C production (μg C g^{-1} d^{-1}); (C) expected number of species [E(51)] and faunal biomass (mg C m^{-2}); (D) functional diversity (number of trophic traits) and faunal biomass (mg C m^{-2}), though biomass can be better as C-stock rather than function. (A) Mediterranean Sea: R^2 = 0.52, Eastern Mediterranean Sea: R^2 = 0.82, North Atlantic: R^2 = 0.77, Equatorial Pacific: R^2 = 0.59, South Pacific: R^2 = 0.67, Central Atlantic: R^2 = 0.81. (B) Mediterranean Sea: R^2 = 0.45, Central Atlantic: R^2 = 0.94, Equatorial Pacific: R^2 = 0.60, South Pacific: R^2 = 0.66. (C) Mediterranean Sea: R^2 = 0.80, Atlantic Ocean: R^2 = 0.80, South Pacific: R^2 = 0.43. (D) Mediterranean Sea: R^2 = 0.41, Atlantic Ocean: R^2 = 0.58, Tropical Pacific: R^2 = 0.60. Data and figures originate from Danovaro et al. (2008).

The cause driving changes in biodiversity and ecosystem functioning in the deep sea is a highly discussed topic (e.g. Danovaro et al. 2010; Paulus 2021) and many hypotheses exist for the potential parameters that contribute to significantly change deep-sea biodiversity such as

temperature, habitat heterogeneity, changes in sediments grain size, environmental disturbance, changing nutrient supply and POC flux (Danovaro et al. 2008; Smith et al. 2008a; Paulus 2021). Now we know that the deep-sea floor is a highly dynamic environment and the different habitats such as wood and whale falls, as well as variations in environmental characters due to burrows and faunal foraging behavior may represent potential reasons for changes in biodiversity (Rex and Etter 2010; Paulus 2021). Sediment disturbance can also contribute to impact deep sea biodiversity, whether anthropogenic in nature such as dredging or deep-sea mining with long lasting effects on the environments (Khripounoff et al. 2006; Stratmann et al. 2018b) or natural processes such as mudslides and changes in ocean chemistry (Paulus 2021). Organic inputs form surface waters such as spring-bloom detritus (Smith et al. 2008b) and jellyfish falls (Sweetman et al. 2016) are also significant events for the benthos and, depending on the inputs, may also contribute to sustain high level of benthic biodiversity for long periods of time (Paulus 2021).

2   Carbon flux to the deep sea

It has long been documented that the downward transfer of biogenic particles, such as POC flux, from the euphotic zone to the deep seafloor represents an important ecological characteristic and, with the exception of chemosynthetic ecosystems, benthic secondary production is often considered to highly depend on this organic input (Fig. 3) (Epply and Peterson 1979; Rex et al. 2006; Honjo et al. 2014; Ruhl et al. 2014; Dunlop et al. 2016; Sweetman et al. 2017). The downward transfer of organic matter plays a significant role in the removal of atmospheric CO_2 and its sequestration in deep-sea sediments for thousands of years buffering Earth's climate system (Sigman and Boyle 2000; Boyd and Trull 2007; Sweetman et al. 2017). Approx. 5-15 Gt C yr^{-1} is transported into the deep sea through POC flux (Boyd and Trull 2007) and the fraction of the net primary productivity (NPP) exported from surface to the deep seabed generally ranges between 0.5-2% (Smith et al. 2008a). Heterotrophic zooplankton

and bacteria consume most of the organic matter in surface and mesopelagic (200-1000m) waters where the majority of organic matter is remineralised to CO_2 and inorganic nutrients (Lee et al. 2004).
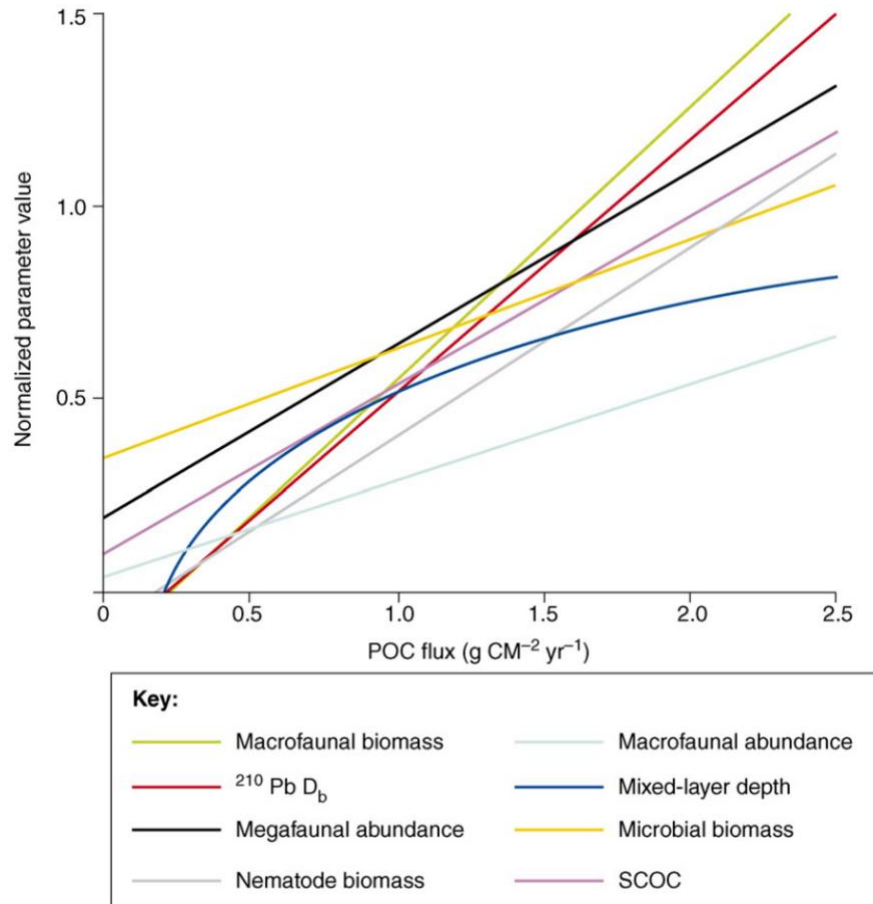
Figure 3: Regression relationships between abyssal benthic ecosystem structure and function and POC flux to the seafloor demonstrate a strong dependence as discussed and showed by Smith et al. (2008a).

As organic matter sinks to the seafloor, its composition changes due to the many physical and biological dynamics such as dissolution due to increasing depth, aggregation/disaggregation, and heterotrophic consumption by zooplankton and microbes (Lee et al. 2004). Once at the seafloor, organic matter is influenced by different phenomena that determined the rate of nutrient input to the benthos including community structure and organization, morphological diversity, body size and faunal composition (Rex et al. 2006).

Similarities exist in benthic community structure and ecosystem function in deep-sea regions where food availability is similar (Danovaro et al. 2008; Campanyà-Llovet et al. 2017). For example, as food declines, key ecosystem characteristics and functions (e.g., organic matter and nutrient recycling, community respiration, and productivity) follow (Danovaro et al. 2008; Smith et al. 2008a). Community abundance and biomass on the continental shelf is much higher in many regions compared to community abundance and biomass at abyssal depths as shallower areas are characterised by greater input of POC to the benthos (Rex et al. 2006). Also, benthic respiration rates have been shown to be higher beneath the eutrophic equatorial Pacific compared to the more oligotrophic areas north and south of the equator (Berelson et al. 1997).

Studies have shown that not only is the quantity of food important for benthic stocks but also the quality (Campanyà-Llovet et al. 2017). Food quality can significantly alter benthic trophic structure and, while the response to quantity and quality of food can vary in different ecosystems, deep-sea benthic community structure relies particularly on both quantity and quality of food input (Campanyà-Llovet et al. 2017). For example, dramatic shifts in benthic community can be correlated to climate variation shifting plankton composition and thus food supply and quality to the deep-sea benthos (Smith et al. 2008a). Here, the benthos prefer fresh organic matter as it is remineralized faster than more refractory organic compounds as seen in the deep-sea sediments of the Benguela Upwelling System (Aspetsberger et al. 2007) and the deep Northeast Atlantic where diatoms were remineralized faster than faecal pellets (Mayor et al. 2012). Furthermore, changes in food quality can often correlate to changes in trophic diversity and structure where the presence of fresh or more degraded material can determine the dominance of a specific faunal group (Wieking and Kröncke 2003).

Interestingly, polar ecosystems are subjected to a strong seasonal flux of organic matter to the benthos as labile food material is deposited on the seafloor following the retreat of winter sea

ice (Mincks et al. 2005; Campanyà-Llovet et al. 2017). The cold temperatures at the seafloor then lead to reduced hydrolysis of organic matter and the build-up of organic "food-banks", which provide food through the winter months when the supply of organic material from the surface is reduced (Mincks et al. 2005).

3   Anthropogenic impacts

Deep-sea mining, climate change, fisheries exploitation and hydrocarbon extraction are only a few of the numerous environmental challenges that the deep sea presently faces and will be exposed to in future (Ramirez-Llodra et al. 2011, Sweetman et al. 2017). Here, the scientific community along with industries and national and international organizations have been called to work together to develop successful management and conservation strategies to preserve and safeguard deep-sea environments (Ramirez-Llodra et al. 2010, 2011; Mengerink et al. 2014; Thurber et al. 2014; Levin and Le Bris 2015; Danovaro et al. 2017). Along with the 1982 United Nations Convention on the Law of the Sea (UNCLOS), a framework set to regulate international ocean management, the International Seabed Authority (ISA) is dedicated to regulating mining in areas of international jurisdiction, helping to monitor and manage anthropogenic impacts and preserve deep-sea resources and ecosystems (Mengerink et al. 2014).

Traditional quantitative approaches to determine the extent of anthropogenic impacts are often difficult as the lack of evidence and baseline studies before impacts have taken place are few and far between. The deep sea has already experienced dramatic changes in the past with the expansion of oxygen minimum zones (OMZ) during warming events in the last deglaciation and during the millennial-scale Dansgaard-Oeschger events (abrupt climate oscillations) (Cannariato and Kennett 1999; Schmittner et al. 2007; Moffitt et al. 2015) and from fluctuations of bottom water temperature and current velocities during the last deglaciation and

Holocene (Cronin and Raymo 1997; Sweetman et al. 2017). However, now anthropogenic impacts are affecting the deep-sea environment on a timescale never experienced before shifting from millennial to decadal timescales, and the task of assessing the full extents of the changes is falling on the scientific community which presents a challenge that is difficult to overcome (Ramirez-Llodra et al. 2010, 2011; Danovaro 2017; Sweetman et al. 2017). In this regards, we should consider that deep-sea environments need long recovery times and have very slow growth rates suggesting that some anthropogenic impacts, if on a large enough scale, such as deep-sea mining, might be irreversible (Stratmann et al. 2018b; Simon-Lledó et al. 2019; de Jonge et al. 2020; Vonnahme et al. 2020).

3.1 Deep-sea mining: the Clarion-Clipperton Zone

The increasing demand for energy and minerals along with a decline in the grade of land-based mineral resources, economic profitability and technological development have resulted in prospecting for new resources, favouring the exploration and exploitation of deep-sea mineral resources (Halfar and Fujita 2002; Wedding et al. 2015; Mullineaux et al. 2018).

The ISA has granted 19 contracts for the exploration of polymetallic nodules in the Clarion-Clipperton Zone (CCZ) (17), the central Indian Ocean Basin (1) and the western Pacific Ocean (1) (International Seabed Authority [ISA] 2010, 2020) (Fig. 4). Polymetallic nodules, characterised by very slow growth rates of < 1 mm million yr^{-1} (Kerr 1984), are found over vast areas of the abyssal seafloor that is characterised by low sedimentation rates. Nodules contain commercially valuable minerals such as manganese, cobalt, copper, nickel, and rare-earth elements. The CCZ, an area in the equatorial Pacific Ocean that extends for 9 million km^2 from Mexico to Hawaii, is of particular interest for commercial deep-sea mining due to nodule concentrations occurring at weights of up to 10-15 kg m^{-2} (International Seabed Authority [ISA] 2020).

States and private contractors have undertaken exploration activities in the CCZ since 2001 following ISA directives that have granted a framework of exploration licenses as well as 13 Areas of Particular Environmental Interest (APEIs) (Wedding et al. 2015; International Seabed Authority [ISA] 2021) or Marine Protected Areas.
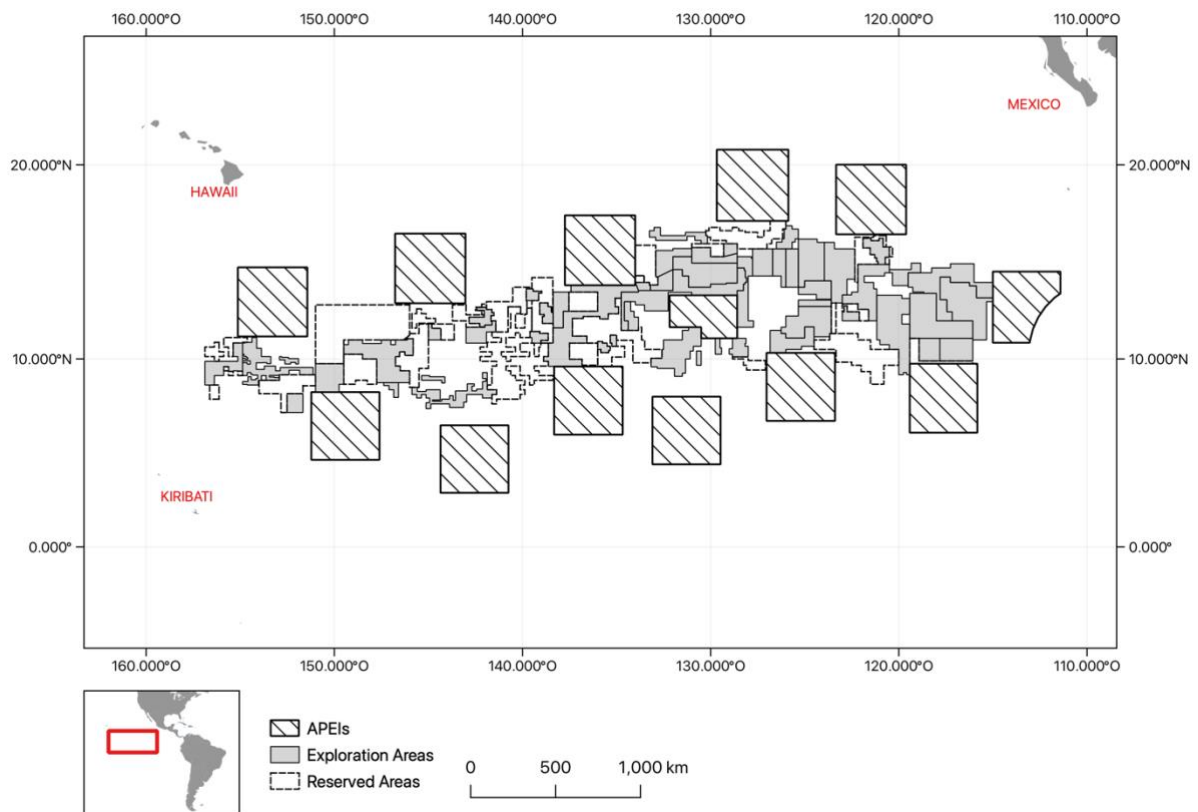
Figure 4: Exploration areas, reserved areas and APEIs in the polymetallic nodule areas of the Clarion-Clipperton Zone.

It is well documented that mining operations will have considerable impacts on the environment but the full extent of these impacts remain speculative until mining is conducted on a commercial scale (Becker et al. 2001; Thiel 2001). Among the many seabed disturbance experiments conducted to evaluate the impact of deep-sea mining conducted in the '80s and '90s (Jones et al. 2017), the "DISturbance and reCOLonization experiment" (DISCOL) conducted in 1989 in the Peru Basin offered the opportunity for long-term environmental monitoring. This area was again surveyed in 2015 providing insights on the recovery of the

local environment after 26 years from the disturbance with data on microbial community and functions (de Jonge et al. 2020; Vonnahme et al. 2020), carbon cycling (Stratmann et al. 2018a), megafauna (Stratmann et al. 2018c; Simon-Lledó et al. 2019), deep-sea fishes and mobile scavengers (Drazen et al. 2019). These studies showed impaired environmental conditions after two decades and estimated long recovery times (e.g., over 50 years, Vonnahme et al. 2020) to recover to undisturbed levels. Based on these studies it is suggested that deep-sea mining could potentially lead to irreversible loss of biodiversity and ecosystem functions (Simon-Lledó et al. 2019). Thus, conservation strategies (e.g., the establishment of APEIs) for the protection and conservation of biodiversity and ecosystem function become vital as a precautionary measure against deep-sea mining (Dunn et al. 2018).

While numerous environmental studies have been conducted in the CCZ looking at microbial communities (e.g., Shulse et al. 2017; Sweetman et al. 2019; Wear et al. 2021), foraminifera (e.g., Nozawa et al. 2006; Gooday et al. 2015, 2017; Goineau and Gooday 2017), meiofauna (e.g., Radziejewska 2002; Miljutina et al. 2010; Miljutin et al. 2011; Pape et al. 2017), megafauna abundance and biodiversity (e.g., Amon et al. 2017; Leitner et al. 2017; Durden et al. 2021), and larval dispersal (Kersten et al. 2017), there is still a need for baseline studies to improve our understanding of benthic ecosystem functioning, biodiversity and resilience in mining zones, as well as in areas set aside for protection to see if the ecosystems here are representative for mining lease areas (Rex et al. 2006; Kaiser et al. 2017).

As discussed previously, food availability in the form of organic matter flux to the benthos plays a significant role in driving benthic ecosystem functioning in the deep sea and more in particular on abyssal plains (Smith et al. 2008a). The strong POC flux gradient in the CCZ, increasing from north to south and from east to west (Lutz et al. 2007), has been shown to lead to changes in the faunal communities in this area. As such, POC flux and its influence on the ecosystems found in the CCZ may be important aspects to include in future management and

environmental considerations going forward (Vanreusel et al. 2016; Bonifácio et al. 2020; McQuaid et al. 2020).

3.2 *Climate change*

Rapid climate change is now a well-documented phenomenon marked by, among the many impacts, increasing water temperatures, melting polar ice sheets, rising sea levels, ocean density stratification and acidification, and impacts on oceanic surface primary production as well as the transport of organic material to the benthos (Bopp et al. 2013; Levin and Le Bris 2015; Sweetman et al. 2017).

There are numerous studies that highlight the challenges that deep-sea ecosystems are facing and some predict significant impacts will be felt by continental margin, abyssal and polar settings by 2100 due to climate change and other anthropogenic impacts (e.g., Levin and Le Bris 2015; Sweetman et al. 2017; Kerr et al. 2018).

Oxygen utilization rates and ventilation processes determine mid-depth O_2 minimum areas, also known as oxygen minimum zones (OMZs) where O_2 levels are considerably low (O_2 <0.5 ml L^{-1}). OMZs are usually located between 400 and 1200 m depth, close to the base of the permanent thermocline (Keeling et al. 2010; Sweetman et al. 2017). These areas are found along the continental margins of the east Pacific, southeast Atlantic, west Pacific and north Indian Oceans (Levin 2003; Helly and Levin 2004) and will likely be significantly affected and experience volume expansion in the presence of greenhouse warming and changes in thermohaline circulation patterns (Rahmstorf 2002; Sweetman et al. 2017). Many OMZs have already expanded in volume in the last half century (Stramma et al. 2008, 2010; Gilly et al. 2013) and will likely experience lower O_2 levels by 2100 where changes in ocean circulation patterns will alter their intensity (Schmittner et al. 2007; Sweetman et al. 2017).

Higher water stratification will not only reduce deep-water ventilation but will also affect POC flux to abyssal environments by reducing the nutrient supply to, and hence the production of organic material by photosynthesis in the euphotic zone (Smith et al. 2008a; Jones et al. 2014; Levin and Le Bris 2015; Sweetman et al. 2017). Most of the deep sea, with the exception of continental margin and chemosynthetic habitats, is already characterised by energy limitation (POC flux of 1-2 g C m^{-2} yr^{-1} Smith et al. 2008a; Sweetman et al. 2017), and generally, high latitudes are characterised by higher POC export than lower latitudes (Sweetman et al. 2017). The isolation of the upper water column by increased stratification will lead to a reduction in nutrient supply, which is predicted to cause a change in phytoplankton community composition, with shifts from fast sinking diatoms to low sinking picoplankton, that will ultimately limit the export and the transfer efficiency to the seafloor (Buesseler et al. 2007; Smith et al. 2008a). Benthic biomass, respiration and bioturbation rates in the deep sea (in particular on abyssal plains) will be significantly affected leading to a reduction in the capacity of the deep-sea benthos to sustain and provide ecosystem services (Smith et al. 2008a; Levin and Le Bris 2015; Sweetman et al. 2017).

Further environmental stressors will be observed in the form of increasing CO_2 levels in addition to biological respiration in the water column, causing water acidification at intermediate depths throughout the oceans (Byrne et al. 2010). Major pH reductions are expected by 2100 across the world's oceans where excess atmospheric CO_2 is introduced into deep-water masses at down-welling sites and distributed across the world by meridional overturning circulation (Sweetman et al. 2017). Predictions indicate that seamounts and canyons will be particularly affected by pH reductions as well as bathyal depths with reductions ranging between 0.2 to 0.06 units by 2100 (Sweetman et al. 2017). Predicted pH reductions are of particular concern for deep-water corals as future elevated CO_2 values will reduce suitable habitats and constrain calcifying organisms to shallower waters (Levin and Le Bris 2015).

However, direct observations on deep-water organisms are still rare and biological consequences of elevated CO_2 on deep-water organisms are lacking as our capacity for studying deep-water organisms in laboratory conditions is still limited (Levin and Le Bris 2015). It is well acknowledged that polar environments will be the most affected regions of the planet by climate warming and will exhibit rapid and drastic changes especially in relation to sea ice extent and ocean dynamics (Barnes and Tarling 2017; Kerr et al. 2018).

3.2.1 The West Antarctic Peninsula

The coasts of the West Antarctic Peninsula (WAP) are characterized by an extensive system of glacio-marine fjords, deep inlets excavated by glaciers, that typically represent important boundary zones between glacial ice and the ocean (Grange and Smith 2013). Due to the close relationship between glaciers and the oceans, these areas are highly sensitive to changes in environmental conditions caused by climate change, however these same conditions infer unique ecosystem characteristics that distinguish them from the adjacent continental shelves (Grange and Smith 2013).

In the last decade, the WAP has shown an increase in the number of environmental impacts related to climate warming and glacial melt disturbance events (Kerr et al. 2018) and a significant change in important ecosystem functions such as primary productivity and energy transfer (Gutt et al. 2020), including shifts in benthic community metabolism (Braeckman et al. 2021) and distribution (Grange and Smith 2013; Kim et al. 2021). However, if the benthic response to climate change impacts in Arctic fjords is well documented (Wlodarska-Kowalczuk et al. 2005; Wesławski et al. 2011; Morata et al. 2020), and even though there are numerous studies that have looked into the fate of organic matter across the WAP and the potential impacts of climate warming in this region (e.g. Kaehler et al. 2000; Smith et al. 2008; Nowacek et al. 2011; Ducklow et al. 2018), there is a lack of information regarding the

environment and ecosystems in glaciomarine fjords of the WAP coastal margins and the effect of a warming climate on these ecosystems (Grange and Smith 2013; Lundesgaard et al. 2020; Ziegler et al. 2020).

Arctic fjords have been shown to be characterised by decreasing benthic abundance and biodiversity into fjords due to enhanced glacial runoff and burial disturbance with the lowest benthic biomass, species richness and trophic complexity near the glacier in the inner part of the fjords (Wlodarska-Kowalczuk et al. 2005). Also, as climate change will lead to less ice cover, the carbon input to the benthic habitat will likely change allowing more regular and continuous carbon inputs to the seafloor by flooding the system with detritus and potentially affecting benthic ecosystem functioning (Morata et al. 2020).

However, Antarctic fjords have been shown from limited observations to exhibit the opposite pattern seen in Arctic fjords. Seasonality and low temperatures allow the formation of "food banks" in the sediments of the Antarctic fjords providing hotspots for benthic biodiversity and functions (Grange and Smith 2013). Benthic ecosystem functioning and the impacts of climate change on the continental shelf of the WAP have been previously assessed by the FOODBANCS 1 and 2 programs, which studied pelagic benthic coupling along the WAP and provided key insights on the fate of organic matter in the region and the importance of sea-ice cover along the WAP (Suhr et al. 2002; Glover et al. 2008; Hartnett et al. 2008; Smith et al. 2008b, 2012). Macrofaunal abundances were consistent with the sediment "food bank" hypothesis with relatively high abundances being observed throughout the year that is caused by the build-up of labile organic material at the seafloor during summer, which persists and provides food to benthic communities during winter (Glover et al. 2008). Similarly, this benthic food bank contributed to sustain benthic oxygen consumption and denitrification rates throughout the year even though the sinking flux of organic carbon showed considerable temporal variability between summer and winter seasons (Hartnett et al. 2008). Thus, benthic

ecosystem function is heavily influenced and sustained by these sediment deposit of labile organic material that accumulates following summer blooms and offers energy throughout the winter when the export of carbon from the surface is considerably less (Smith et al. 2012). There are growing concerns for the ecosystems of the Antarctic Peninsula in relation to climate change and further baseline studies are needed to better understand fjord responses to climate warming and their resilience to a rapidly changing environment (Grange and Smith 2013; Kerr et al. 2018).

4 Pulse-chase experiments

Pulse-chase experiments have been used to study and better understand food webs and the fate of organic labile detritus in different deep-sea benthic communities from those found in polar environments (van Oevelen et al. 2011; Sweetman et al. 2014; Hoffmann et al. 2017) to abyssal plains (Aberle and Witte 2003; Witte et al. 2003a; b; van Oevelen et al. 2012; Sweetman et al. 2019). These studies have assessed the long and short-term response to inputs of phytodetritus (e.g., Moodley et al. 2002; Witte et al. 2003a; Woulds et al. 2009) or larger food falls such as jellyfish (Sweetman et al. 2016) providing unique insights into the functioning of deep-sea benthic communities (Witte et al. 2003a; Gontikaki et al. 2011; Sweetman et al. 2014).

For examples, these experiments shed light on the roles of the different benthic communities in the short-term C-cycling showing contrasting results in the presence of oligotrophic or eutrophic environments (Witte et al. 2003b; Sweetman et al. 2019). Short-term C-cycling in oligotrophic regions appears to be dominated by the microbial community (Sweetman et al. 2019) while the macrofaunal community tends to dominate under eutrophic environments (Witte et al. 2003b). The use of fresh labile organic material in these experiments also allows us to better understand feeding preferences of the major macrofaunal taxa in the sediments emphasizing high heterogeneity and plasticity for the macrofaunal community whether at

family, taxon or community levels (Sweetman and Witte 2008). Furthermore, Sweetman et al. (2016) investigated the implication of jellyfish decomposition for the benthic food webs in an Arctic fjord noting the significant importance that these deposits have on benthic C-uptake dynamics by altering biogeochemical cycling and C-flow through the benthos.

Currently, there is a significant gap on our knowledge on the ecology of the western CCZ. To date, only four studies have examined benthic ecosystem functioning in the equatorial Pacific (Hammond et al. 1996; Berelson et al. 1997; Khripounoff et al. 2006; Sweetman et al. 2019), and only two have focused in the parts of the CCZ targeted for mining (central CCZ: Khripounoff et al. 2006; eastern CCZ: Sweetman et al. 2019). There is also a considerable gap on our knowledge about benthic ecosystem functioning in glaciomarine fjords along the WAP and the effect of climate warming on Antarctic environments (Grange and Smith 2013; Lundesgaard et al. 2020; Ziegler et al. 2020). The current PhD project therefore consisted of assessing benthic ecosystem functioning of the abyssal seafloor in the western CCZ to assess how representative the western APEIs are to other areas of the CCZ (Fig. 5), and in a bathyal fjord and on the continental shelf in the WAP to assess how unique Antarctic fjord ecosystems are to adjacent shelf habitats and the implications of a rapidly warming WAP environment. Pulse-chase experiments with labelled ^{13}C phytodetritus were carried out in these two very diverse deep-sea environments to observe the benthic response to a sudden input of fresh organic matter and trace the enriched material throughout the different ecosystem compartments (e.g., bacteria vs macrofauna). At the same time, I measured sediment community oxygen consumption (SCOC) rates, and nutrient and DIC fluxes across the sediment water interface. This study improves our understandings of regional benthic ecosystem functioning across the CCZ and across natural gradients of POC flux, as well as improves our knowledge on the implications of a warming environment on glaciomarine fjords and the continental shelf of the WAP.

22
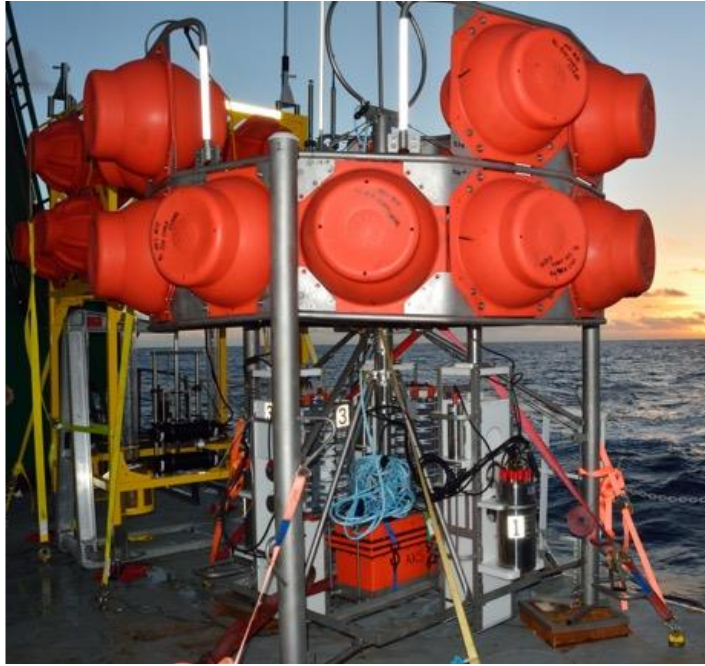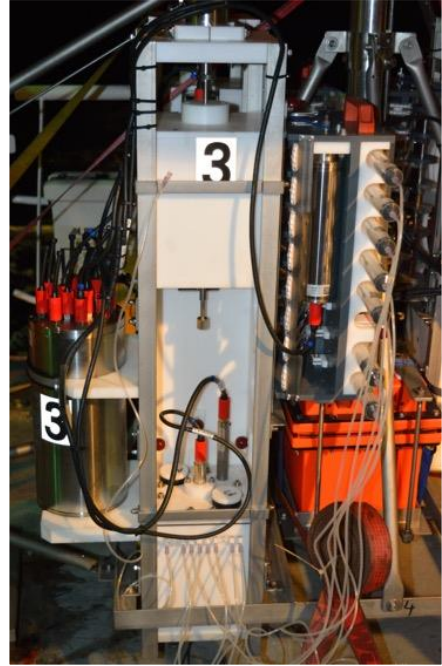
Figure 5: (A) Respirometer lander deployed in the western CCZ and (B) example of a chamber used to carry out in situ experiments.

CHAPTER 2

ABYSSAL SEAFLOOR RESPONSE TO FRESH PHYTODETRITAL INPUT IN THREE AREAS OF PARTICULAR ENVIRONMENTAL INTEREST (APEIs) IN THE POLYMETALLIC NODULE-RICH CLARION-CLIPPERTON ZONE (CCZ)

Abstract

The abyssal seafloor (3500-6000m) remains largely unexplored but with deep-sea mining imminent, anthropogenic impacts may soon reach abyssal communities. Thus, there is a growing need for baseline studies of biodiversity, ecosystem functioning, and connectivity in both potential mining and no-mining areas across the Clarion-Clipperton Zone (CCZ), a key target region for polymetallic nodule mining. In this study, in situ pulse-chase experiments were conducted for 1.5 days in three no-mining areas (Areas of Particular Environmental Interest, or APEIs) in the western CCZ, a region with a seafloor particulate organic carbon (POC) flux gradient. Mean seafloor respiration, macrofaunal abundance, and biomass showed a decreasing trend from the more eutrophic APEI 7 to the more oligotrophic APEI 1, although this trend was not statistically significant (p = 0.18), likely due to small samples sizes. Most (96%) of the ^{13}C-labelled processed phytodetritus was respired within 1.5 days. Uptake of phytodetritus by macrofauna and bacteria was detected but was lower than in the previously studied and more eutrophic eastern CCZ over similar time scales. Bacteria dominated the short-term (~1.5d) uptake of organic carbon at the seafloor, yet macrofauna processed more organic carbon per unit biomass than previously found in the eastern CCZ. Our study provides information on benthic ecosystem functioning in areas set aside from mining in the western CCZ to use while designing APEIs and suggests high variability may occur in the rates of benthic C_{org}-cycling across the CCZ. Our results confirm the utility POC flux as an environmental factor in future marine spatial planning studies.

1 Introduction

Concerns about the depletion of land-based high-grade mineral ores and the worlds growing population necessitating a greater need to access high-grade ores has led to significant international attention being directed at the deep seafloor (Sparenberg 2019; Levin et al. 2020a). The deep sea is the largest ecosystem on Earth with the abyssal seafloor making up the largest deep-sea benthic ecosystem and the only region on the planet aside from Antarctica that has remained untouched from commercial mining (Smith et al. 2008a; Ramirez-Llodra et al. 2010, 2011; Sweetman et al. 2017).

Abyssal ecosystems are characterized by severe organic-carbon limitation (Smith et al. 2008a) with some of the most oligotrophic abyssal regions relying on a particulate organic carbon (POC) flux of only 0.5 g C m^{-2} yr^{-1}. The rate of POC flux to the seafloor plays a major role in structuring benthic biodiversity, community structure and ecosystem functioning, including sediment community oxygen consumption, calcite dissolution, and bioturbation (Archer and Maier-Reimer 1994; Wenzhoefer et al. 2001; Smith et al. 2008a; Ruhl et al. 2014; Thurber et al. 2014).

Parts of the abyssal seafloor of the western equatorial Pacific receive an annual POC flux of ~1 g C m^{-2} yr^{-1} (Smith et al. 1997; Smith and Demopoulos 2003; Washburn et al. 2021b; a), which allows the precipitation of manganese and iron oxides from the water column and sediment pore waters in the form of polymetallic nodules at the seafloor (Hein et al. 2013). In the Clarion-Clipperton Fracture Zone (CCZ), these nodules are rich in nickel, copper, cobalt, lithium and molybdenum (Paulikas et al. 2022) and the high abundances of polymetallic nodules found near the surface of the seafloor may be containing higher ore grades than for land-based mines (e.g., cobalt and nickel may be 3-6 times more concentrated in nodules in the CCZ than in deposits on land, Levin et al. 2020a). Their high mineral content and abundance

make polymetallic nodules targets for commercial extraction by a nascent deep-sea mining industry (International Seabed Authority [ISA] 2010; Hein et al. 2013; Kuhn et al. 2017).

Deep-sea mining will represent a significant disturbance for the seafloor as direct nodule removal and the consequent sediment plumes will affect approx. 600-800 km^2 of seabed and the overlying water column per mining operation per year (Levin et al. 2016; Drazen et al. 2020; Smith et al. 2020), with long-lasting impacts on benthic microbiota (Stratmann et al. 2018b; a; Vonnahme et al. 2020), meiofauna (Stratmann et al. 2018a), macrofauna and megafauna (Jones et al. 2017; Stratmann et al. 2018b; a) and ecosystem function predicted (de Jonge et al. 2020). Deep-sea mining will result in habitat removal, sediment plume generation and burial of seafloor biota and likely species extinction due to connectivity and biodiversity loss (Borowski and Thiel 1998; Niner et al. 2018; Ardron et al. 2019).

Based on environmental proxies of seafloor biodiversity, the ISA recently established 9 no-mining areas, termed "Areas of Particular Environmental Interest" or APEIs, to safeguard regional biodiversity in the face of polymetallic nodule mining in the CCZ (Wedding et al. 2013, 2015; Cuvelier et al. 2020; McQuaid et al. 2020). However, very few studies have compared benthic ecology in the APEIs (e.g., Simon-Lledó et al. 2019) to the license areas to determine whether the APEIs are representative of exploration claims in terms of seafloor biodiversity and ecosystem function. Previous research into deep CCZ ecology relied on observations and measurements of claim areas in the eastern and central CCZ and APEIs situated on the edge of the eastern CCZ (e.g. Jones et al. 2017; Kersten et al. 2017; Volz et al. 2018; Wiklund et al. 2019), leaving a significant gap in our knowledge on the environment and ecology of the western CCZ and how pattern change with changing overlying productivity that decreases northward. Furthermore, current knowledge on benthic ecosystem functioning in the equatorial Pacific, and in particular in the CCZ, is scarce and isolated (Khripounoff et al. 2006; Stratmann et al. 2018c; a, 2019; Sweetman et al. 2019; de Jonge et al. 2020) and is non-existent

for the western APEIs. To date, only 4 studies have addressed benthic ecosystem functioning in the equatorial Pacific (Hammond et al. 1996; Berelson et al. 1997; Khripounoff et al. 2006; Sweetman et al. 2019), and only two have focused in the parts of the CCZ targeted for mining (central CCZ: Khripounoff et al. 2006; eastern CCZ: Sweetman et al. 2019). This makes it difficult to make generalization across the CCZ and APEIs, and to assess how representative APEIs are of exploration claim areas.

The CCZ has a distinctive pattern for POC flux to the seafloor (Lutz et al. 2007; McQuaid et al. 2020). Here we focus on two dominant POC flux gradients: a first trend east to west, and a second trend south to north (Lutz et al. 2007; McQuaid et al. 2020). The first trend involves the whole CCZ where the higher POC flux in the east ($\sim$1.5-2 g C_{org} m^{-2} yr^{-1}) diminishes towards the western boundaries (0.8 – 1.5 g C_{org} m^{-2} yr^{-1}) (Lutz et al. 2007; McQuaid et al. 2020). The second gradient refers only to the western CCZ, where POC flux to the seafloor decreases northward (APEI 7 to APEI 1) from $\sim$2 g C_{org} m^{-2} yr^{-1} in APEI 7, $\sim$1.5 g C_{org} m^{-2} yr^{-1} in APEI 4 and $\sim$1 g C_{org} m^{-2} yr^{-1} in APEI 1 (Lutz et al. 2007; McQuaid et al. 2020). Data from these unstudied western CCZ would be a step further to assess whether POC flux gradient is indeed a useful proxy to delineate APEIs in the CCZ.

In this study, we undertook in situ benthic lander experiments in the westernmost APEIs (1, 4 and 7) of the CCZ over a gradient of POC flux that decreased northwards from APEI 7 to APEI 1 to evaluate seafloor respiration rates and nutrient fluxes across the sediment-water interface, and to measure C-flow through the benthic macrofauna and bacteria by injecting and tracing ^{13}C-labelled phytodetritus. We also compared the C-uptake rate data from these western APEIs to similar data collected in the UK1 and Ocean Minerals of Singapore claim area in the eastern CCZ (Sweetman et al. 2019) to generate regional insights of benthic ecosystem function across the CCZ. By comparing data collected in the more eutrophic eastern to the more oligotrophic western CCZ, and from the more eutrophic APEI 7 to more oligotrophic APEI 1, it was possible

to assess changes in benthic processes over natural gradients in POC flux. We specifically tested the following hypotheses: (1) *No significant change exists in SCOC, nutrient fluxes or C-uptake rates of bacteria and macrofauna between the westernmost APEIs*; and (2) *No significant change exists in C-uptake rates of bacteria and macrofauna between western and eastern sides of the CCZ.* Falsifying these hypotheses would demonstrate a significant structuring effect of POC flux on the seafloor of the CCZ and can be reliably used as one of the environmental proxies in the selection of APEIs.

2 Methods

2.1 Study sites

During the KM1808 cruise aboard RV *Kilo Moana* in May-June 2018 in situ pulse-chase experiments were carried out in APEI 1, 4 and 7 in the western CCZ (Fig. 6) during a total of five deployments of a deep-sea benthic chamber lander, also called a benthic respirometer, equipped with 3 chambers (22 x 22 cm plan area). Deployment depths ranged from 4,861 m to 5,216 m (Table 1). In 3/5 lander experiments (AKS 252, AKS 254, and AKS 261), the phytodetritus injectors malfunctioned in some of the chambers and the samples from these "failed" chambers were used to gather information on natural non enriched, also defined as "background", sediment community oxygen consumption (SCOC), nutrient and dissolved inorganic carbon (DIC) flux rates, and to collect samples for background stable-isotopes signatures of the fauna and bacteria.
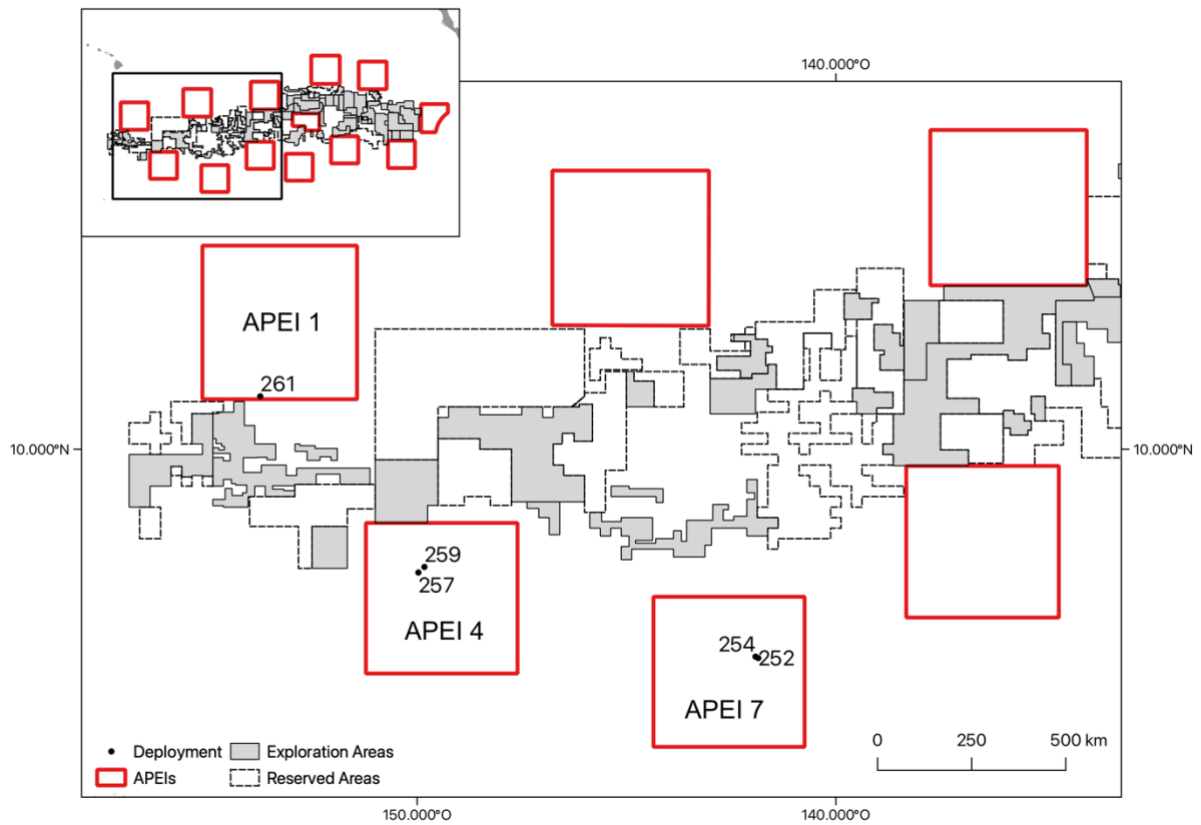
Figure 6: Areas surveyed in the western CCZ. The deployments sites are shown by the different AKS numbers.

Table 1: Deployment depths and locations in the western CCZ. A total of 15 incubations were carried out over five deployments, of which seven were pulse-chase experiments ad four 'control' incubations. No sediments were collected in the remaining four experiments.

Deployment AKS #	Depth (m)	APEI #	Lat	Lon	Pulse-chase Experiments	Control Incubations
252	4887	APEI7	5.02	-141.85	2	1
254	4861	APEI 7	5.05	-141.91	1	2
257	5043	APEI 4	7.06	-149.96	1	
259	4891	APEI 4	7.20	-149.82	2	
261	5216	APEI 1	11.24	-153.74	1	1

2.2 Labelled algae preparation

An axenic clone of the diatom *Phaeodactylum tricornutum* was used as a labelled C-source in the experiments, since it occurs throughout the Pacific Ocean (Martino et al. 2007) and was previously used in pulse-chase experiments carried in the eastern CCZ by Sweetman et al. (2019). The diatoms were cultured in artificial seawater and F/2 culture medium replacing 25% of the $NaHCO_3$ with 25% $NaH^{13}CO_3$. The algae were grown for 4-5 weeks at 16°C under a 12 h light dark cycle. Algae were harvested by centrifugation (408 rpm x 3 min), rinsed 5 times with unlabeled artificial seawater to remove labelled inorganic C, frozen and freeze-dried. The algal biomass had a mean molar C:N ratio of 8.9 ± 0.1 (SD), a mean organic C content of 8% and a mean ^{13}C content of 22.04 ± 0.12 atom% (SD).

Prior to the deployment of the lander, 122 mg dry weight of freeze-dried, ground up and homogenized axenic diatoms were hydrated with cold, filtered (0.2 μm) deep-sea water collected at the deployment sites by CTD, and loaded into an algal injector on top of each chamber. The algal addition corresponded to an organic C input of 200 mg C m^{-2}, which was equivalent to approximately 20% of the annual POC seafloor flux in this region of the southernmost APEI 7 (Lutz et al. 2007).

2.3 Lander deployments and in situ experiments

After the lander was deployed it reached the seafloor 2 to 3 h later. After 2 h, to allow any resuspended sediments to be carried away by the bottom current or resettle to the seafloor, the chambers were slowly driven into the sediment by onboard motors, and stirrers mounted in the chamber lids were activated to maintain mixing of the water overlying the sediments in the chamber. The algae were injected over the chamber seafloor 1.5 h after the chambers began pushing into the sediment. Once the algae were injected, it was mixed into the water overlying the sediments by a stirrer for 2 minutes. Subsequently, the stirrers were switched off for 1 h to

allow settling of the algae which was a sufficient amount of time based on experience from previous experiments (e.g Sweetman et al. 2014, 2016, 2019). After 1 h, the stirrers were then switched on again and remained on and stirring (60 rpm) for the remainder of the 36-h incubation. During each 36-h incubation, seven water samples were collected for total DIC, $DI^{13}C$ and nutrients from above the sediment-water interface by a syringe sampler attached to the chambers. Water samples were collected 1 h, 4.5 h, 13 h, 19.5 h, 26.5 h and 33.5 h after algae injection from the top of the camber assuming uniform water distribution as a result of the stirring. A control water sample was collected before the algae was injected and it was used to evaluate the natural background water conditions in the chamber. Contros Hydroflash® oxygen optodes mounted in the chamber lids continuously measured the oxygen concentration during the incubation (assuming a DIC: O_2 respiratory quotient of 1). At the end of the experiments, the chambers were sealed, and the lander was acoustically recalled from the seabed, arriving at the sea surface approximately 2 h later. Once the lander was aboard the ship, the depth of the overlying water in each chamber was measured to determine the volume of the overlying water. Subsequently, the top water was siphoned off and filtered through 63-µm mesh, and the sediment enclosed in each chamber were recovered from 0-2 cm and 2-5 cm deep sediment horizons. No nodules were collected as they were either not present or were too small to be relevant. Sediments from each vertical stratum were removed by a spackle knife, transferred to a bucket, and homogenized by gentle stirring. Approximately 50 ml of sediment was transferred to 50 ml plastic Falcon tubes for total organic carbon (TOC), bacterial specific phospholipid fatty acid (PLFA), and sediment density analysis. TOC, bacterial PLFA and sediment density samples were then frozen at -80°C. The remaining sediments and nodule granules sieved with cold (4°C), 0.2-µm filtered seawater on a 300-µm mesh and fixed in 4% buffered formaldehyde seawater for macrofauna analysis. Syringe water samples were filtered with sterile 0.2 µm cellulose acetate syringe filters into 12 ml and 3 ml exetainer vials and

preserved with 10 µl of 6% $HgCl_2$ for total DIC and ^{13}C-signature analysis. The remaining water was filtered into previously acid (HCl)-washed, 60 ml scintillation plastic bottles and frozen at -80°C for nutrient analysis.

2.4 Samples processing and analysis

Ashore, water samples were sent to the Royal Netherlands Institute for Sea Research (NIOZ) in Yerseke for analyses of DIC concentrations and $DI^{13}C$ signatures on an Apollo SciTech AS-C3 and an elemental analyzer Flash 1112, THERMO Electron S.p.A.) coupled to an isotope ratio mass spectrometer (EA-IRMS, DELTA-V, THERMO Electron Corporation), and for nutrient concentrations (SiO_2, NO_2, NO_3, NH_4 and PO_4) as described by Maier et al. (2019). Fixed macrofauna samples were sieved on a 300-µm sieve, sorted under a microscope in cool, artificial seawater, and identified to family (Polychaeta), or to other major taxa. Separate sorting utensils were used for background and enriched isotope samples to avoid contamination with enriched ^{13}C. Organisms were washed to remove attached organic debris in cooled, filtered seawater. Due to insufficient biomass being available for measuring isotope signatures of individual animals, macrofauna were pooled into polychaete family, crustacean order, or other major taxa where possible. Calcareous shelled organisms were placed into silver (Ag) caps while all other organisms were placed into tin (Sn) caps. Caps were dried at 35-40°C for 7 days and calcareous shelled organisms were decalcified with 0.5 M HCl and 2 M HCl following the approach described in Sweetman et al. (2009). Samples were then sent to UC Davis Stable Isotope Facility in California, USA, to measure C-content and ^{13}C-isotopic ratios. Bacterial specific PLFA analysis was carried out at the James Hutton Institute in Aberdeen, UK. PLFA extraction and derivatization to fatty acids methyl esters (FAMEs) followed Shahbaz et al. (2020). A GC Trace Ultra with combustion column attached via a GC Combustion III to a Delta V Advantage isotope ratio mass spectrometer (all Thermo Finniga,

Bremen, Germany) was used to quantify and determine the isotopic composition and concentration of individual FAMEs as described by Thornton et al. (2011). The bacterial specific PLFAs, $iC_{14:00}$; $iC_{15:00}$; $aiC_{15:00}$; $iC_{16:1}$; $iC_{16:0}$; $C_{16:1w5c}$; $aiC_{17:0}$; $C_{17:1w8c}$; $C_{18:1w9}$; $C_{18:1w7}$; $C_{18:00}$; cyclo $C_{19:0}$, were used for biomass and C-uptake measurements following the lists of Willers et al. (2015) and Bühring et al. (2006, 2010).

Macrofaunal specific ^{13}C uptake, expressed as $\Delta^{13}C$ (‰), was calculated as the difference between the $\delta^{13}C_{sample}$ and $\delta^{13}C_{background}$ values of closely related taxa. Uptake of ^{13}C was then calculated as the product excess of atom% ^{13}C (samples – background) and C content expressed as a unit weight: ^{13}C uptake (unit wt C) = (atom% $^{13}C_{samples}$ – atom% $^{13}C_{background}$) x (unit wt C of organism). This was then adjusted to total C uptake by accounting for the ^{13}C algal labeling: C uptake = ^{13}C uptake / 22.04 atom%.

Bacterial biomass was calculated from the weighted-average PLFA ($iC_{14:00}$; $iC_{15:00}$; $aiC_{15:00}$; $iC_{16:1}$; $iC_{16:0}$; $C_{16:1w5c}$; $aiC_{17:0}$; $C_{17:1w8c}$; $C_{18:1w9}$; $C_{18:1w7}$; $C_{18:00}$; cyclo $C_{19:0}$) concentration (μmol) mL^{-1} sediment/ (a x b), where a is the average PLFA concentration in bacteria (for this study we assumed 0.056 g C PLFA g^{-1} biomass, Brinch-Iversen and King 1990), and b is the average fraction-specific bacterial PLFA encountered in sediment dominated by bacteria (0.48; calculated after Rajendran et al. 1993, 1994). The prefixes ´i´ and ´ai´ refer to ´iso´ and ´$antiso$´, respectively. Total bacterial assimilation (mg ^{13}C m^{-2}) of ^{13}C was calculated from label incorporation into the bacterial fatty acids ($iC_{14:00}$; $iC_{15:00}$; $aiC_{15:00}$; $iC_{16:1}$; $iC_{16:0}$; $C_{16:1w5c}$; $aiC_{17:0}$; $C_{17:1w8c}$; $C_{18:1w9}$; $C_{18:1w7}$; $C_{18:00}$; cyclo $C_{19:0}$) following the methods of Sweetman et al. (2010, 2014, 2016, 2019) using an average fraction-specific bacterial PLFA encountered in sediment dominated by bacteria (0.48; calculated after Rajendran et al. 1993, 1994). The ^{13}C assimilation values (mg ^{13}C m^{-2}) for bacteria were then converted to daily C assimilation rates (mg C m^{-2} d^{-1}) by accounting for the fractional abundance of ^{13}C in the added algae as: C

assimilation = ^{13}C incorporated (mg ^{13}C m^{-2})/ fractional abundance of ^{13}C in algae and dividing by 1.5 to account for the 1.5 d experiment.

2.5 Data analysis

All data analysis was carried out in R. Significant differences in mean SCOC rates and the total microbial and macrofaunal biomass and C-uptake between APEIs were analysed using a One-Way ANOVA test. T-tests were used to test for significant differences in SCOC, DIC, or nutrient fluxes in the presence or absence of the labeled substrate. Differences in C-uptake between macrofauna and bacteria across APEIs and the eastern CCZ were analysed using a Two-Way ANOVA with organism and site set as fixed factors. Prior to analysis, datasets were first checked for normality and heteroscedasticity, and a square-root or logarithmic transformation applied where necessary to achieve normality and homoscedasticity. Regression analysis was carried out to study the relationship between SCOC, phytodetritus-derived DIC production, biomass and C-uptake to the observed POC flux gradient across the APEIs. POC flux values were extracted using QGIS from the POC flux values from Lutz et al. (2007). An alpha level of 0.05 was chosen as the criterion of statistical significance.

3 Results

3.1 Sediment community oxygen consumption and nutrient fluxes

Mean total oxygen consumption rates increased from 3.74 ± 1.86 mg C m^{-2} d^{-1} ($n = 2$, Standard Deviation [SD]) (0.37 ± 0.18 mmol O_2 m^{-2} d^{-1}) to 5.22 ± 0.92 mg C m^{-2} d^{-1} ($n = 3$, SD) (0.51 ± 0.09 mmol O_2 m^{-2} d^{-1}) between APEI 1 and APEI 7 (Fig. 7). Although the mean respiration rate increased from APEI 1 to APEI 7, mean total SCOC rates were not significantly different between APEIs (One-Way ANOVA, $p = 0.60$). In terms of mean respiration rates between the enriched and background (i.e., non-algal addition) experiments, mean respiration rates in the

enriched cores were 17% higher than background rates, varying from 4.25 ± 1.83 mg C m^{-2} d^{-1} ($n = 3$, SD) (0.42 ± 0.18 mmol O$_2$ m^{-2} d^{-1}) for background to 4.99 ± 1.24 mg C m^{-2} d^{-1} ($n = 4$, SD) (0.49 ± 0.06 mmol O$_2$ m^{-2} d^{-1}) for enriched rates, but this increase was not statistically significant (t-test, $p = 0.23$).

Nutrient fluxes were not significantly different between the algal-enriched chambers and background incubations (Table 2), very possibly because of the high variability in the fluxes seen amongst the chambers and APEIs. For both the algal and non-algal injection experiments, total silicate and nitrate fluxes were directed into the sediment, while ammonium, nitrite and phosphate showed efflux. Total ammonium fluxes were positive (i.e., out of the sediment) in APEI 1 (0.12 ± 0.68 mmol m^{-2} d^{-1} [SD]) and APEI 7 (0.15 ± 0.13 mmol m^{-2} d^{-1} [SD]) and negative (i.e., into the sediment) in APEI 4 (-0.05 ± 0.15 mmol m^{-2} d^{-1} [SD]). Total nitrite fluxes showed a mean efflux from the sediment in APEI 1 (2.79 ± 7.40 x 10^{-3} mmol m^{-2} d^{-1} [SD]) and APEI 4 (1.01 ± 1.63 x 10^{-3} mmol m^{-2} d^{-1} [SD]) and influx in APEI 7 (0.13 ± 2.17 x 10^{-3} mmol m^{-2} d^{-1} [SD]). Contrastingly, total phosphate fluxes were into the sediment in APEI 1 (0.22 ± 3.33 x 10^{-2} mmol m^{-2} d^{-1} [SD]) and 4 (-0.01 ± 0.03 mmol m^{-2} d^{-1} [SD]) and out of the sediment in APEI 7 (0.41 ± 1.03 x 10^{-2} mmol m^{-2} d^{-1} [SD]).
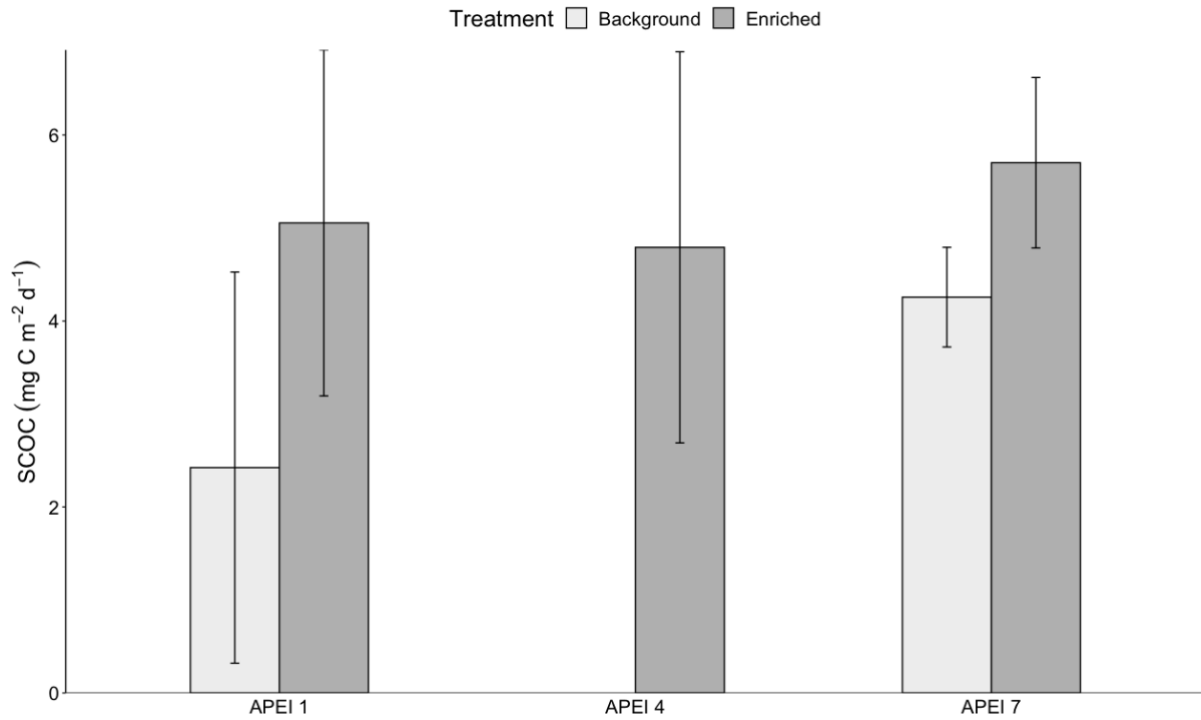
Figure 7: SCOC rates (mean ± SD) in the different study areas of the western CCZ. Mean SCOC rates observed in the algal-addition (Enriched) and control (Background) experiments.

Table 2: Mean nutrient fluxes and *p*-values of the Welch two sample t-test comparing fluxes between background and enriched conditions. Positive flux means flux out of the sediment and negative flux means flux into the sediments.

	Ammonium (mmol m^{-2} d^{-1})	Nitrite (mmol m^{-2} d^{-1})	Nitrate (mmol m^{-2} d^{-1})	Phosphate (mmol m^{-2} d^{-1})	Silicate (mmol m^{-2} d^{-1})
Background	0.05 ± 0.04	0.00176 ± 0.002	-0.06 ± 0.08	-0.01 ± 0.002	-0.33 ± 0.46
Enriched	0.17 ± 0.09	0.00180 ± 0.004	-0.11 ± 0.03	0.02 ± 0.002	-0.40 ± 0.56
p	0.30	0.27	0.60	0.22	0.92

3.2   Dissolved inorganic carbon

Production of phytodetritus-derived DIC increased over time from 0 mg C m^{-2} to 0.10 ± 0.17 mg C m^{-2} (*n* = 5, SD) within the first hour of the experiment and then to 0.71 ± 0.35 mg C m^{-2} (*n* = 5, SD) after 36 hours of incubation. DIC production spiked within the first hours of

incubation rising from 0.10 ± 0.17 mg C m^{-2} ($n = 5$, SD) to 0.33 ± 0.24 mg C m^{-2} ($n = 7$, SD)

within the first 5 h (an increase of 67%). Following this first rapid increase, DIC production

then slowed down. Mean DIC production rates at APEI 1, 4 and 7 were 0.75 mg C m^{-2} d^{-1}, 0.51

± 0.30 mg C m^{-2} d^{-1} ($n = 3$, SD) and 0.53 ± 0.24 mg C m^{-2} d^{-1} ($n = 3$, SD), respectively. Only

one DIC production measurement was possible at APEI 1 (0.75 mg C m^{-2} d^{-1}) (Fig. 8). No

significant differences were found in mean DIC production in the different APEIs ($p = 0.33$,

One-Way ANOVA).
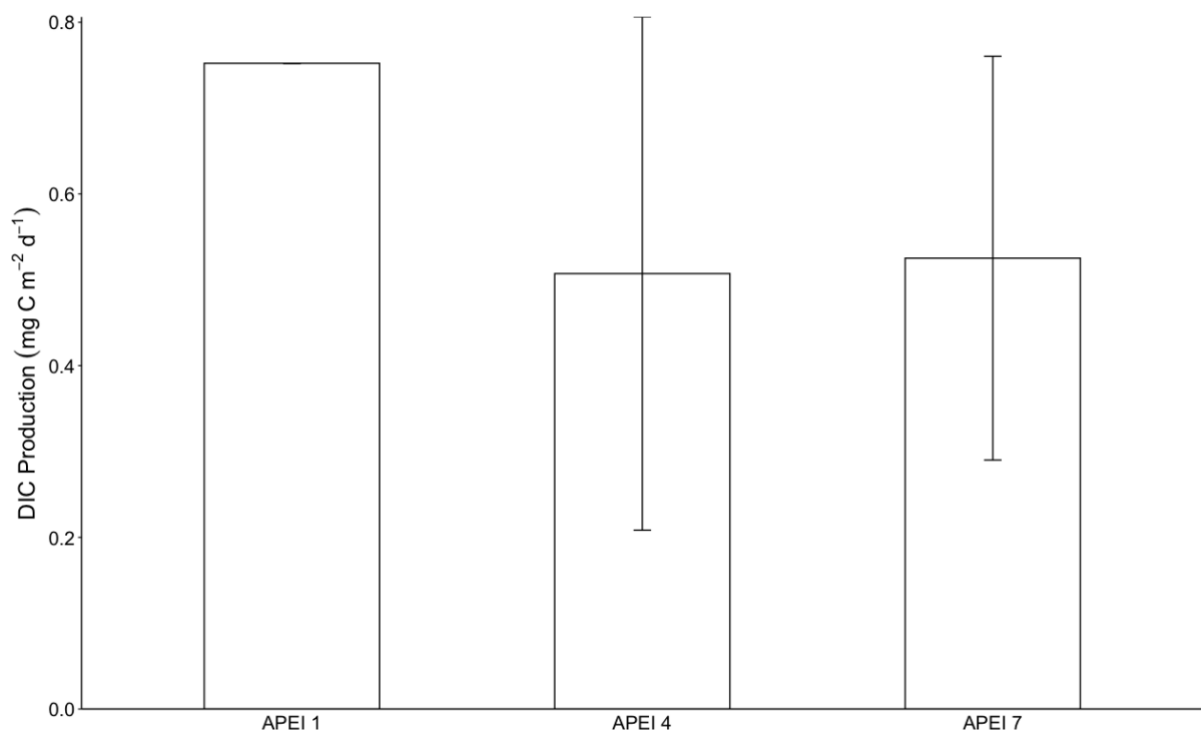
Figure 8: Phytodetritus-derived DIC production in the 36-h incubations across the different APEIs of the western CCZ. Error bars denote ± SD. Only one measurement was available for APEI 1.

3.3 Benthic community structure

The total number of macrofauna individuals collected in each APEI is stated in SI1.

Macrofaunal community abundance decreased northwards from a mean of 1739 ± 197 ind. m^{-2} ($n = 6$, SD) in APEI 7 to 366 ± 32 ind. m^{-2} ($n = 2$, SD) in APEI 1 (Fig. 9), albeit no significant

differences were detected ($p = 0.078$, One-Way ANOVA,). Macrofaunal biomass decreased

northward, from 4.87 ± 4.36 mg C m^{-2} ($n = 6$, SD) in APEI 7 to 1.76 ± 1.28 mg C m^{-2} ($n = 2$, SD) in APEI 4 and 0.55 ± 0.35 mg C m^{-2} ($n = 2$, SD) in APEI 1 (Fig. 10). Mean bacterial biomass (Fig. 10) across the western APEIs showed a northward decrease, varying from 3.25 ± 0.92 mg C m^{-2} ($n = 4$, SEM) in APEI 7, the most southern station, to 2.79 ± 0.42 mg C m^{-2} ($n = 3$, SEM) in APEI 4 and 1.35 ± 0.46 mg C m^{-2} ($n = 2$, SEM) in APEI 1. However, no statistically significant differences were observed across the APEIs ($p = 0.71$, Two-Way ANOVA).
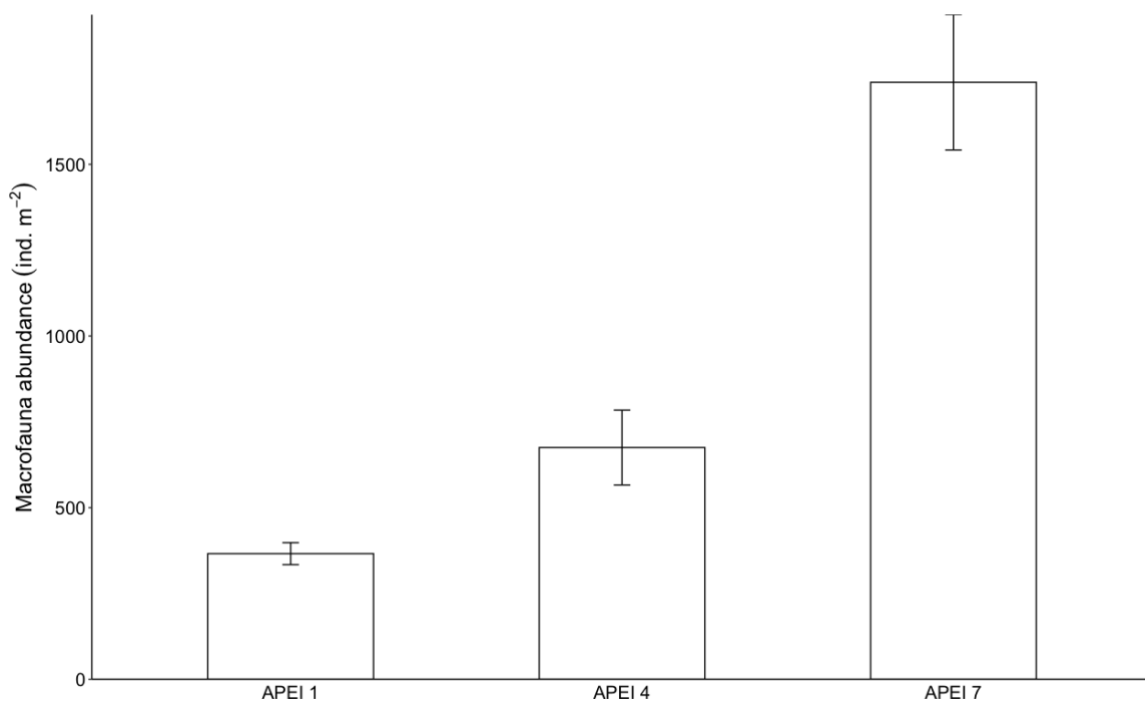
Figure 9: Mean macrofauna abundance in the three different APEIs study regions. Error bars denote $\pm$ SD.
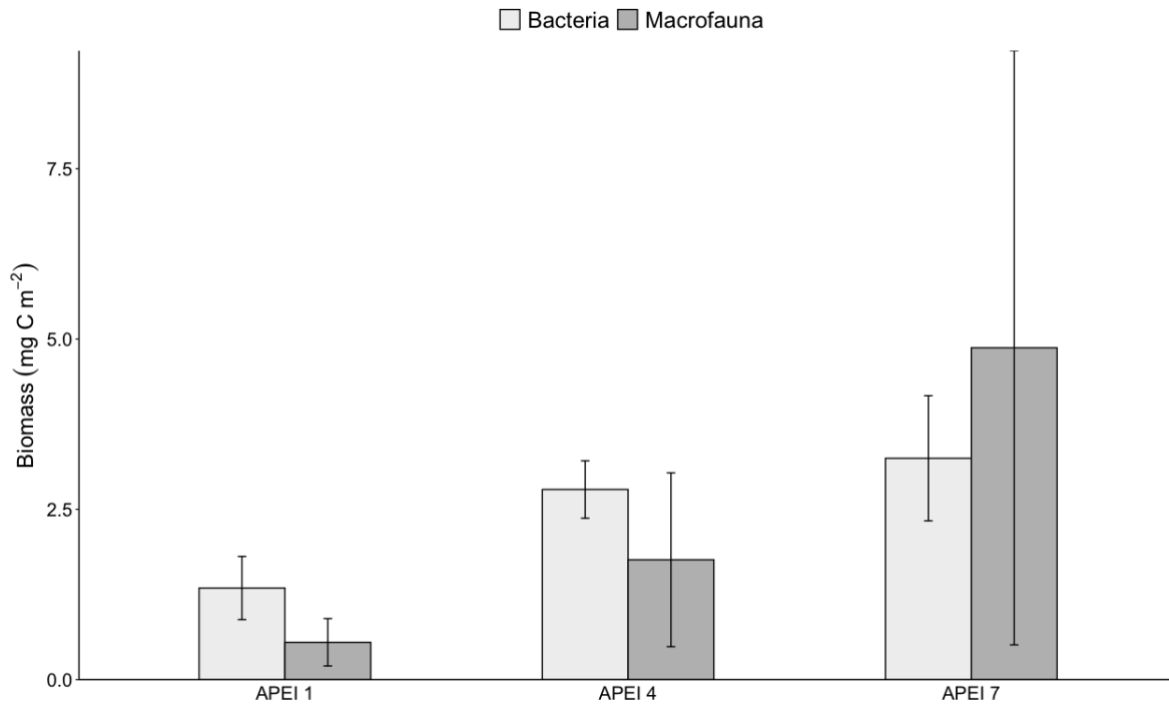
Figure 10: Mean bacterial and macrofaunal biomass (mg C m^{-2}) across the three different APEIs in the western CCZ. Error bars denote ± SD.

3.4 Benthic C-uptake

The range in $\Delta\delta^{13}$C signatures found in the macrofauna was large and varied from 0.5 to 1568‰, with the lowest value observed for a nemertean and the highest value for a gastropod in APEI 7. Crustacea isotopic signatures were highly variable with low $\Delta\delta^{13}$C values (Copepoda: 7.9‰) and some very high values (Ostracoda: 588‰) from APEI 7. Polychaeta $\Delta\delta^{13}$C signatures ranged from 4.3‰ for a lumbrinerid in APEI 4 to 71‰ for paraonids in APEI 7. Bivalves (687‰) along with the gastropod in APEI 7 (1568‰) exhibited some of the highest isotopic signatures measured. Taxon-specific isotope signatures and C-carbon uptake rates in the different APEIs are summarized in Table 3. When data from all sampling stations were pooled, the Mollusca dominated macrofauna C-uptake (molluscan C-uptake: 0.09 ± 0.03 mg C m^{-2} d^{-1} [n = 3, SD]), followed by Crustacea (5.59 ± 4.02 x10^{-3} mg C m^{-2} d^{-1}, n = 9, SD), and other metazoans made up of a mixture of less common macrofaunal taxa such as nematodes, nemerteans and sipunculid worms had a mean C-uptake rate of 1.33 ± 1.55 x10^{-3} mg C m^{-2} d^{-1}

($n = 6$, SD) (Table 3). The Polychaeta contributed the least to total macrofaunal C-uptake when data were pooled across from all experiments (8.06 ± 8.47 x10^{-4} mg C m^{-2} d^{-1}, $n = 11$, SD) (Table 3).

While a gradient of decreasing macrofaunal C-uptake was observed between the southernmost (relatively eutrophic) and northernmost (relatively oligotrophic) APEIs, macrofauna C-uptake rates in the different APEIs showed great variability (Fig. 11). The means C-uptake rate was highest in the APEI 7 (0.02 ± 0.04 mg C m^{-2} d^{-1}, $n = 4$, SD), with rates decreasing to 1.64 ± 1.78 x 10^{-3} mg C m^{-2} d^{-1} ($n = 2$, SD) and 1.80 ± 0.73 x 10^{-4} mg C m^{-2} d^{-1} ($n = 2$, SD) in APEI 4 and APEI 1, respectively.

As with the macrofaunal C-uptake data, a pattern of decreasing bacterial C-uptake was observed from APEI 7 to 1. Mean bacterial C-uptake decreased from 2.34 ± 0.49 x 10^{-2} mg C m^{-2} d^{-1} ($n = 4$, SD) in APEI 7 to 9.86 ± 6.01 x 10^{-3} mg C m^{-2} d^{-1} ($n = 2$, SD) in APEI 1. Moreover, the high level of variability in the macrofaunal C-uptake data meant that no significant difference was found between mean bacterial and macrofaunal C-uptake (Fig. 11) across study sites in the Western APEIs ($p = 0.82$, Two-Way ANOVA), although the bacterial contribution to the summed macrofauna and bacteria daily C-uptake decreased southward from 98% in APEI 1 to 38% in APEI 7, suggesting a greater importance for macrofauna in C-cycling as POC flux increased. As with the mean macrofaunal and bacterial C-uptake rates, a decrease was observed in mean summed bacteria and macrofauna daily C-uptake rates (Fig. 12) from APEI 7 to APEI 1, though no significant difference between the APEIs was detected ($p = 0.37$, One-Way ANOVA).

Table 3: Total macrofaunal isotopic signatures, C-uptake rates (mg C m^{-2} d^{-1}) and abundance during pulse chase experiments in the different APEIs. Values are represented as ± SD.

Taxon	Biomass (µg C)	No. animals	Δδ^{13}C (‰)	C-uptake (x10^{-4} mg C m^{-2} d^{-1})	Abundance (Ind. m^{-2})
APEI 1					366 ± 32
Polychaeta	38.43	1	4.85	1.28	
Other metazoan	14.66	4	22.96	2.31	
APEI 4					641 ± 109
Crustacea	30.11 ± 1.00	13	258.00 ± 113.55	27.41 ± 12.59	
Polychaeta	140.23 ± 83.06	3	24.34 ± 11.18	5.35 ± 1.56	
APEI 7					1621 ± 197
Crustacea	232.82 ± 33.65	18	692.69 ± 177.58	84.33 ± 16.83	
Mollusca	114.72 ± 25.19	5	2460.69 ± 691.14	900 ± 300	
Polychaeta	455.22 ± 70.00	16	124.29 ± 16.39	17.56 ± 2.19	
Other metazoan	611.72 ± 162.47	44	91.57 ± 21.40	24.20 ± 3.26	
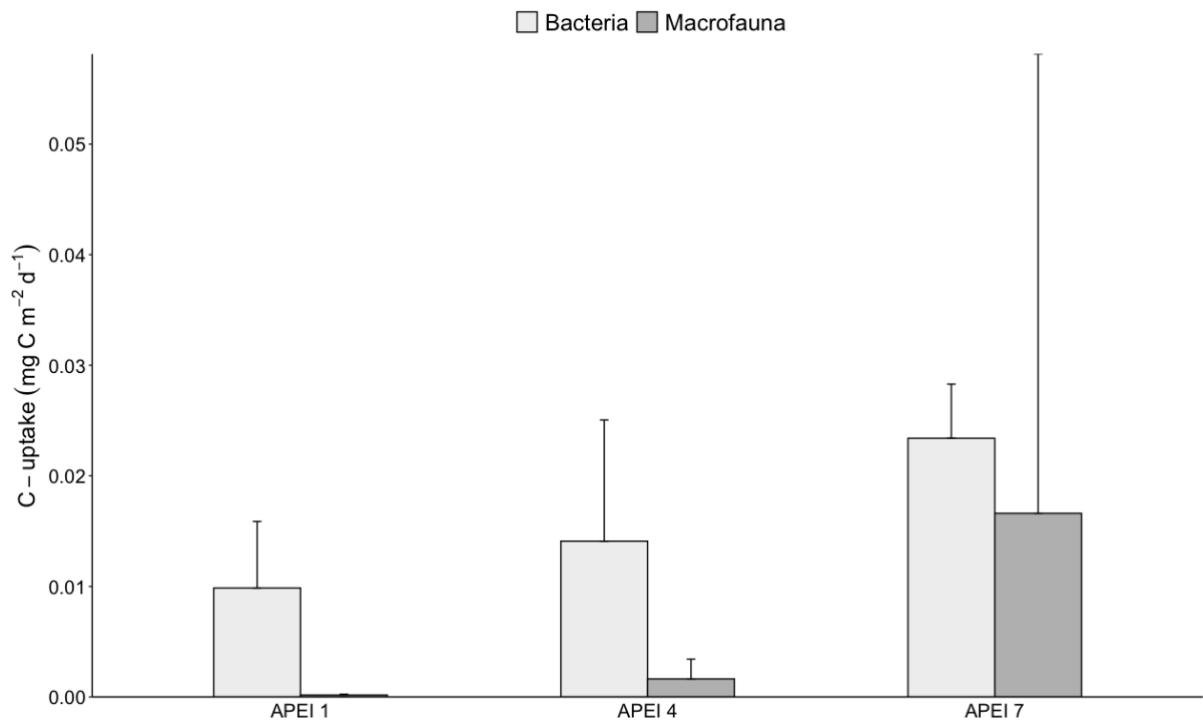
Figure 11: Mean macrofaunal and bacterial C-uptake observed in the three different APEIs of the western CCZ. Error bars denote ± SD.
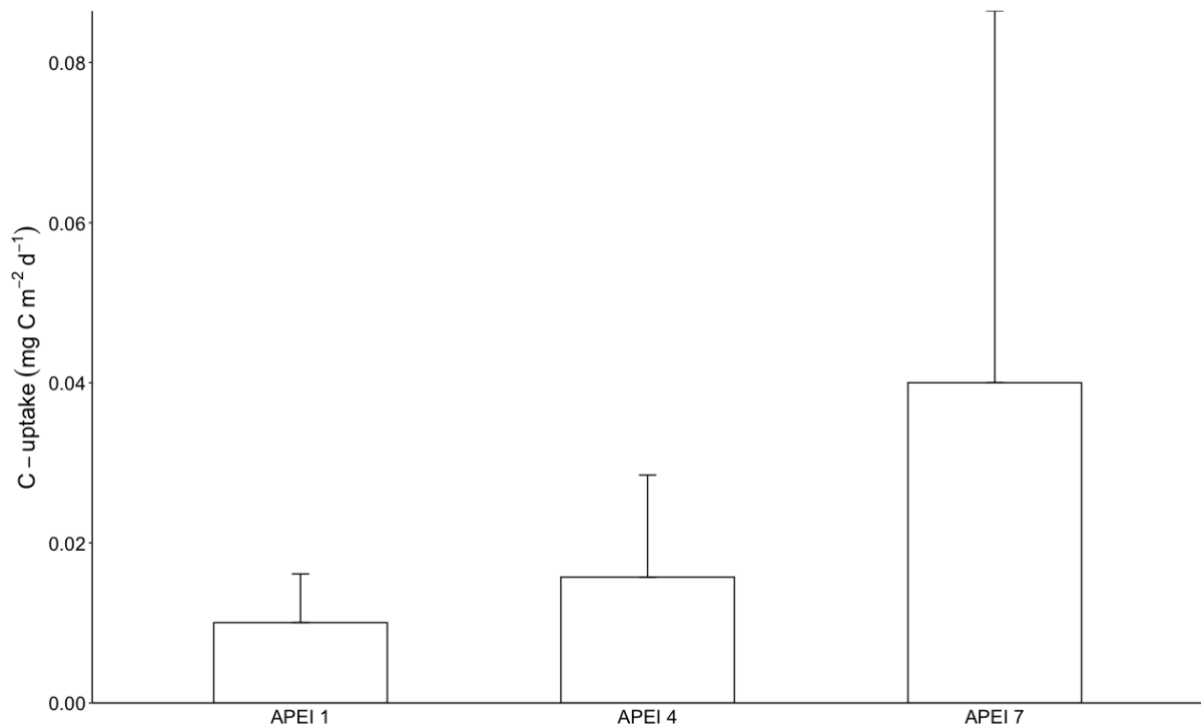
Figure 12: Mean total daily C-uptake (summed macrofauna and bacteria) rates across the western CCZ. Error bars denote ± SD.

4　Discussion

In this study, we conducted multiple in situ pulse chase experiments across 3 APEIs using a benthic chamber lander to document SCOC, DIC and nutrient flux rates and measure C flow through benthic macrofauna and bacteria. While the SCOC rates, macrofaunal abundances and biomasses, bacterial biomasses and C-uptake data were not significantly different across the three APEIs, which confirms our initial hypothesis, these parameters all showed a pattern of decreasing SCOC rates, macrofaunal abundances and biomasses, bacterial biomasses, and C-uptake from the more eutrophic (APEI 7) to the most oligotrophic study region (APEI 1).

4.1　Linkages between deep-sea benthos and surface productivity

While significant differences could not be detected across the APEI network studied, the patterns that we found in the western APEIs were consistent with other studies that have shown spatial changes in benthic community composition, structure and ecosystem function due to

changes in overlying surface productivity (Smith et al. 1996, 1997, 2008a; Berelson et al. 1997; Cosson et al. 1997; McClain et al. 2012). For example, long-term monitoring of POC fluxes at abyssal depths at Station M in the NE Pacific have repeatedly shown positive relationships between episodic POC flux pulse events and benthic respiration (Drazen et al. 1998; Smith et al. 2001, 2018). Increased POC flux to the seafloor around the equator in the central Pacific relative to the more oligotrophic gyre have also been seen in seafloor community oxygen consumption by Berelson et al. (1997). Moreover, further studies (Smith et al. 1997; Ruhl 2004; Johnson et al. 2007) have shown the importance of surface ocean production and deep ocean POC flux in explaining variations in sediment bioturbation (Smith and Rabouille 2002), microbial biomass, macrofaunal and megafaunal abundance in the equatorial Pacific Ocean (Smith et al. 1997, 2008a), and macrofaunal biomass and abundance at abyssal depths in the western North Atlantic (Johnson et al. 2007). Based on our data, it is possible that similar gradients exist in benthic respiration, nutrient fluxes, community structure and C-uptake across APEI 7, 4 and 1 but the limited data set and high variability in our data made these gradients difficult to detect in this study.

4.2 Abyssal macrofaunal abundance

Abyssal macrofaunal abundances measured using relatively small (approx. 0.05 m^2) benthic chambers are difficult to compare to abundances determined from much larger 0.25 m^2 box-core samples. While the macrofaunal abundances documented from the benthic chambers in APEI 7 and 4 were in the same order of magnitude as macrofaunal abundances (Fig. 9) determined by box-core sampling in DOMES site C and PRA of the CCZ (370-774 ind. m^{-2}) by Wilson (2017), the DOMES and PRA study did not include Nematoda and Copepoda (harpacticoids) in its analysis. The exclusion of these taxa from our macrofaunal abundances would yield abundances of 90 ± 32, 117 ± 68 and 625 ± 98 ind. m^{-2} for APEI 1, 4 and 7,

respectively, which is on average 34% lower than the abundances recorded by Wilson (2017). Another study located in the Global Sea Mineral Resources (GSR) license area on the eastern CCZ which also excluded meiofauna found similar abundances to APEI 4, 199 ± 15, 202 ± 22 and 180 ± 30 ind. m^{-2} (De Smet et al. 2017). Also, the POC fluxes in the GSR area was more closely related to APEI 4 than the other two APEIs (1 and 7) surveyed in this study. Nevertheless, macrofaunal abundances (546 ± 51 ind. m^{-2} and 313 ± 64 ind. m^{-2}) from benthic chamber samples collected in the eastern CCZ that also included nematodes and harpacticoids (Sweetman et al. 2019) were comparatively similar to our data. The abundances documented in APEI 1 from the chambers were the lowest recorded in this study (Fig. 9), which most likely was related to the lower POC fluxes to the seafloor in this region as indicated by Washburn et al. (2021b). All the macrofaunal abundances measured during this study were significantly lower than those recorded by Sweetman and Witte (2008) from Station M ($6{,}165 \pm 3{,}751$ ind. m^{-2}) in the NE Pacific that used a similar benthic chamber system to sample the seafloor. However, it is likely that the deeper depths studied (0-10cm), and the inclusion of large numbers of macrofaunal-sized nematodes that contributed 60% of the macrofaunal community in the Sweetman and Witte (2008) study all contributed to this difference since abundances reduced to 228 ± 32, 351 ± 129 and 858 ± 100 ind. m^{-2} for APEI 1, 4 and 7, respectively, when nematodes were excluded. The Sweetman and Witte (2008) study site was also much more eutrophic compared to the CCZ sites studied here.

4.3   Benthic biomass

As stated before, while we did not find a significant change in benthic biomass between the southernmost and northernmost APEIs, we observed a pattern showing a northward decrease in mean biomass that was likely related to declining surface ocean productivity (Smith et al. 2008a). However, the combined biomass of macrofauna and bacteria in the sediments from

APEI 1, 4 and 7 (14.56 ± 7.79 mg C m^{-2}) was lower than the mean total benthic (macrofauna and bacteria) biomass measured in the Sweetman et al. (2019) (461 mg C m^{-2}) in the eastern CCZ despite the Sweetman et al. (2019) being situated in an apparently less productive region (Washburn et al. 2021b; a). Bacterial C-uptake rates at APEI 7 were also two orders of magnitude lower than in the eastern CCZ despite the lander deployment times being identical (36 h). It is unlikely that the significantly lower total benthic biomass and bacterial C-uptake rates in the APEIs compared to the eastern CCZ was due to experimental artefacts associated with the lander (e.g., bow-wave effects blowing surface sediments away). Bacterial biomasses measured between 0-5 cm sediment depth using push cores collected by the ROV 'Luukai' during the same cruise were approx. 4 mg C m^{-2}, which is almost identical to the bacterial biomasses measured from the benthic chamber lander samples. Extremely low bacterial abundances (and by inference, biomass) were found in the south Pacific Gyre by D'Hondt et al. (2009). These authors documented bacterial abundances of approximately 30,000 cells cm^{-3} which is equivalent to a bacterial biomass of 0.02 mg C m^{-2} (assuming a bacterial cell contains 12 fg C [Fukuda et al. 1998] and a constant bacterial abundance between 0 and 5 cm sediment depth). The results from this study, therefore, suggest that the APEIs located in the western CCZ may instead be sites of extremely low bacterial biomass and represent the low biomass sites for the wider CCZ region.

4.4 *Dissolved inorganic carbon fluxes as a response to the addition of labelled material*

The only other directly comparable in situ abyssal experiment that documents C-transfer into the DIC pool, macrofauna and bacteria and which did not include megafauna (Stratmann et al. 2018a; c), was conducted at the Porcupine Abyssal Plain by Witte et al. (2003). These authors found a respiration of 4 mg C m^{-2} d^{-1}, which is substantially higher than our study (0.5 to 0.75 mg C m^{-2} d^{-1}). The percentage of introduced organic C going into the DIC pool was dominant

at both sites (70% of the C went into the DIC pool at PAP vs. 96% in the western CCZ) which suggests, as with all detritus-based ecosystems, that the western CCZ sites are respiration-dominated ecosystems as has also been suggested for the abyssal eastern Mediterranean and bathyal NE Atlantic (Woulds et al. 2009). The higher DIC flux rate in the (Witte et al. 2003b) study could partly be explained by the higher POC fluxes at the PAP, as well as the higher biomass of microbes (2.5 g C m^{-2}) and macrofauna (120 mg C m^{-2}) compared to the more oligotrophic western CCZ (microbial biomass: 7.39 mg C m^{-2}; macrofaunal biomass: 7.18 mg C m^{-2}). Furthermore, the different response could also be a function of the amount of C injected at the seafloor. The PAP study simulated a POC input event of 1 g C m^{-2}, which was equivalent to the yearly flux of POC to the PAP seafloor at 4800 m. However, we introduced the equivalent of 0.2 g C m^{-2} which was approximately 20% of the annual flux to the seafloor in the CCZ, which could explain our labelled DIC flux rates being between 13-19% that of the DIC fluxes measured in the abyssal NE Atlantic. In the more eutrophic SE Pacific, Stratmann et al. (2018c) found respiration rates measured using ROV-operated benthic chambers after an algal-addition equivalent to 0.48 mg C m^{-2} were within the same order of magnitude (11.31 mg C m^{-2} d^{-1}) as at the PAP, and significantly higher than in the western CCZ. Again, the higher rate was potentially caused by the greater C addition as well as the inclusion of large holothurian megafauna in their benthic chambers that processed significant amounts of introduced organic material. While the study sites from the western CCZ seemed to function differently to the PAP in terms of the total amount of C cycled, the phytodetritus turnover rate was similar between the western APEIs and PAP. Assuming a respiratory quotient between O_2 and CO_2 of 1 (Middelburg et al. 2005), the mean C-degradation rate in our experiments was 0.76 mg C m^{-2} d^{-1} after correcting for the background SCOC rate. Therefore, assuming that the degradation rate in the algal-addition chambers was exclusively due to the added phytodetritus (200 mg C m^{-2}), the added tracer had a turnover rate of 0.0038 d^{-1}, which compares well to

turnover rates for labile phytodetritus at the seafloor in the PAP (0.0048 d^{-1}). However, our turnover rate is lower than in the eastern CCZ at 0.012 d^{-1} (Sweetman et al. 2019) and the model by Snelgrove et al. (2018) on global carbon cycling at 0.02-0.05 d^{-1}.

4.5   Sediment community oxygen consumption rates

Although DIC flux rates at our sites were 10-20% of the rates seen in the eutrophic NE Atlantic, SCOC rates from the western CCZ (range: mean of 3.74 ± 1.86 mg C m^{-2} d^{-1} and 5.22 ± 0.92 mg C m^{-2} d^{-1}) showed more similarity to the eutrophic abyssal NE Atlantic (4.49 mg C m^{-2} d^{-1}, Witte et al. 2003) than the NE Pacific (12.1 mg C m^{-2} d^{-1}, Smith et al. 2018). Interestingly, the rates we recorded in the western CCZ were ~2X higher than background SCOC rates measured on the eastern side of the CCZ in the UK1 and OMS (2.24 mg C m^{-2} d^{-1}, Sweetman et al. 2019). The study sites of Sweetman et al. (2019) were situated in a less productive region compared to the APEI 7 study sites (Washburn et al. 2021a; b), which could provide one explanation for this difference. The lower benthic biomass and total C-uptake rates in the western CCZ combined with relatively high SCOC rates suggest the heterotrophic community was either actively consuming other OM sources in the sediments and/or other benthic groups (e.g., Archaea) were consuming oxygen though not necessarily remineralizing organic material. Bacterial chemoautotrophy has been shown to be an important C-cycling process in sediments in the SE Pacific (Vonnahme et al. 2020) and Mediterranean Sea (Molari et al. 2013). Sweetman et al. (2019) also documented abyssal benthic bacteria are capable of fixing significant quantities of inorganic C into biomass possibly via chemoautotrophic pathways, which could lead to oxygen being consumed at the seafloor. If chemoautotrophy did in fact contribute to the SCOC rates measured in this study, the positive efflux of ammonium out of the sediment in many of the study sites (e.g., APEIs 1 and 7) would suggest that electron donors other than ammonium were being used. Further studies should be directed at resolving this.

4.6   Community response to the introduction of labelled material

As already observed by Sweetman et al. (2019) from the eastern CCZ as well as other studies that have incubated deep-sea sediments in the laboratory (Rowe and Deming 1985; Lochte and Turley 1988; Boetius and Lochte 1996; Kanzog et al. 2009; Hoffmann et al. 2017), the dominance of the microbial community in cycling organic matter in this study (especially in APEIs 4 and 1) highlights the importance of microbial communities in benthic ecosystem functioning in the abyssal ocean. This contrasts with Witte et al. (2003) who found a dominance by macrofauna in cycling organic matter over the short-term, which could have been due to the shorter duration of the APEI experiments (36 h) compared to those of Witte et al. (2003) (2.5 d). Upper bathyal depth experiments have shown macrofaunal dominating benthic C-cycling dynamics over longer-term time scales (3d), with bacteria dominating on shorter-term timescales (1.5d) (Witte et al. 2003b). Differences in benthic community structure could explain the lower macrobenthic response to phytodetritus in our study compared to at the PAP. At our study sites, total macrofaunal biomass was lower (7.18 ± 5.98 mg C m-2) and known surface deposit-feeding fauna (e.g., cirratulids, spionids, terebellids) contributed little to macrofaunal abundance (13% of polychaetes) and a negligible amount to C assimilation (Table 3). In contrast to this, at the PAP, benthic biomass was much greater (total biomass: ~ 2.6 g C m^{-2}) and surface-feeding cirratulid and spionid polychaetes were highly abundant contributing 50% of all polychaetes and 57% of polychaete biomass (Aberle and Witte 2003; Witte et al. 2003b). They were also important in cycling organic material that was introduced to the seafloor (Aberle and Witte 2003; Witte et al. 2003b). The smaller amounts of phytodetritus added to sediments in our study may have also played a role as modelling studies of abyssal benthic C cycling have revealed that the contribution of bacteria to total benthic C cycling increases under low POC flux relative to high POC flux conditions (Dunlop et al. 2016). Here, bacteria have been seen to outcompete macrofauna for organic substrates at low concentrations

(van Nugteren et al. 2009). While the bacteria were key players in the short-term cycling of C at the seafloor in the eastern and western CCZ, total (i.e., summed bacteria and macrofauna) C-uptake was much greater in the eastern CCZ than in the western APEIs (Fig. 13) despite the eastern CCZ being apparently more oligotrophic (Washburn et al. 2021a; b). Nevertheless, macrofauna in the western CCZ processed more C per unit area per unit time than metazoan macrofauna in the eastern CCZ (Sweetman et al. 2019) when rates were normalized to metazoan macrofaunal biomass (0.003 mg C m^{-2} d^{-1} and 0.5 x 10^{-5} mg C m^{-2} d^{-1} for the western and eastern CCZ, respectively), suggesting that even though the total (i.e., summed bacteria and macrofauna) C-uptake was lower in this study than in Sweetman et al. (2019), and macrofaunal community biomass in the western CCZ was an order of magnitude lower than in the eastern CCZ, western CCZ macrofauna were better able to exploit the fresh organic material when it was supplied to the sediment.
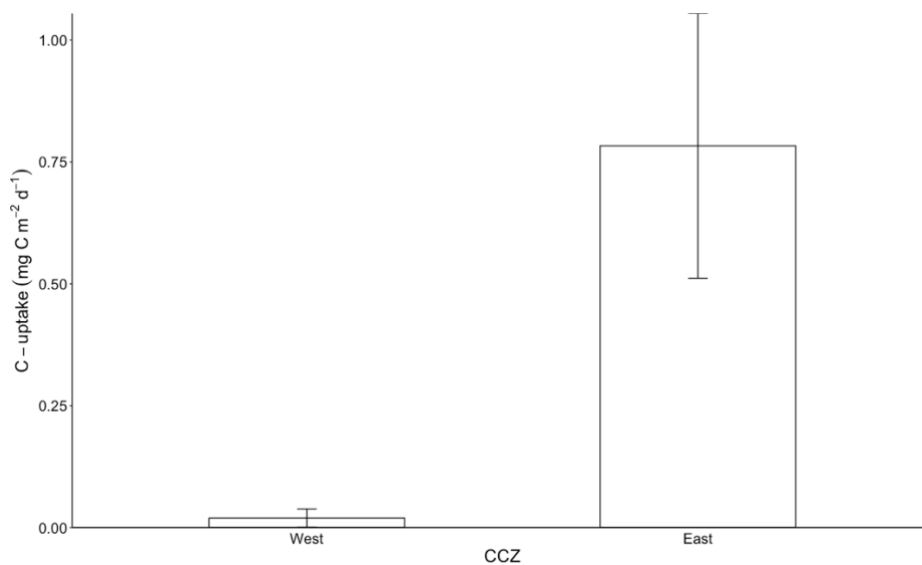
Figure 13: Mean total (summed macrofauna and bacteria) C-uptake rates between the eastern (Sweetman et al. 2019) and the three APEIs in the western CCZ. Mean total C-uptake measurements for the individual APEIs in the western CCZ are reported in Fig. 12. Error bars denote ± SD.

5 Conclusions

Our findings show variable benthic ecosystem structure and function across the western APEI network as well as variability between western and eastern regions of the CCZ. Our results suggest that POC flux is an important driver affecting benthic community structure (e.g., total biomass) and very possibly benthic C-turnover, though more studies are needed to confirm this in this region of the Pacific. Nevertheless, based on the data collected at this time we recommend that POC flux be considered a major environmental factor driving ecosystem dynamics in the CCZ and support its use in future marine spatial planning studies. Our data confirms that the benthos in the western APEI network are respiration-dominated systems, and thus share attributes with other deep-sea regions such as in the North Atlantic and Mediterranean Sea. Our results also confirm that bacteria are key players in the short-term processing of organic material at the seafloor in APEIs 1, 4, and 7 as has been shown in the eastern CCZ. Overall, our data emphasize the clear need for baseline studies assessing benthic ecosystem function within the APEI network in the CCZ in order to better understand the implications of deep-sea mining and the effectiveness of the APEIs in protecting the full range of ecosystem characteristics of these deep-sea environments.

CHAPTER 3

BENTHIC ECOSYSTEM RESPONSE TO FRESH PHYTODETRITAL INPUT ALONG A SUB-POLAR

ANTARCTIC BATHYAL FJORD AND THE BATHYAL CONTINENTAL SHELF OF THE WEST

ANTARCTIC PENINSULA

Abstract

Glaciomarine fjords dominate the coastal margins of the West Antarctic Peninsula (WAP) and in contrast to extensive studies in the Arctic, benthic ecosystem functioning in subpolar Antarctic fjords remain largely understudied. Currently, benthic ecosystem functioning in the inner and middle basins of Arctic fjord tend to be heavily affected by meltwater and sedimentation inputs due to climate warming while Antarctic fjord are characterized by biodiversity hotspots sites. Here, pulse-chase experiments were conducted along Andvord Bay, Gerlache Strait and the continental shelf in the WAP to observe how benthic metabolism and C-cycling activity change along the different basins of the fjord and the continental shelf under different organic matter inputs. Contrary to the Arctic counterparts, the inner parts of Andvord Bay showed significantly higher seafloor respiration, benthic abundances, biomass and dissolved inorganic carbon production. Interestingly, the macrofauna community was responsible for most of the C-uptake in the inner parts of the fjord (>45%) while the fjord mouth to the continental shelf appeared to predominantly release carbon through respiration (>80%). The inner parts of Andvord Bay appear to be hotspots for benthic C-cycling and metabolism; however, climate change will likely alter this pattern by changing the availability of labile detritus and POC flux in the region.

1 Introduction

Fjords are deep coastal inlets excavated by glaciers (Syvitski et al. 1987; Howe et al. 2010) and, at high latitudes, they are widely recognized as critical sites for observing sediment deposition from past climatic conditions (Cottier et al. 2010) and high biomass, biodiversity and primary and secondary production (Nowacek et al. 2011; Grange and Smith 2013; Grange et al. 2017; Ziegler et al. 2017). In the Arctic, elevated levels of warming have led to the transition of many marine-terminating glaciers to land-terminating glaciers. As such, ecosystem structure and function has become heavily influenced by meltwater and turbidity plumes leading to reduced primary and secondary productivity in the water column (Hop et al. 2002; Powell and Domack 2002; Al-Habahbeh et al. 2020; Morata et al. 2020). Predicted loss of glaciers over time associated with climate warming may lead to increased Arctic fjord productivity, biomass and biodiversity (Kedra et al. 2010; Parkinson and Cavalieri 2012). In contrast, some subpolar Antarctic fjords are characterized by "hotspots" of biological production, with krill densities of 2000 animals m^{-3} (Nowacek et al. 2011; Grange et al. 2017), which is thought to result from a combination of limited local wind forcing (due to fjord topography) and weak meltwater influences, enhancing water-column stratification, light penetration, phytoplankton production (PP) and detrital fluxes (Griffith and Anderson 1989; Nowacek et al. 2011; Grange and Smith 2013; Grange et al. 2017).

Along the full extent of the Western Antarctic Peninsula (WAP), coastal margins tend to be dominated by glaciomarine fjords (with marine-terminating glaciers) and these represent a major corridor for the transfer of glacial ice to the ocean (Grange and Smith 2013). While many marine-terminating glaciers along the WAP are characterized as hotspots of biological production and biodiversity, the WAP has been exposed to significant environmental change over the last 100 years (Hendry et al. 2018). Temperature has increased steadily during this time (e.g. approx. 1°C increase in sea-surface temperature since the 1950s, (Vaughan et al.

2001; Cook et al. 2005; Meredith and King 2005), and now the peninsula is recognized as the fastest warming region on the planet (Kerr et al. 2018). This temperature increase has significantly impacted the local marine environment (Smith et al. 2012; Ziegler et al. 2017; Kerr et al. 2018), as well as changing the areal extent of ice-sheets and marine-terminating glaciers (Cook et al. 2016; Hendry et al. 2018). In fact, more than 87% of the glaciers have now retreated as a consequence of regional climatic warming that has increased surface and sub-surface temperatures and changed ocean circulation (Cook et al. 2005, 2016; Hendry et al. 2018).

Benthic ecosystems in Arctic fjords tend to show a gradient of increasing biodiversity from inner to outer fjord regions and continental shelf, as a result of less chronic burial disturbance from meltwater intrusion, and high labile organic matter concentrations in the sediment in outer fjord locations (Wlodarska-Kowalczuk et al. 2005; Renaud et al. 2007; Wesławski et al. 2011). While Antarctic subpolar fjord systems are starting to transition to the fjord landscape often seen in the Arctic, limited investigations along the WAP have revealed that benthic biodiversity and biomass in inner fjord locations can be greater compared to outer fjord regions and the adjacent continental shelf. Moreover, the seafloor of inner fjord locations tends to be characterized by much larger taxa as a result of the inner portion of fjords being subject to less sedimentation and chronic burial effects due to marine-terminating glaciers being at an earlier stage of warming compared to their Arctic counterparts (Grange and Smith 2013; Lundesgaard et al. 2020; Ziegler et al. 2020). However, despite the studies that have assessed the state of benthic biodiversity and biomass in glaciomarine fjords in the subpolar Antarctic (Glover et al. 2008; Grange and Smith 2013; Ducklow et al. 2018; Braeckman et al. 2021), very few studies have assessed how benthic metabolism and C-cycling dynamics change along the fjord to shelf continuum (Ziegler et al. 2020). Given that ecosystem function and structure in subpolar fjords along the WAP are predicted to show increasing similarities with Arctic fjord systems as time

progresses (Grange and Smith 2013), understanding current benthic ecosystem processes and environmental conditions will help in documenting the scale of ecosystem impacts we can expect in the future.

In this study, pulse chase experiments were carried out on sediment cores recovered from multiple sites in Andvord Bay, a subpolar Antarctic fjord situated along the WAP, as well Gerlache Strait immediately outside Andvord Bay and a continental shelf site, Station B. Cores were used to document benthic community structure and compare seafloor community oxygen consumption (SCOC) rates, nutrient fluxes and C-flow through the benthic macrofaunal and microbial community. We then compared these findings to observed Arctic fjord systems and discuss the negative implications of a rapidly warming environment for Antarctic subpolar fjord in the future. We specifically tested the hypotheses that: *No significant change spatial differences in SCOC, nutrient fluxes or bacterial and macrofaunal C-uptake rates within the fjord and between the fjord and the continental shelf.*

2 Methods

2.1 Study sites and experimental design

During the cruise NBP1603 on the RV '*Nathaniel B. Palmer*' in the fall of 2016 (April-May), a Bowers and Connolly megacorer was used to collect seafloor sediments from three study sites (inner, middle and outer basin) in Andvord Bay, Gerlache Strait (intermediate station between Andvord Bay and the continental shelf) and Station B located on the continental shelf on the Western Antarctic Peninsula (Fig. 14). Upon retrieval, sediment cores that would later be used for incubation experiments were immediately transferred from the 10 cm diameter megacore tubes to 10 cm diameter incubation core tubes (45 cm long). They were then sealed at the bottom with a rubber bung. All incubation core sediments (four per site) were then gently

covered with 25 cm of 5-μm filtered, oxygenated seawater. The cores were then placed in a water bath, aerated and incubated in an incubator at in-situ temperature (-1℃) for 24 h.
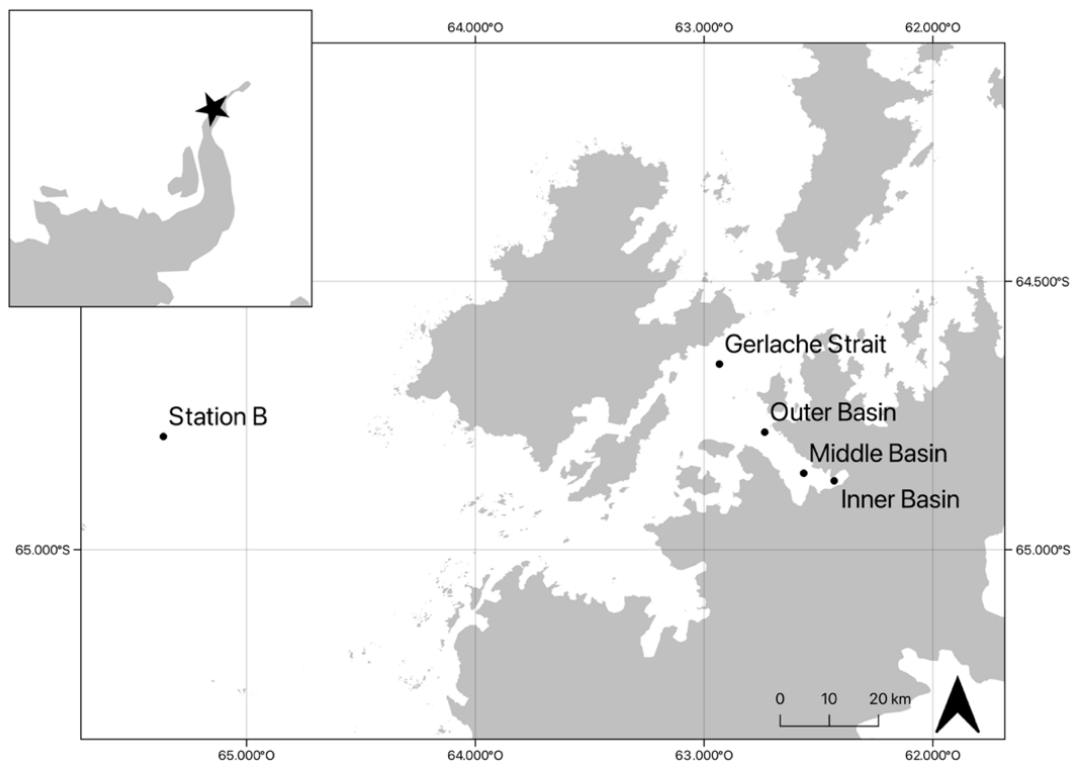
Figure 14: Study sites in Andvord Bay, Gerlache Strait and Station B on the continental shelf in the West Antarctic Peninsula.

2.2 *Labelled organic material preparation*

An axenic clone of the diatom *Phaeodactylum tricornutum* was used as a labelled food source in this experiment. Diatoms were cultured in artificial seawater modified with F/2 algal culture medium (Grasshoff et al. 1999) and labelled by replacing 50% of ^{12}C bicarbonate in the culture medium with $NaH^{13}CO_3$. The algae had an organic content of 18.6% and a ^{13}C content of 37.8 atom%. To harvest the algae, the cultures were concentrated by filtration over a 0.45-μm filter (cellulose acetate), washed five times by centrifugation with un-labelled F/2 medium to remove excess labelled bicarbonate, and freeze dried. The absence of microbes was verified by microscopic observations after staining some inoculum with Sybr Gold.

2.3   Shipboard experiments

Twenty-four hours after the cores were collected, water was exchanged with filtered fully oxygenated seawater (at the same in situ temperature) to remove toxic metabolites such as ammonium or sulphides produced in the chambers. Chamber waters were allowed to exchange and overflow each chamber into the surrounding water bath (that was periodically emptied), which maintained the independence of replicates. Because of the slow rate of water exchange, no sediment was resuspended during this procedure. A 50 ml sample of water was then collected from each chamber by syringe for dissolved inorganic carbon (DIC) concentration and ^{13}C isotope signatures and nutrient concentration analysis. The DIC samples were filtered with a 0.2-μm filter and preserved in 12 ml exetainers with 10 μl of 6% $HgCl_2$ for later analysis. Nutrient samples were filtered with a 0.2-μm filter into acid-washed 50 ml Falcon tubes and stored in a fridge before analysis on a shipboard autoanalyzer later the same day. A black 10 cm diameter core top and stirrer were then placed on top of the core tube making sure to not introduce air bubbles, and a previously calibrated (2-point calibration) robust oxygen probe (Pyroscience ®) was inserted into each core lid, which continuously logged O_2 conditions in the chambers. The stirrer mounted in the lid of each core tube was then turned on, which mixed the chamber water at 30 revolutions per minute (rpm) to create enough shear stress at the sediment-water interface to maintain a sufficiently thin diffusive boundary layer. The cores were then incubated for 24 h. Chamber water column O_2 concentrations never decreased more than 20% relative to the initial O_2 concentration throughout the 24 h incubations. After 24 h, the core tops were removed and another 50 ml syringe sample was collected for DIC (concentration and ^{13}C isotope signatures) and nutrient concentration analysis, before the overlying water was replaced as before with fully oxygenated filter seawater.

Then 45 mg of freeze-dried algae was added to each chamber, which was equivalent to 8.37 mg C m^{-2} or 15% of the annual POC flux (7.45 g C m^{-2} yr^{-1} [Smith et al. 2008]) and allowed to

settle on the sediment surface for 1 h as in previous experiments (Sweetman et al. 2014, 2016, 2019, Cecchetto et al. in review). After 1 h, a third 50 ml sample of water was then collected by syringe from each chamber for DIC (concentration and ^{13}C isotope signatures) and nutrient concentration analysis as before. The chamber was then sealed ensuring no air bubbles were present, and the cores were incubated with stirring for another 24 h while continuously logging the O_2 concentration in the overlying water. After 24 h, the lids were removed, and a fourth 50 ml sample of water was collected by syringe for DIC (concentration and ^{13}C isotope signatures) and nutrient concentration analysis. The chambers were then removed from the water bath, and the top water sieved through a 32-μm sieve before being added to a sample bottle.

2.4   Sample processing and analysis

To sample bacteria and macrofauna, sediment was extruded and sectioned into 0-2, 2-5, and 5-10 cm depth layers. During this procedure, some macrofauna were observed burrowing deeper into sediment layers. Thus, differences in ecosystem processes (e.g., C-uptake) as a function of sediment depth will not be addressed in this study. The extracted sediments were placed into a clean bowl and homogenized. Approximately 10 ml of sediment was removed and placed in Falcon tubes for bacterial phospholipid fatty acid (PLFA) analysis and subsequently frozen at -80°C. The remaining sediment from each layer was sieved on a 300-μm mesh with cold (0-1°C), filtered seawater to isolate macrofauna. The fauna was then transferred to the same plastic bottle as the 32-micron fraction (see above) and fixed with 4% buffered formaldehyde in seawater. DIC (concentration and ^{13}C isotope signatures) samples were analyzed on an Apollo SciTech AS-C3 and an elemental analyzer Flash 1112, THERMO Electron S.p.A.) coupled to an isotope ratio mass spectrometer (EA-IRMS, DELTA-V, THERMO Electron Corporation) as described by Maier et al. (2019).

2.4.1 Macrofaunal structure and C-uptake

Fixed macrofaunal samples were washed with artificial seawater in the laboratory over a 300-μm mesh sieve and picked under a microscope in artificial seawater. All fauna were identified to order or major taxa, except for polychaetes, which were identified to family. Organisms were pooled into either the same polychaete family, crustacean order, or major taxon to measure biomass. Calcareous organisms were placed into silver (Ag) caps while all other organisms were placed into tin (Sn) caps for biomass measurements. All organisms were dried at 35-40°C for a maximum of 7 days and all calcareous organisms were decalcified using two rounds of acidification as in Sweetman et al. (2009). To do this, 20 µl MilliQ water was initially added to each silver cup followed by 40 µl of 0.5 M HCl and subsequently dried at 50°C for 48 h. After this, a further 20 µl MilliQ water was added followed by 40 µl of 2 M HCl and then the caps were dried again at 50°C for 48 h to remove any residual calcareous material. Some samples were then combined to meet UC Davis Stable Isotope Facility biomass requirements for C-isotopic analysis.

Macrofaunal specific ^{13}C uptake, expressed as $\Delta^{13}C$ (‰) was calculated as the difference between the $\delta^{13}C_{enriched\ sample}$ and $\delta^{13}C_{background}$ values of closely-related taxa. Uptake of ^{13}C was calculated as the product of excess of atom% ^{13}C (enriched - background) and C content of the enriched sample expressed as a unit weight: ^{13}C uptake (unit wt C) = (atom% $^{13}C_{samples}$ – atom% $^{13}C_{background}$) x (unit wt C of organism). This was then adjusted to total C uptake by taking into account the ^{13}C algal labeling: C uptake = ^{13}C uptake / 37.8 atom%. Background macrofaunal isotope ($\delta^{13}C_{background}$) signatures were extrapolated from Pasotti et al. (2015).

2.4.2 Bacterial phospholipid fatty acid analysis and C-uptake

Sediment samples for bacterial specific PLFA analysis were sent to the James Hutton Institute in Aberdeen, UK. The method for PLFA extraction and derivatization to fatty acids methyl

esters (FAMEs) is described by Shahbaz et al. (2020). Individual FAMEs quantification and their isotopic composition and concentration was determined using a GC Trace Ultra with combustion column attached via a GC Combustion III to a Delta V Advantage isotope ratio mass spectrometer (all Thermo Finniga, Bremen, Germany) as described by Thornton et al. (2011).

Bacterial biomass was calculated from the weighted-average PLFA ($iC_{14:0}$; $iC_{15:0}$; $aiC_{15:0}$; $iC_{16:0}$; $C_{16:1w5c}$; $iC_{17:0}$; $aiC_{17:0}$; $C_{17:1w8c}$; $C_{17:1w7c}$; $C_{17:0}$; $C_{18:1w7}$; cyclo $C_{19:0}$) concentration (μmol) mL^{-1} sediment/ (a x b), where a is the average PLFA concentration in bacteria (0.056 g C PLFA g^{-1} biomass after Brinch-Iversen and King 1990), and b is the average fraction-specific bacterial PLFA encountered in sediment dominated by bacteria (0.584; calculated after Rajendran et al. 1993, 1994). The prefixes ´i´ and ´ai´ refer to ´iso´ and ´antiso´, respectively. Total bacterial assimilation (mg ^{13}C m^{-2}) of ^{13}C was calculated from label incorporation into the bacterial fatty acids ($iC_{14:0}$; $iC_{15:0}$; $aiC_{15:0}$; $iC_{16:0}$; $C_{16:1w5c}$; $iC_{17:0}$; $aiC_{17:0}$; $C_{17:1w8c}$; $C_{17:1w7c}$; $C_{17:0}$; $C_{18:1w7}$; cyclo $C_{19:0}$) following the methods of Sweetman et al. (2010, 2014, 2016, 2019) using an average fraction-specific bacterial PLFA encountered in sediment dominated by bacteria (0.584; calculated after Rajendran et al. 1993, 1994). The ^{13}C assimilation values (mg ^{13}C m^{-2}) for bacteria were then converted to daily C assimilation rates (mg C m^{-2} d^{-1}) by accounting for the fractional abundance of ^{13}C in the added algae as: C assimilation = ^{13}C incorporated (mg ^{13}C m^{-2})/ fractional abundance of ^{13}C in algae (37.8%).

2.5 Data analysis

The software R was used to carry out all statistical data analysis. Before carrying out any analysis, datasets were checked for normality and heteroscedasticity, and a logarithmic transformation was applied when necessary to make data sets satisfy parametric assumptions. Differences in SCOC (factor 1: before vs. after agal addition), nutrient flux rates (factor 1:

before vs. after agal addition), C-uptake rates and biomasses (factor 1: macrofauna vs. bacteria) as a function of site (factor 2) were tested using a Two-Way ANOVA test. Significant differences in SCOC, macrofaunal abundance, DIC fluxes, total biomass and C-uptake) across the different study sites were analyzed using One-Way ANOVA tests. If transformations failed, non-parametric a Scheirer-Ray-Hare test and Kruskal-Wallis test followed for two factor and one factor analysis, respectively. Post-hoc tests are reported on the graphs. The criterion for statistical significance was an alpha level of 0.05.

3 Results

3.1 Sediment Community Oxygen Consumption (SCOC) rates

Mean SCOC rates ranged between 29.35 ± 4.61 mg C m^{-2} d^{-1} (Station B [$n = 4$, SD]), to 65.22 ± 9.46 mg C m^{-2} d^{-1} (Inner Basin [$n = 4$, SD]) during the initial 24 h incubation across all study sites, and between 34.03 ± 7.20 mg C m^{-2} d^{-1} (Station B [$n = 4$, SD]) to 72.59 ± 4.69 mg C m^{-2} d^{-1} (Gerlache Strait, $n = 4$, SD) during the algal-amended incubation (Fig. 15).

Statistical analysis of the interaction between sites and the different experiment conditions revealed significant differences ($p = 0.003$, Two-Way ANOVA); in particular, the background SCOC rates in the Inner and the Outer Basins were significantly different as well as background rates at Station B versus rates in the Inner Basin, Middle Basin and Gerlache Strait (Fig. 15). Significant differences between the non-algal and algal amended incubations were revealed at Gerlache Strait where SCOC rates increased from 50.07 ± 4.39 mg C m^{-2} d^{-1} ($n = 4$, SD) to 72.59 ± 4.69 mg C m^{-2} d^{-1} ($n = 4$, SD), respectively, and at the Outer Basin where SCOC increased from 37.50 ± 11.02 mg C m^{-2} d^{-1} ($n = 3$, SD) to 69.19 ± 5.38 mg C m^{-2} d^{-1} ($n = 3$, SD) (Fig. 15).
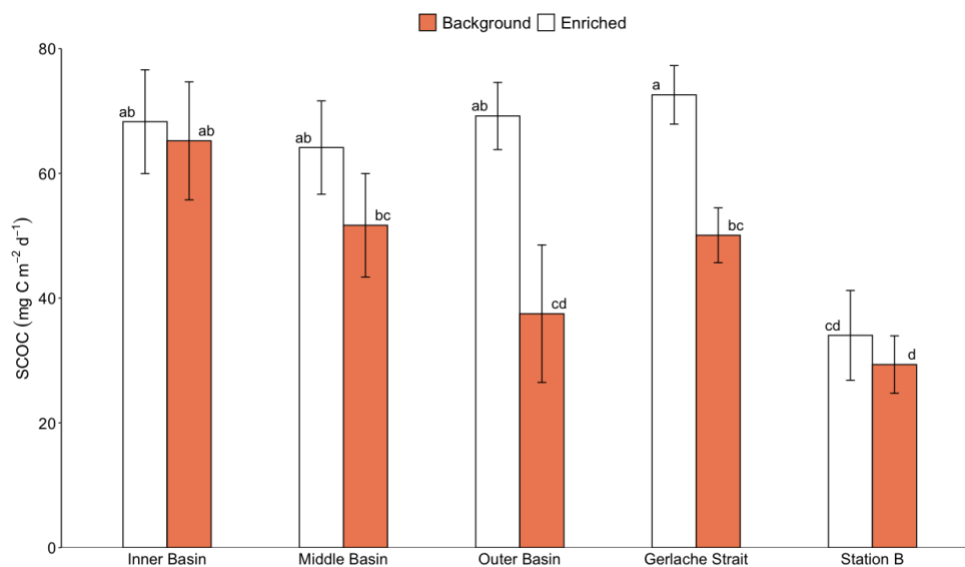
Figure 15: Mean SCOC rates in Andvord Bay, Gerlache Strait and Station B for background (white) and enriched (lines) conditions. Two-Way ANOVA was carried out with treatments (Background and Enriched) and Station as factors. Significant differences ($p < 0.05$) between sites and treatments are designated by different letters. Error bars denote $\pm$ SD.

3.2   Nutrient Fluxes

Background phosphate fluxes ranged between 3.23 ± 9.01 µmol m^{-2} d^{-1} ($n = 4$, SD) in Gerlache Strait to 43.69 ± 21.18 µmol m^{-2} d^{-1} ($n = 4$, SD) in the Inner Basin of Andvord Bay. Here, positive numbers denote effluxes from the sediments while negative number denote influxes into the sediments. Andvord Bay exhibited the highest background phosphate fluxes amongst the study sites (Fig. 16A). The phosphate fluxes in the algal amended incubations were significantly different to background conditions at all sites ($p = 0.04$, Two-Way ANOVA) and ranged from 92.02 ± 15.98 µmol m^{-2} d^{-1} ($n = 4$, SD) in the Middle Basin to 218.05 ± 56.94 µmol m^{-2} d^{-1} ($n = 4$, SD) in the Inner Basin.

Background silicate fluxes ranged from $1{,}610.83 \pm 415.42$ µmol m^{-2} d^{-1} ($n = 4$, SD) in the Middle Basin to $3{,}379.44 \pm 253.26$ µmol m^{-2} d^{-1} ($n = 4$, SD) at Station B. Enriched fluxes varied from $1{,}142.86 \pm 273.95$ µmol m^{-2} d^{-1} ($n = 4$, SD) to $3{,}698.06 \pm 290.70$ µmol m^{-2} d^{-1} ($n = 4$, SD) in the Middle Basin and Station B, respectively. Enriched and background silicate fluxes were

63

significantly different among stations ($p = 0.001$, Two-Way ANOVA) and differences can be found in Fig. 16B. Only at the inner station were fluxes significantly greater in the algal incubation versus the background experiment (Fig. 16B).

Background ammonium fluxes ranged between -75.62 ± 47.23 µmol m^{-2} d^{-1} ($n = 4$, SD) at Station B to 136.25 ± 117.74 µmol m^{-2} d^{-1} ($n = 4$, SD) in the Inner Basin of Andvord Bay. Gerlache Strait (5.23 ± 30.76 µmol m^{-2} d^{-1} [$n = 4$, SD]) along with the Inner Basin were the only two sites showing an efflux of ammonium for the non-algal amended incubations (Fig. 16C). Enriched incubations showed an increase in ammonium fluxes in all sites, except for the outer basin which exhibited similar values for the non-algal and algal amended incubations (-50.84 ± 26.12 and -50.47 ± 32.69 µmol m^{-2} d^{-1} [$n = 3$, SD], respectively). Enriched algal amended ammonium fluxes ranged between -50.47 ± 32.69 µmol m^{-2} d^{-1} ($n = 3$, SD) in the Outer Basin to 233.93 ± 175.75 µmol m^{-2} d^{-1} ($n = 4$, SD) in the Inner Basin of Andvord Bay. Statistical analysis revealed no significant difference between enriched and background experiments, nor between the different stations.

Background nitrite fluxes varied from -18.36 ± 8.71 µmol m^{-2} d^{-1} ($n = 4$, SD) in Gerlache Strait to 2.68 ± 3.04 µmol m^{-2} d^{-1} ($n = 4$, SD) at Station B on the continental shelf (Fig. 16D). Station B along with the Outer Basin site in Andvord Bay (2.01 ± 0.92 µmol m^{-2} d^{-1} [$n = 4$, SD]) were the only two sites that exhibited positive nitrite efflux in the background incubations. Two factor statistical analysis between stations and treatments revealed significant differences in nitrite fluxes ($p = 0.0001$, Two-Way ANOVA). Enriched nitrite fluxes ranged between -45.81 ± 22.46 µmol m^{-2} d^{-1} ($n = 4$, SD) in the Inner Basin to 21.64 ± 16.98 µmol m^{-2} d^{-1} ($n = 4$, SD) in the Middle Basin in Andvord Bay. The Middle Basin site showed a significant difference between the two experimental treatments (Fig. 16D), which was not the case for the Inner or Outer Basin.

Background nitrate fluxes ranged between -236.07 ± 80.65 µmol m^{-2} d^{-1} (n = 4, SD) in the Inner Basin to 148.46 ± 8.12 µmol m^{-2} d^{-1} (n = 4, SD) at Station B on the continental shelf. Station B and the Middle Basin sites (90.88 ± 56.79 µmol m^{-2} d^{-1} [n = 4, SD]) were the only stations showing positive efflux of nitrate (Fig. 16E). Enriched nitrate fluxes ranged between -139.50 ± 42.08 µmol m^{-2} d^{-1} (n = 4, SD) in the Middle Basin site in Andvord Bay to 124.53 ± 51.74 µmol m^{-2} d^{-1} (n = 4, SD) at Station B. Here, all sites exhibited negative influx of nitrate except Station B. Nitrate fluxes differed significantly among stations and between treatments ($p < 0.001$, Two-Way ANOVA). Fig. 16 presents post-hoc test results for all nutrient fluxes.
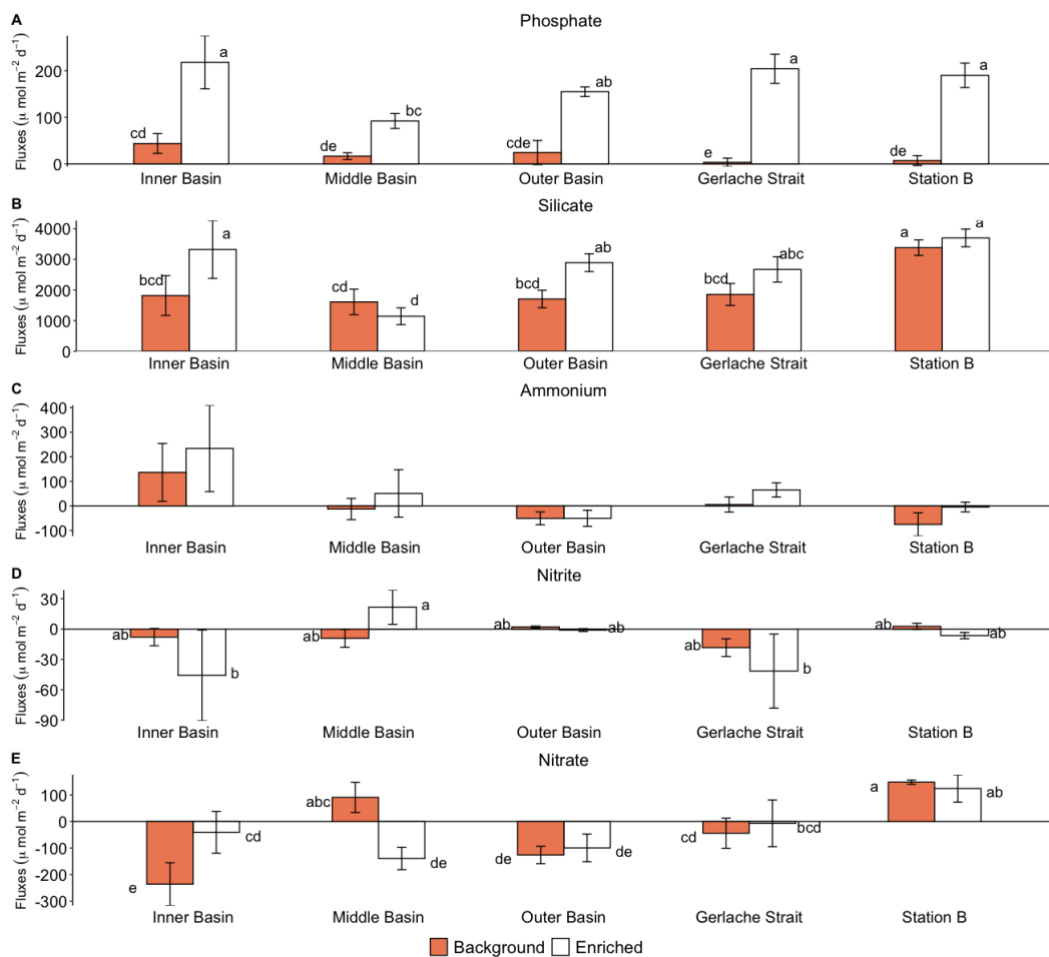

Figure 16: Phosphate (A), silicate (B), ammonium (C), nitrite (D) and nitrate (E) fluxes along Andvord Bay, Gerlache Strait and Station B. Two-Way ANOVA was carried out with treatments (Background and Enriched) and station as factors. Significant differences ($p < 0.05$) between sites and treatments are designated by different letters. Error bars denote ± SD.

3.3 Dissolved Inorganic Carbon (DIC)

Remineralisation rates of algal C to DIC decreased along the fjord from the inner to outer basin from 8.24 ± 0.76 mg C m^{-2} d^{-1} ($n = 4$, SD) in the inner part, to 6.63 ± 1.30 mg C m^{-2} d^{-1} ($n = 4$, SD) in the middle and finally to 4.88 ± 0.52 mg C m^{-2} d^{-1} ($n = 3$, SD) in the outer basin of the fjord (Fig. 17). The site in Gerlache Strait remineralised more algal C to DIC per unit time (10.01 ± 1.92 mg C m^{-2} d^{-1} [$n = 4$, SD]) than any station and DIC production was significantly different here compared to the other stations within the fjord (Middle and Outer Basin) and on the continental shelf ($p < 0.001$, One-Way ANOVA). The DIC productions rates in the Inner Basin were significantly higher than for the Outer Basin site (Fig. 17).
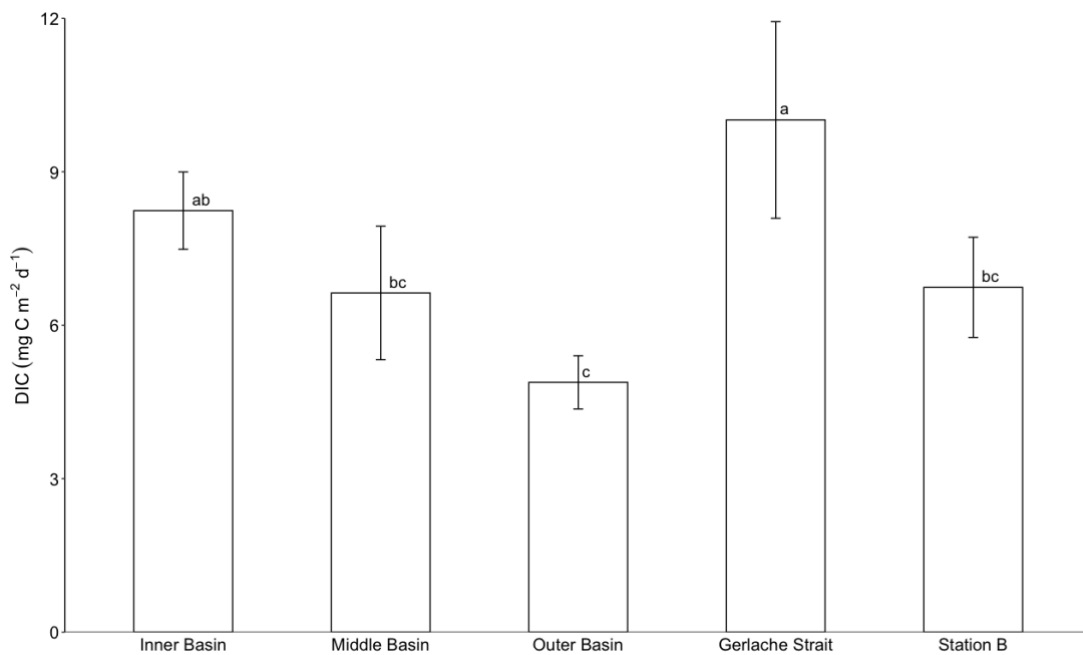
Figure 17: Mean DIC production rates from all study sites on the WAP. One-Way ANOVA tested significant differences ($p < 0.05$) between stations and differences are designated by different letters. Error bars denote $\pm$ SD.

3.4 Benthic community structure

The highest total macrofaunal abundance was found in Gerlache Strait ($69,710 \pm 19,386$ ind. m^{-2} [$n = 4$, SD]) and the lowest at Station B ($6,425 \pm 1,058$ ind. m^{-2} [$n = 4$, SD]) (Fig. 18).

Macrofaunal abundance within the fjord varied from 35,432 ± 6,662 ind. m^{-2} ($n = 4$, SD) in the Inner Basin, to 41,567 ± 8,917 ind. m^{-2} ($n = 4$, SD) in the Middle Basin and 28,736 ± 4,902 ind. m^{-2} ($n = 3$, SD) in the Outer Basin (Fig. 18). Removal of macrofaunal-sized nematodes reduced macrofaunal abundance considerably at all sites especially at Gerlache Strait (Fig. 18). Macrofaunal abundance (exc. Nematoda) at Gerlache Strait was 53% lower than the total abundance with nematodes (32,615 ± 7,874 ind. m^{-2} [$n = 4$, SD]) (Fig. 18). The highest macrofaunal abundance (exc. Nematoda) was the Middle Basin (34,133 ± 7,685 ind. m^{-2} [$n = 4$, SD]) and the lowest abundance was again found Station B (4,659 ± 407 ind. m^{-2} [$n = 4$, SD]). All macrofaunal abundances calculated with and without Nematoda were significantly different among sites ($p < 0.001$ and $p < 0.001$, respectively) (Fig. 18). Macrofaunal abundance in the fjord and at Gerlache Strait (with and without nematodes) were significantly higher than at Station B (Fig. 18).

Figure 18: Mean macrofaunal abundance across Andvord Bay, Gerlache Strait and Station B for total number of individuals (ind. m^{-2}) with ("Total", a, b, c) and without ("No Nematoda", d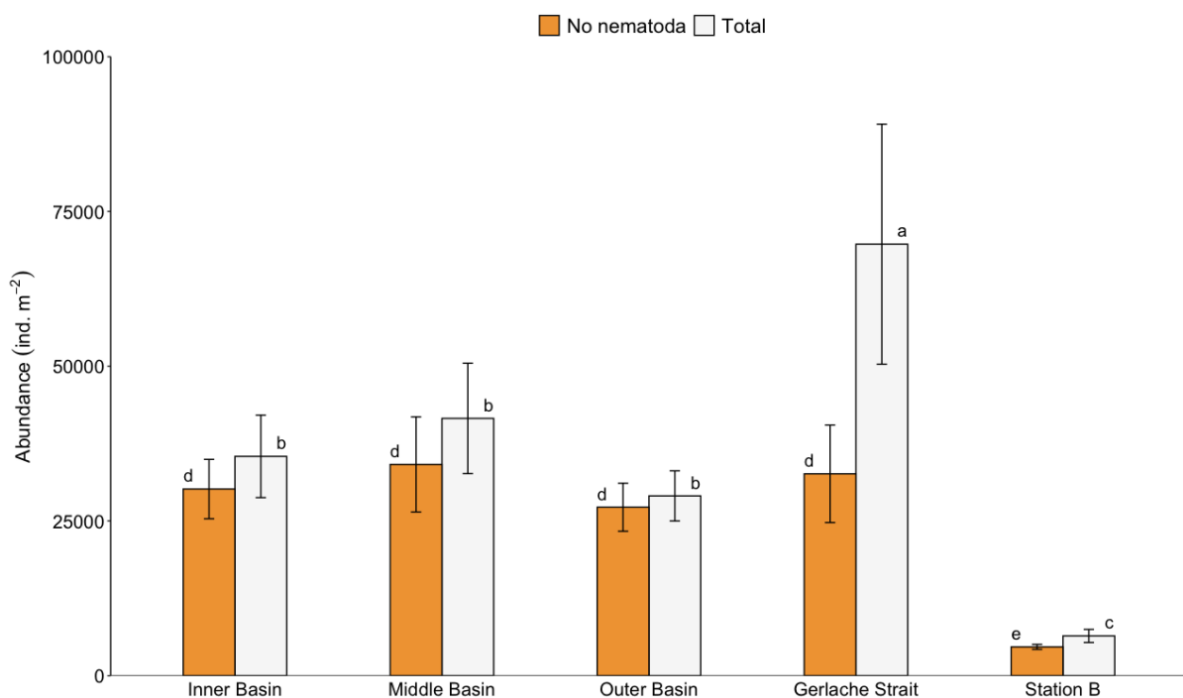, e) nematodes. One-Way ANOVA tested significant differences ($p < 0.05$) between stations using "Total" and "No Nematoda" as single factors. Significant differences are designated by different letters. Error bars denote ± SD.

Macrofaunal biomass ranged from 0.36 ± 0.15 g C m^{-2} ($n = 3$, SD) in the Outer Basin to 10.72 ± 8.11 g C m^{-2} ($n = 4$, SD) in the Middle Basin (Fig. 19). The Inner Basin exhibited the second highest macrofaunal biomass (10.00 ± 3.33 g C m^{-2} [$n = 4$, SD]) followed by Gerlache Strait (5.27 ± 1.48 g C m^{-2} [$n = 4$, SD]) and Station B on the continental shelf (0.59 ± 0.64 g C m^{-2} [$n = 4$, SD]) (Fig. 19). Bacterial biomass ranged from 0.10 ± 0.006 g C m^{-2} ($n = 4$, SD) at Station B on the continental shelf to 1.36 ± 0.59 g C m^{-2} ($n = 4$, SD) in the Middle Basin (Fig. 19). Andvord Bay exhibited the highest bacterial biomasses overall (Outer Basin: 1.24 ± 0.42 g C m^{-2} [$n = 3$, SD]; Inner Basin: 0.68 ± 0.08 g C m^{-2} [$n = 4$, SD]) and Gerlache Strait (0.59 ± 0.20 g C m^{-2} [$n = 4$, SD]) was the intermediate site between the continental shelf and the fjord. The interaction between the two factors, site and organism type (macrofauna and bacteria) was not significantly different ($p = 0.07$, Scheirer-Ray-Hare) (Fig. 19). Total biomass (the sum of bacteria and macrofauna biomasses) reflected the pattern already seen in macrofaunal biomass (Fig. 20) with significantly higher biomasses in the Inner and Middle Basin of Andvord Bay and Gerlache Strait ($p < 0.001$, One-Way ANOVA) versus the Outer Basin and Station B (Fig. 20).
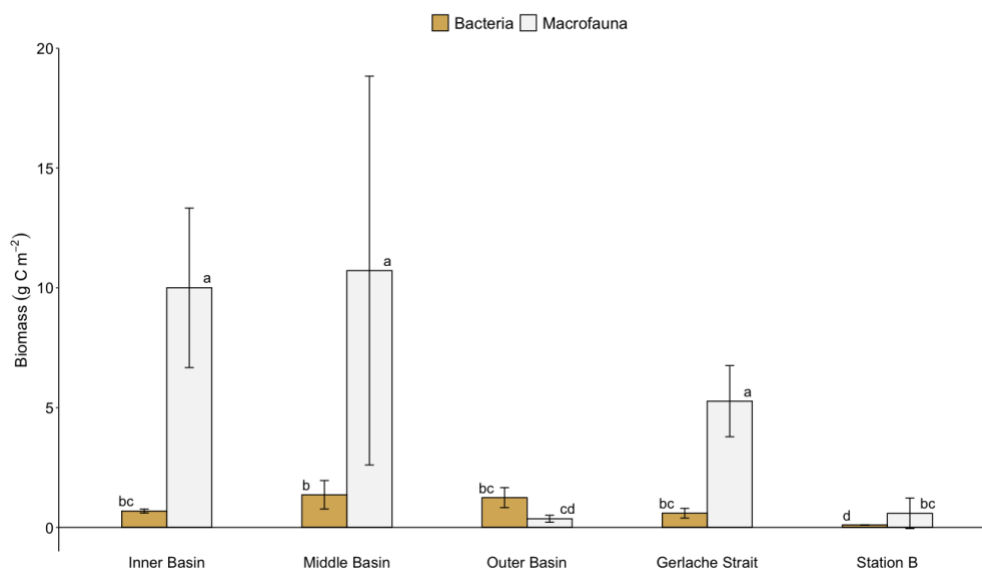
Figure 19: Mean bacterial and macrofaunal biomass across Andvord Bay, Gerlache Strait and at Station B. Scheirer-Ray-Hare test was carried out with organisms (Bacteria and Macrofauna) and stations as factors. Significant differences (p < 0.05) are designated by different letters. Error bars denote ± SD.
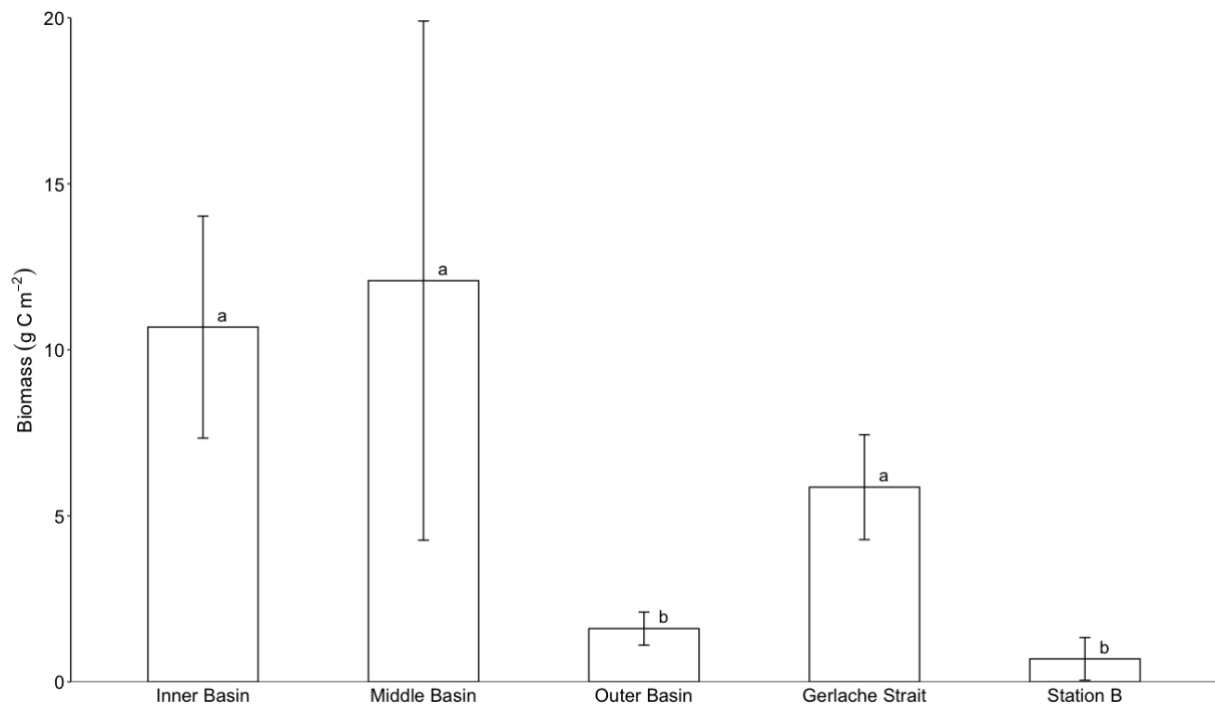
Figure 20: Total biomass (summed bacterial and macrofaunal biomasses) across Andvord Bay, Gerlache Strait and Station B. A One-Way ANOVA was carried out to test for significant differences ($p < 0.05$) between stations and differences are designated by different letters. Error bars denote ± SD.

3.5 C-uptake

Statistical analysis revealed significant differences in total (sum of bacteria, macrofauna and DIC respiration) C-uptake rates between the different sites ($p < 0.001$, One-Way ANOVA) (Fig. 21). The highest total C-uptake rates were seen at the Inner and Middle Basins of Andvord Bay (Inner Basin: 19.37 ± 4.69 mg C m^{-2} d^{-1} [$n = 4$, SD]; Middle Basin: 20.56 ± 3.74 mg C m^{-2} d^{-1} [$n = 4$, SD]) compared to the other sites (Gerlache Strait: 10.65 ± 1.70 mg C m^{-2} d^{-1} [$n = 4$, SD]; Outer Basin: 6.15 ± 1.12 mg C m^{-2} d^{-1} [$n = 3$, SD]; Station B: 7.38 ± 1.54 mg C m^{-2} d^{-1} [$n = 4$, SD]).
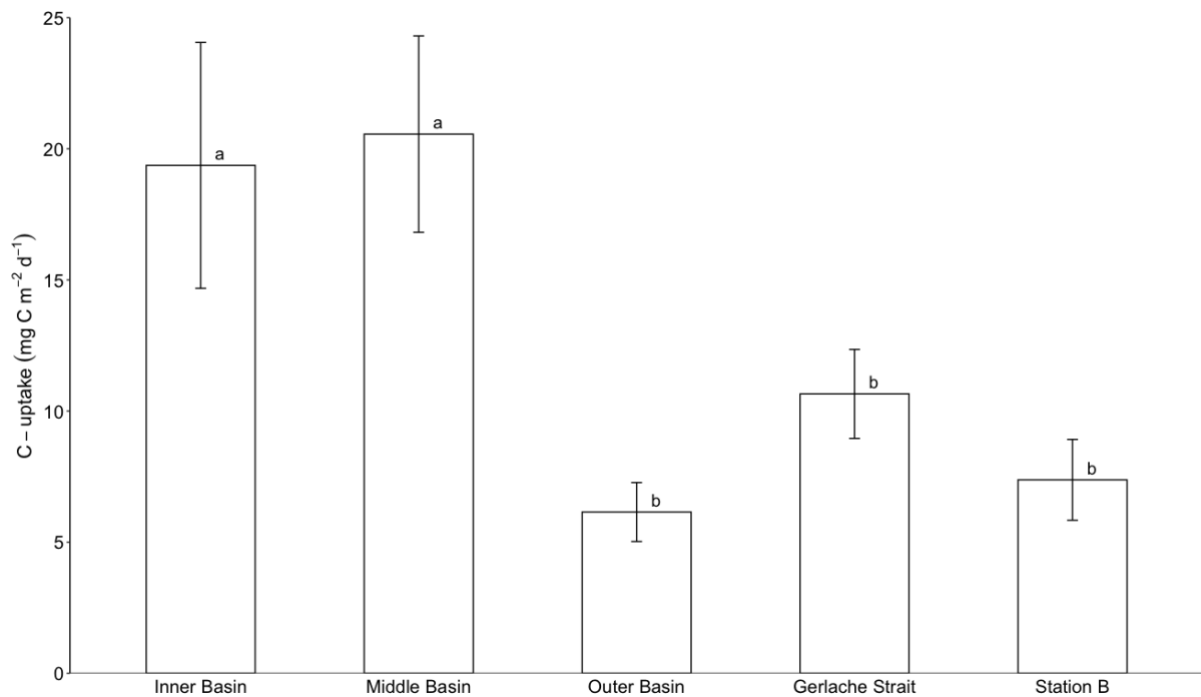
Figure 21: Total summed (bacterial, macrofaunal and respiration) C-uptake observed along Andvord Bay, Gerlache Strait and Station B. One-Way ANOVA was carried out to test for significant differences ($p <$ 0.05) between stations and differences are designated by different letters. Error bars denote ± SD.

Microbial and macrofaunal C-uptake relationships between the different stations and each other were significantly different ($p < 0.001$, Two-Way ANOVA). Interestingly, although no significant difference was found among study sites, microbial C-uptake rates showed a decreasing pattern from Andvord Bay (Inner Basin: 1.58 ± 1.07 mg C m^{-2} d^{-1} [$n = 4$, SD]; Middle Basin: 1.17 ± 1.03 mg C m^{-2} d^{-1} [$n = 4$, SD]; Outer Basin: 1.03 ± 0.81 mg C m^{-2} d^{-1} [$n = 3$, SD]), to Gerlache Strait (0.27 ± 0.37 mg C m^{-2} d^{-1} [$n = 4$, SD]) and eventually to Station B (0.08 ± 0.05 mg C m^{-2} d^{-1} [$n = 4$, SD]) (Fig. 22). The highest macrofaunal C-uptake rates were detected at the inner and middle basin sites of Andvord Bay (Fig. 22), and these rates were significantly higher than microbial C-uptake rates at all sites, plus macrofaunal C-uptake rates at the Outer Basin, Gerlache Strait and Station B sites. Gerlache Strait, despite having higher macrofaunal biomass here compared to station B and the Outer Basin site, exhibited among the lowest macrofaunal C-uptake rates in the study.
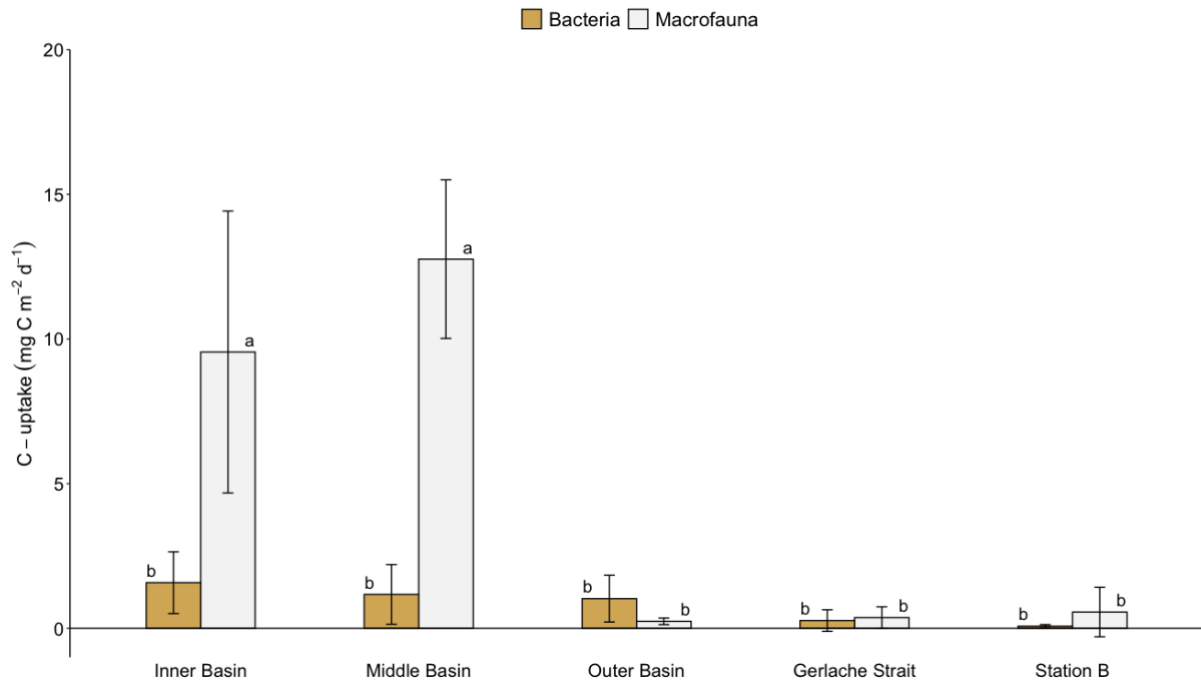
Figure 22: Mean bacterial and macrofaunal C-uptake observed across Andvord Bay, Gerlache Strait and Station B. Two-Way ANOVA was carried out with organisms (Bacteria and Macrofauna) and station set as factors and differences ($p < 0.05$) are designated by different letters. Error bars denote ± SD.

In the Inner and Middle Basin, most of the algal C was used by the macrofauna (47% and 62%, respectively) followed by DIC respiration (44% and 33%, respectively) and microbial uptake (9% and 5%, respectively) (Fig. 23). Most of the algal C in the Outer Basin of the fjord, Gerlache Strait and Station B was diverted into the DIC pool (80%, 94% and 92%, respectively). Interestingly, macrofauna in the Outer Basin used the less amount of C while in Gerlache Strait and Station B, the bacteria were the least consumers.
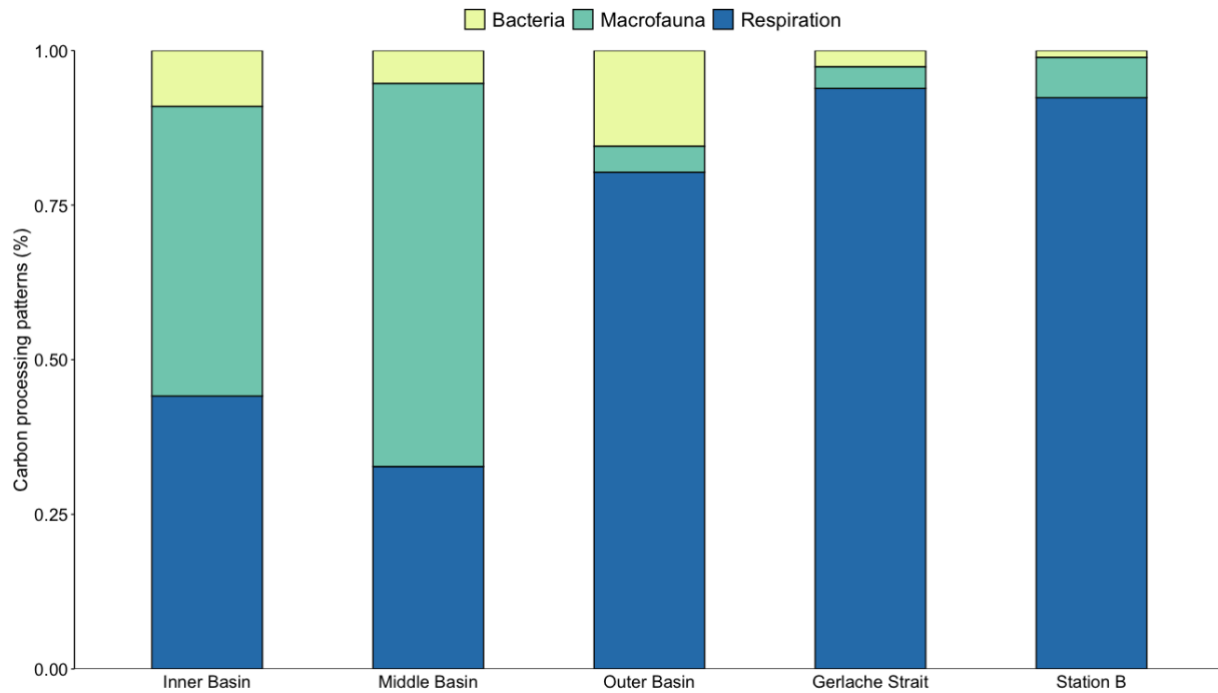
Figure 23: Bacterial, macrofaunal and respiration contribution to total C-uptake in Andvord Bay, Gerlache Strait and Station B.

4 Discussion

This study undertook benthic incubation experiments down Andvord Bay to document ecosystem function and structure in a glaciomarine fjord and compare these results to the benthic ecosystem outside the fjord and onto the continental shelf. We found significantly higher SCOC rates in the Inner and Middle Basins and Gerlache Strait compared to Station B on the continental shelf for non-algal experiments and these trends continued after the addition of algae. Furthermore, we detected significantly higher nutrient fluxes (e.g., phosphate), macrofaunal abundances, bacterial and macrofaunal biomasses in the fjord compared to the adjacent shelf. Interestingly, we found that the total (summed macrofaunal and bacterial) and macrofaunal C-uptake in the Inner and Middle Basin were significantly higher than from the other sites. Therefore, our hypothesis that "*No significant change exists in SCOC, nutrient fluxes or bacterial and macrofaunal C-uptake rates within the fjord and between the fjord and the continental shelf*" is only partially supported.

Glacio-marine fjords in the Arctic paint a picture of future environmental conditions in Antarctic fjords as the severe impacts of climate change on the regional Arctic environment which exhibits fjords with high meltwater disturbances, increase sedimentation events and limited food supply (Wlodarska-Kowalczuk et al. 2005; Wesławski et al. 2011; Al-Habahbeh et al. 2020).

Climate alteration related events have rapidly increased in the last 20 years in Antarctica (Kerr et al. 2018; Convey and Peck 2019) and Arctic fjord models and predictions on glacial melt impacts on regional ecosystems (Wlodarska-Kowalczuk et al. 2005; Wesławski et al. 2011) suggest what Antarctic fjords may see in the coming years (Amesbury et al. 2017).

Generally, benthic ecosystems in the WAP play a critical role in biogeochemical cycling sequestrating carbon and often acting as a sink for C produced during primary productivity in the overlying water column (Barnes 2017; Henley et al. 2019). In particular, benthic organisms can assimilate the carbon fixed by primary producers at the sea surface and on the ice for periods of time, that vary depending on sea-ice dynamics as well as organisms' lifespan and behavior, algal blooms and oceanographic conditions (Barnes et al. 2018).

4.1   Benthic oxygen rates and nutrient fluxes

Background SCOC rates decreased along Andvord Bay with the highest rate in the Inner Basin of the fjord (65.22 ± 9.46 mg C m^{-2} d^{-1}) and the lowest fjord SCOC rate in the fjord mouth (37.50 ± 11.02 mg C m^{-2} d^{-1}). Background SCOC rates at Gerlache Strait (50.07 ± 4.39 mg C m^{-2} d^{-1}) were higher than the Outer Basin, albeit not significantly and Station B on the continental shelf (29.35 ± 4.61 mg C m^{-2} d^{-1}), which was the lowest rate detected. Background respiration rates at Station B were significantly different to the Inner and Middle Basins of Andvord Bay and Gerlache Strait.

Shallow and deep-water environments strongly depend on benthic-pelagic coupling as an effective C transport pathway. In particular, the deep-water environments of the WAP greatly rely on C export from the surface, which experiences high seasonality (Smith et al. 2008b). The seabed of the WAP receives on average 7.45 g C m^{-2} y^{-1} (0.02 g C m^{-2} d^{-1}) (Smith et al. 2008b) and we added 8.37 mg C m^{-2} of C enriched phytodetritus to mimic a sudden POC flux event. This POC addition led to a significant rise in SCOC in the Outer Basin experiments and at Gerlache Strait suggesting that the other stations might experience availability of labile and semi-labile POC more frequently, either in the form of bloom-derived phytodetritus or a continually available "food bank" as observed for Station B in the studies of Hartnett et al. (2008) and Smith et al. (2008). Similar oxygen consumption rates to ours were observed at Station B during the FOODBANCS project (9.38 - 31.72 mg C m^{-2} d^{-1}, Hartnett et al. 2008). In contrast, SCOC rates in Potter Cove, Antarctica, were higher than our rates most likely due to the shallower depth of their study sites and greater C-flux to the seafloor, ranging from -436.56 and 192.78 mg C m^{-2} d^{-1} where negative value indicates when more oxygen is consumed than produced (Braeckman et al. 2021). Community metabolism in Potter Cove varied greatly in the presence of chlorophyll-*a* after a bloom event (Braeckman et al. 2021) and showed higher benthic respiration rates following the deposition of algal material. Andvord Bay experiences a strong seasonal cycle of sea-ice cover, which affects seafloor phytodetritus cover by altering light availability and stratification in surface waters and allowing for high C-fluxes and higher respiration rates within the inner parts of the fjords (Lundesgaard et al. 2020; Ziegler et al. 2020). Interestingly, background oxygen respiration rates in this study are similar to SCOC rates measured at 8°C from Norwegian fjord sediments collected at 200m depth, which ranged from 7.14 ±. 3.06 mg C m^{-2} d^{-1} to 1701.36 ± 36.72 mg C m^{-2} d^{-1} (Sweetman et al. 2014). Furthermore, SCOC rates in Sognefjord, in the Arctic, at 1,250 m depth at 7°C were lower than this study (14.69 ± 2.45 mg C m^{-2} d^{-1}, Witte et al. 2003) suggesting that SCOC rates measured

in Andvord Bay are exceptionally high for fjord sediments given the incubations were undertaken at -1°C.

Nutrient fluxes varied greatly in the different stations and for the different treatments and generally, the addition of algae contributed to significantly changes in nutrient fluxes (Fig. 16). Previously, experiments on the WAP continental shelf identified the presence of coupled nitrification-denitrification where denitrification ranged from 0.66 to 1.45 mmol N m^{-2} d^{-1} accounting for about 1-2% of global sediment nitrification rates (Hartnett et al. 2008). Nitrate fluxes measured during the FOODBANCS program were lower at Station B (-0.01 ± 0.05 mmol N m^{-2} d^{-1}) than this study (0.15 ± 0.04 mmol m^{-2} d^{-1}). The higher rates measured in this study suggest that localized upwelling of shelf waters could help fuel intense primary production and lead to strong benthic pelagic coupling in the region. Similar phosphate fluxes to the different basins in Andvord Bay were found in the inner, middle and outer basins of Kongsfjorden (Svalbard), though ammonium fluxes were generally higher (Morata et al. 2020). Nitrification activity at Station B was suggested by the uptake of NH_4^+ in the sediment and flux of NO_3^- from the sediments (Fig. 16C and E). In contrast, nitrate influx into the sediments in the Inner Basin of Andvord Bay suggested denitrification activity most likely driven by the intense primary production and detrital fluxes (Lundesgaard et al. 2020; Ziegler et al. 2020) in this area that support the high macrofaunal abundance and biomass (Fig. 18 and 19), and megafaunal abundance and diversity (Grange and Smith 2013).

Interestingly, silica fluxes were all out of the sediment along the length of Andvord Bay, Gerlache Strait and Station B for both enriched and background conditions and fluxes at Station B were the highest measured (Fig. 16B) suggesting elevated opal dissolution likely caused by the sedimentation of intense diatom pulses to the seafloor and the introduction of the labelled algal culture. In the Arctic, ice sheets have been suggested to play an important role in the

global silicon cycle as meltwater and icebergs affect diatom growth and productivity in surface waters (Hawkings et al. 2017).

4.2 Benthic community structure

Benthic macrofaunal abundances documented at Station B on the continental shelf of the WAP (4,659 ind. m^{-2}) were 66% lower than the abundances measured during the FOODBANCS project (13,844 ± 3,948 ind. m^{-2}, $n = 4$, SD) by Glover et al. (2008) who used the same Bowers and Connelly megacoring system that we used. The mismatch in macrofaunal abundances between this study and that of Glover et al. (2008) could reflect seasonal differences; macrofaunal abundances at Station B have been shown to fluctuate by 2-3 times during an annual cycle Glover et al. (2008). Similarly to Grange and Smith (2013) who observed high soft-sediment epibenthic megafaunal abundances in Andvord Bay, macrofaunal abundances were higher in Andvord Bay (91,193 ind. m^{-2}) and Gerlache Strait (32,615 ind. m^{-2}) compared to the continental shelf (4,659 ind. m^{-2}, Station B).

Generally, microbes represent one of the key organisms dominating deep-sea sediments (Danovaro et al. 2015) and, in Antarctica, the microbial community dominates the genetic pools and biomass of the different ecosystems highlighting the importance of these organisms for both oceanic food-webs and carbon transport and sequestration (Wilkins et al. 2013). Similarly, in the deep Sognefjord in western Norway, microbial and macrofaunal biomass are 8.5 g C m^{-2} and 250 mg C m^{-2}, respectively (Witte et al. 2003a) and in Hardangerfjorden, bacterial biomass exceeds macrofaunal biomass (Sweetman et al. 2014). In our study, however, macrofauna biomasses exceeded microbial biomass at all stations except the Outer Basin, and the inner and middle basins of the fjord had significantly higher macrofaunal biomasses than the Outer Basin and Station B (Fig. 18). Here, the elevated biomass, SCOC and nutrient data indicating denitrification activity in the inner fjord basin of Andvord Bay is consistent with the

megafaunal data of Grange and Smith (2013), and suggests that inner fjord basins along the WAP are 'hotspots' of benthic ecosystem function in contrast to their Arctic counterparts due to less sedimentation and burial disturbance, and high levels of primary production and POC flux to the seafloor (Grange and Smith 2013; Lundesgaard et al. 2020; Ziegler et al. 2020).

4.3 *Dissolved inorganic carbon fluxes and community response to the introduction of labelled material*

DIC production rates decreased steadily along Andvord Bay from the highest rate in the Inner Basin (8.24 ± 0.76 mg C m^{-2} d^{-1}) to the lower rate in the Outer Basin (4.88 ± 0.52 mg C m^{-2} d^{-1}) (Fig. 17). Gerlache Strait showed the highest DIC production rate in our experiments (10.01 ± 1.92 mg C m^{-2} d^{-1}) while Station B and the Middle Basin of the fjord showed similar rates (6.74 ± 0.97 mg C m^{-2} d^{-1} and 6.63 ± 1.30 mg C m^{-2} d^{-1}, respectively). This trend reflects background SCOC rates while the total (summed DIC, bacteria and macrofauna) C-uptake showed a different pattern (Fig. 21). Total C-uptake rates as well as macrofaunal uptake were significantly higher in the Inner and Middle Basins in contrast to the other stations, while bacterial C-uptake decreased steadily from the Inner Basin (1.58 ± 0.03 mg C m^{-2} d^{-1}) to Station B (0.08 ± 0.03 mg C m^{-2} d^{-1}) (Fig. 22). Again, the significantly higher total C-uptake rate in the inner and middle basins of Andvord Bay suggests that inner parts of the fjord are intense sites of C-cycling activity compared to the rest of the outer fjord and the continental shelf.

Total daily C-uptake rates from the inner and middle parts of the fjord (Inner Basin: 19.37 ± 4.69 mg C m^{-2} d^{-1}; Middle Basin: 20.56 ± 3.74 mg C m^{-2} d^{-1}) were higher than total daily C-uptake rates (6.15 ± 1.12 mg C m^{-2} d^{-1} and 7.38 ± 1.54 mg C m^{-2} d^{-1}, respectively) measured in situ at 7-8°C in Sognefjorden, western Norway (>1200 m depth: 3-6 mg C m^{-2} d^{-1}, Witte et al. 2003a). The Sognefjord total C-uptake rates were, however, similar to total C-uptake rates measured with sediments from the Outer Basin and Station B (6.15 ± 1.12 mg C m^{-2} d^{-1} and 7.38 ± 1.54 mg C m^{-2} d^{-1}, respectively). Given that the temperature of our incubations was -

1°C, the higher total C-uptake rates measured in the inner reaches of the fjord adds additional evidence that the Inner and Middle Basin of Andvord Bay are "hotspots" of ecosystem function.

In the Inner and Middle Basins, macrofaunal C-uptake and biomass were both significantly higher than the other stations (Outer Basin, Station B) and as biomass increased, macrofauna consumed more material (Fig. 19 and 22). In Gerlache Strait, however, macrofaunal C-uptake rates were some of the lowest rates recorded (0.37 ± 0.37 mg C m^{-2} d^{-1}) despite the higher macrofaunal biomass (5.27 ± 1.48 mg C m^{-2}), suggesting low macrofauna C-cycling activity here. The slightly higher macrofaunal biomasses and C-uptake rates in the middle locations of the fjord and the relationship between macrofaunal biomass and C-uptake suggest that there may be an organic-enrichment gradient existing within the fjord. Intense organic pulses from the surface may lead to elevated, yet slightly lower macrofaunal biomass and lower C-uptake (Pearson and Rosenberg 1978) right next to the glacier compared to the middle station which is less organically enriched as exhibited by biomass and activity maxima.

Bacterial C-uptake was higher in the inner parts of the fjord and decreased towards the continental shelf (Fig. 22). The highest bacterial C-uptake rates were found in Inner Basin where microbial biomass was comparatively low suggesting that microbes in the inner fjord are extremely active in cycling C compared to other sites (e.g., Gerlache Strait) where bacterial C-uptake rates were very low, yet biomass was similar (Fig. 22 and 19). The majority of C in the outer basin, Gerlache Strait and Station B was directed into respiration (i.e., the DIC pool) suggesting that the outer fjord region and the WAP continental shelf are respiration-dominated ecosystems as previous datasets from other detrital fueled food-webs suggest (e.g., Witte et al. 2003a; b; Woulds et al. 2009; Sweetman et al. 2010). While macrofaunal C-uptake dominated over microbial C-cycling in Gerlache Strait and Station B, the microbial pool at the fjord mouth represented the second most important pool for C (15%) followed by macrofauna (4%). Many

pulse chase studies have shown that bacteria are key players in the short-term remineralization of organic C in the deep sea (Witte et al. 2003b; Woulds et al. 2009; Sweetman et al. 2016, 2019), asserting the importance of bacteria in deep-sea benthic ecosystem functioning and organic matter cycling in particular at the seafloor (Lochte and Turley 1988; Boetius and Lochte 1996; Wilkins et al. 2013; Hoffmann et al. 2017; Jørgensen et al. 2021). Similarly, this seems to be the case in the Outer Basin of Andvord Bay. However, the inner parts of the fjord seem to be an exception as most C was shunted into the macrofauna in the Inner Basin and Middle Basin (47% and 62%, respectively), followed by the DIC pool (44% and 33%, respectively) and then the microbes (9% and 5%, respectively) (Fig. 23). Previous studies report dominance of macrofauna over bacteria in short-term C cycling processes in n boreal fjords p (Witte et al. 2003a; Sweetman et al. 2014, 2016). In the Sognefjord, while respiration always remained the main pool for remineralized C, macrofauna processed more C than bacteria after 1.5d whereas the microbial community became the main consumer after 3d (Witte et al. 2003a). Here, despite the lower biomass, macrofauna accounted for 17% of the processed material, that a large fraction of the added tracer first passed through larger animals before becoming available to the microbial community. Similarly, in the Hardangerfjorden, the macrofaunal community, despite the lower biomass compared to the Anterctic, was responsible for the highest C-uptake rates after 48 h incubations under the excessive exposure to organic matter waste from fish farming (Sweetman et al. 2014). Incubations carried out with sediments from Fanafjorden, also, showed that the macrofaunal community was responsible for higher daily C-uptake rates compared to bacteria when sediments were exposed to phytodetritus (Sweetman et al. 2016).

5 Conclusions

Contrary to glacio-marine fjords in the Arctic that see macrofaunal community and trophic structure increase towards the fjords mouth (Wlodarska-Kowalczuk et al. 2005), our study has shown that ecosystem functioning and structure in the inner parts of the fjords are significantly different from the fjord's outer basin and the continental shelf indicating that the inner and middle basins of Andvord Bay are "hotspots" of benthic biomass and ecosystem function. We show how different POC flux inputs drive different ecosystem dynamics O along Andvord Bay, Gerlache Strait and Station B. Our study shows the macrofaunal community importance in the short-term C-cycling at the seafloor under the presence of high organic matter inputs within the inner Andvord Bay. Because availability of labile detritus and POC flux is predicted to change (van Oevelen et al. 2011; O'Daly et al. 2020), and glacial retreat in predicted to increase along the WAP in relation to climate warming events it will be important to undertake studies to assess how these hotspots of biomass and ecosystem function will change. Only through these studies and baseline studies will we be able to assess how climate change along the WAP will impact benthic ecosystem functioning and biogeochemical processes along the fastest warming region on the planet Earth.

CHAPTER 4

THE BENTHIC MACROFAUNAL COMMUNITY RESPONSE TO PHYTODETRITAL INPUTS ALONG A SUB-POLAR ANTARCTIC BATHYAL FJORD AND CONTINENTAL SHELF GRADIENT ON THE WESTERN ANTARCTIC PENINSULA

Abstract

Glaciomarine fjords dominate the coastal margins of the West Antarctic Peninsula (WAP), one of the fastest warming regions of the planet. WAP fjords are hotspots of biological productivity and biodiversity and thus there is the necessity to better understand their sensitiveness to climate warming events. Here, we investigate the macrofaunal response to phytodetrital inputs in Andvord Bay, Gerlache Strait a deep channel situated immediately outside of Andvord Bay and Station B on the continental shelf of the WAP. Pulse-chase experiments were conducted to study macrofaunal C-cycling activity, biomass and community structure. Here, macrofaunal communities were different among Andvord Bay, Gerlache Strait and Station B where the Antarctic continental shelf present the highest taxonomic richness and macrofaunal evenness in our study (30 different taxa for <1000 individuals). The benthic community response under different POC flux inputs was different among the stations along the fjord and the continental shelf and biogeochemical cycling activity appeared to be a lot higher in the inner parts of the Andvord Bay compared to the other sites and the continental shelf with C-turnover rates as high as about one day (1.14 d^{-1}). We postulate that as climate warming and glacial retreat progresses, macrofaunal C-cycling activity as well as biomass and community structure will likely change, and further research is urgent to better understand Antarctic fjord climate sensitivity and the resilience of these environments to environmental changes.

1 Introduction

Warming air and sea temperatures caused by climate change have heavily influenced fjord ecosystem structure and function in polar habitats (Sweetman et al. 2017; Ingels et al. 2021). In the Arctic, for example, warming has enhanced glacial retreat and meltwater runoff from land-terminating glaciers leading to turbidity events, which have resulted in reduced primary and secondary productivity in the water column (Hop et al. 2002; Powell and Domack 2002; Al-Habahbeh et al. 2020; Morata et al. 2020). Elevated particle loads running off the melting glaciers in inner fjord locations leads to extensive burial disturbance at the seafloor that smoothers seafloor life and reduces organic-matter quality in seafloor sediments (Wlodarska-Kowalczuk et al. 2005; Renaud et al. 2007; Wesławski et al. 2011). As such, gradients of increasing benthic biomass and biodiversity from the inner parts of the fjords to the adjacent shelf are often observed in the Arctic (Wlodarska-Kowalczuk et al. 2005; Renaud et al. 2007; Wesławski et al. 2011).

The Western Antarctic Peninsula (WAP) is one of the fastest warming regions on the planet and significant environmental changes have occurred here over the last 100 years (Hendry et al. 2018). For example, changes in ocean circulation and regional climatic warming such as a 6°C increase in mean winter air temperature and an increase of ~1°C in sea-surface temperature have been observed since the 1950s (Vaughan et al. 2001; Cook et al. 2005; Meredith and King 2005) resulting in the retreat of more than 87% of the glaciers along the WAP (Cook et al. 2005; Hendry et al. 2018).

The margins of the WAP are dominated by glaciomarine fjords (Syvitski et al. 1987; Howe et al. 2010) that offer critical points of observation of past climatic conditions (Cottier et al. 2010) as well as an environment in which to observe how benthic ecosystem structure and function change across environmental gradients of primary production and C-export to the seafloor (Nowacek et al. 2011; Grange and Smith 2013; Grange et al. 2017; Ziegler et al. 2017). In

contrast to their Arctic counterparts, inner and mid-fjord basins in glaciomarine fjords along the WAP have been recognized as "hotspots" of biological production (krill density of 2000 animals m^{-3}, Nowacek et al. 2011; Grange et al. 2017) relative to the continental shelf. This is thought to be the result of a combination of fjord topography limiting local wind forcing, weak meltwater processes, enhanced water-column stratification, and high light penetration that collectively act to increase primary production and detrital fluxes (Griffith and Anderson 1989; Nowacek et al. 2011; Grange and Smith 2013; Grange et al. 2017; Lundesgaard et al. 2020). Continued warming of the WAP will likely eventually result in glaciomarine fjord systems shifting to the ecosystem state now seen in many Arctic fjords with significant changes in important ecosystem functions such as primary productivity, energy transfer (Gutt et al. 2020), community metabolism (Braeckman et al. 2021) and distribution (Kim et al. 2021). Investigations in subpolar Antarctic fjord systems have revealed that benthic megafaunal communities exhibit greater biodiversity and biomass in inner fjord locations compared to the fjord mouth and continental shelf sites (Grange and Smith 2013; Grange et al. 2017; Ziegler et al. 2020) due to less sedimentation and lower chronic burial effects (Grange and Smith 2013; Ziegler et al. 2020).

Differences in benthic community structure have been shown repeatedly to have significant effects on benthic ecosystem functions, such as nutrient fluxes and carbon cycling (Solan et al. 2004; Norling et al. 2007; Sweetman et al. 2010, 2014). Studies from Andvord Bay, a glaciomarine fjord situated on the WAP have revealed significant changes in benthic community structure along the fjord to shelf continuum with much higher abundances of surface feeding megafauna (e.g., the ampharetid polychaete, *Amythas membranifera*) dominating inner, middle and outer basins compared to the adjacent continental shelf that tends to be dominated by a more carnivorous (e.g., pycnogonids) and omnivorous (e.g., brittle stars) assemblage (Grange and Smith, 2013). The clear change in benthic community composition

(abundance and biomass) along Andvord Bay and out onto the shelf is almost certainly likely to lead to significant changes in benthic carbon cycling activity at different positions in the fjord and the shelf since surface feeding fauna tend to consume more phytodetrital C than other feeding guilds (Aberle and Witte 2003; Sweetman and Witte 2008; Sweetman et al. 2010, 2014).

Given the WAP fjords are currently hotspots of biological productivity and biodiversity (Glover et al. 2008; Smith et al. 2008b; Grange and Smith 2013) but are likely to be severely impacted by climate change, there is an urgent need to develop a better understanding of baseline functioning of fjord communities to assess their sensitivity to climate warming events. This study aimed to identify the benthic macrofaunal response to phytodetrital inputs in Andvord Bay, Gerlache Strait a deep channel situated immediately outside of Andvord Bay and Station B on the continental shelf. We hypothesized that higher abundances and biomasses of macrofauna would be found in the fjord compared to the shelf, and elevated abundances of surface-feeding fauna in Andvord Bay would lead to elevated levels of C-cycling by the community here compared to Station B on the adjacent continental slope.

2 Methods

2.1 Study sites & experimental design

In April and May 2016, during the cruise NBP1603 on the R.V. *Nathaniel B. Palmer*, pulse-chase experiments were conducted with sediments from three study sites in Andvord Bay (inner, middle and outer basin), Gerlache Strait - an intermediate station between Andvord Bay and the continental shelf - and Station B located on the continental shelf of the WAP (Fig. 24). For detailed hydrography of the region see Lundesgaard et al. (2020). Sediments were collected between 537-631 m depth with a Bowers and Connolly megacorer. Four replicate sediment samples were collected from each station. Upon retrieval, cores were transferred to 10 cm

diameter flux chambers (45 cm long). To avoid sediment disturbance, all cored sediments were gently covered with 25 cm of 5-µm filtered, oxygenated seawater and then they were incubated in a water bath in an incubator for 48 h that was set to *in-situ* temperature (-1°C).
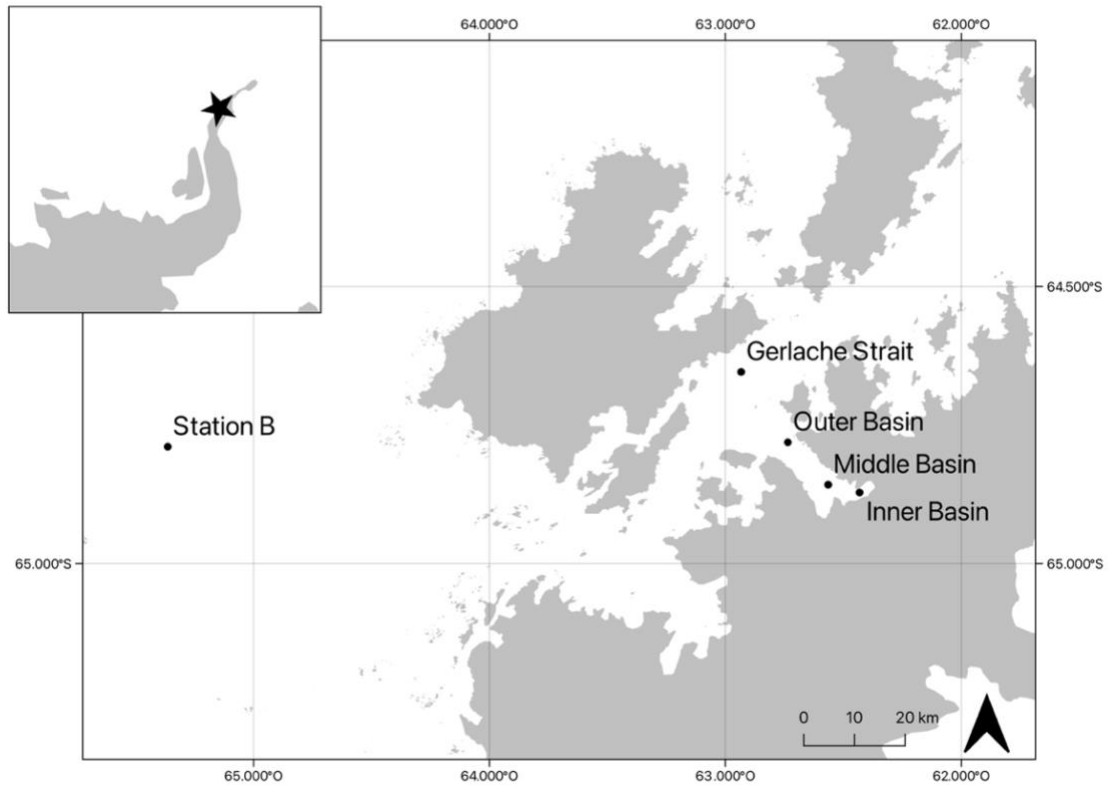
Figure 24: Study sites in Andvord Bay, Gerlache Strait and Station B on the continental shelf.

2.2 *Labelled food source preparation*

An axenic clone of the diatom *Phaeodactylum tricornutum* was used as a labelled food source in our experiments, and cultured in artificial seawater modified with F/2 algal culture medium (Grasshoff et al. 1999). Diatoms were labelled by replacing 50% of ^{12}C bicarbonate in the culture medium with $NaH^{13}CO_3$. Algae were grown for three weeks. After three weeks, the algae were harvested by filtering the algae over a 0.45-µm filter (cellulose acetate) and by centrifuging the algae five times with un-labelled F/2 medium to remove labelled bicarbonate. The algae were then freeze dried. Later analysis on the algae revealed that they had a final organic content of 18.6% and a ^{13}C content of 37.8 atom%.

2.3 Addition of labelled algae

Forty eight hours after the cores were collected 8.37 mg C m^{-2} of labile C (45 mg dry weight of algae) which was equivalent to 15% of the annual POC flux (7.45 g C m^{-2} y^{-1}) (Smith et al. 2008b) was added to the top of each core and allowed to settle to the sediment surface for 1 h. The cores were then treated to periodic bubbling and stirring for 24 h as described in Chapter 2, which maintained oxygen levels and a sufficiently thin diffusive boundary layer.

2.4 Sample processing and analysis

We collected sediment samples from each core 24 h after the start of the algal incubation. Sediments were extruded and sectioned between 0-10 cm depth. During this procedure, some macrofauna were observed burrowing deeper into the sediment core. Thus, changes in ecosystem parameters as a function of sediment depth were not addressed in this study. Approximately, 10 ml of these sediments were removed for bacterial phospholipid fatty acid (PLFA) analysis that has been described in Chapter 2, and the remaining sediments were placed into a bowl and sieved with cold, filtered seawater over a 300-µm mesh. The fauna was then transferred to plastic bottles and fixed with 4% buffered formaldehyde in seawater.

Back in the laboratory, fixed macrofauna samples were sieved on a 300-µm sieve with filtered seawater, picked under a microscope in artificial seawater and identified to order or major taxa while polychaetas were identified to family. All organisms were dried on foil or in pre-weighed tin cups (depending on their size) at 35-40°C for a maximum of 7 days. Calcareous organisms were placed into silver (Ag) cups and dried using the same conditions as described above. Calcareous organisms were decalcified following the methods described in Sweetman et al. (2009). Here, 20 µl MilliQ water was added to each silver cup followed by 40 µl of 0.5 M HCl and subsequently dried at 50°C for 48 h. After this, a further 20 µl MilliQ water was added followed by 40 µl of 2 M HCl and the cups were again dried at 50°C for 48 h to remove any

residual calcareous material. Depending on dry weight biomass measurements, some samples were then combined to meet UC Davis Stable Isotope Facility biomass requirements for C-isotopic analysis. Samples of the same taxa were combined. When this was not possible, samples (polychaetes) were combined according to their dominant feeding guild.

Macrofaunal specific ^{13}C uptake, expressed as $\Delta^{13}C$ (‰), was calculated as the difference between the $\delta^{13}C_{enriched\ sample}$ and $\delta^{13}C_{background}$ values of closely-related taxa. Uptake of ^{13}C was calculated as the product of excess of atom% ^{13}C (enriched - background) and C content of the enriched samples expressed as a unit weight: ^{13}C uptake (unit wt C) = (atom% $^{13}C_{enriched\ sample}$ – atom% $^{13}C_{background}$) x (unit wt C). This uptake was then adjusted to total C uptake by accounting for the added ^{13}C algal labeling: C uptake = ^{13}C uptake / 37.8 atom%, the fractional abundance of ^{13}C in algae. Background macrofaunal isotope ($\delta^{13}C_{background}$) signatures used in the aforementioned analysis were extrapolated from Pasotti et al. (2015).

2.5   Data analysis

The statistical software package R and Primer 7 were used to carry out all statistical analysis. Differences in macrofaunal abundance, biomass and C-uptake between sites were tested using One-Way ANOVA tests if the data were normally distributed, and homogeneity of variance was present within the data. A Scheirer-Ray-Hare (SRH) test was carried out to test for differences in polychaeta feeding guilds between sites since the assumptions of normality and homoscedasticity were not satisfied. PRIMER was used to carry out non-metric multi-dimensional scaling (nMDS) analysis and graphic visualization of Bray-Curtis similarities between macrofauna abundances and conduct ANOSIM and SIMPER analyses to assess which fauna were driving the differences in macrofaunal community structure between sites. An alpha level of 0.05 was the criterion for statistical significance.

3 Results

3.1 Benthic macrofaunal community abundance and structure

A total of 934, 1,090, 763, 1,851 and 171 individual macrofaunal organisms were picked and identified from the inner, middle and outer basins of Andvord Bay, Gerlache Strait and Station B, respectively. When nematodes were included, the highest macrofaunal abundance was found in Gerlache Strait ($69,710 \pm 9,694$ ind. m^{-2} [$n = 4$, SD]). When nematodes were excluded, the highest macrofaunal abundance was found in Middle Basin ($34,133 \pm 7,685$ ind. m^{-2} [$n = 4$, SD]) (Fig. 25). Station B had the lowest macrofaunal abundance with $6,425 \pm 1,058$ ind. m^{-2} ($n = 4$, SD) including nematode and $4,659 \pm 407$ ind. m^{-2} ($n = 4$, SD) excluding nematodes (Fig. 25). Macrofaunal abundance (inc. nematodes) differed among stations, with significantly greater abundance at Gerlache Strait than at all the other stations in Andvord Bay and Station B ($p < 0.001$, One-Way ANOVA) (Fig. 25).
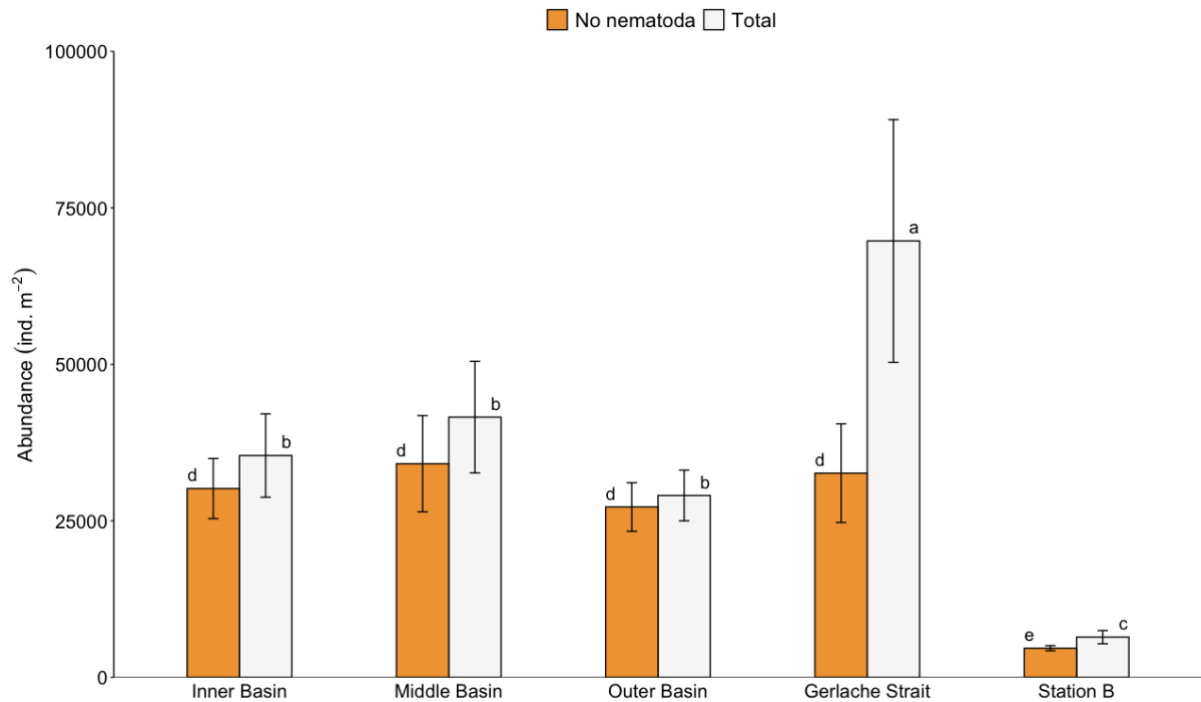
Figure 25: Mean macrofaunal abundance across Andvord Bay, Gerlache Strait and Station B for total number of individuals (ind. m^{-2}) with ("Total", a, b, c) and without ("No Nematoda", d, e) nematodes. One-Way ANOVA tested significant differences ($p < 0.05$) between stations using "Total" and "No Nematoda" as single factors. Significant differences are designated by different letters. Error bars denote ± SD.

Taxa accumulation curves generated for the sites in Andvord Bay, Gerlache Strait and Station B approached an asymptote after 4 cores were sampled suggesting that additional sampling was probably not needed to get a better picture of the macrofaunal communities in the area (Fig. 26). Rarefaction curves showed that the locations in Andvord Bay had similar taxonomic richness, Gerlache Strait supported more than 30 different types of taxa (3,000 individuals). Although fewer animals were sampled at Station B, taxonomic richness was higher at Station B compared to all other sites (30 taxa in 1,000 individuals), and with no signs of an asymptote macrofaunal evenness was also greater (Fig. 26).
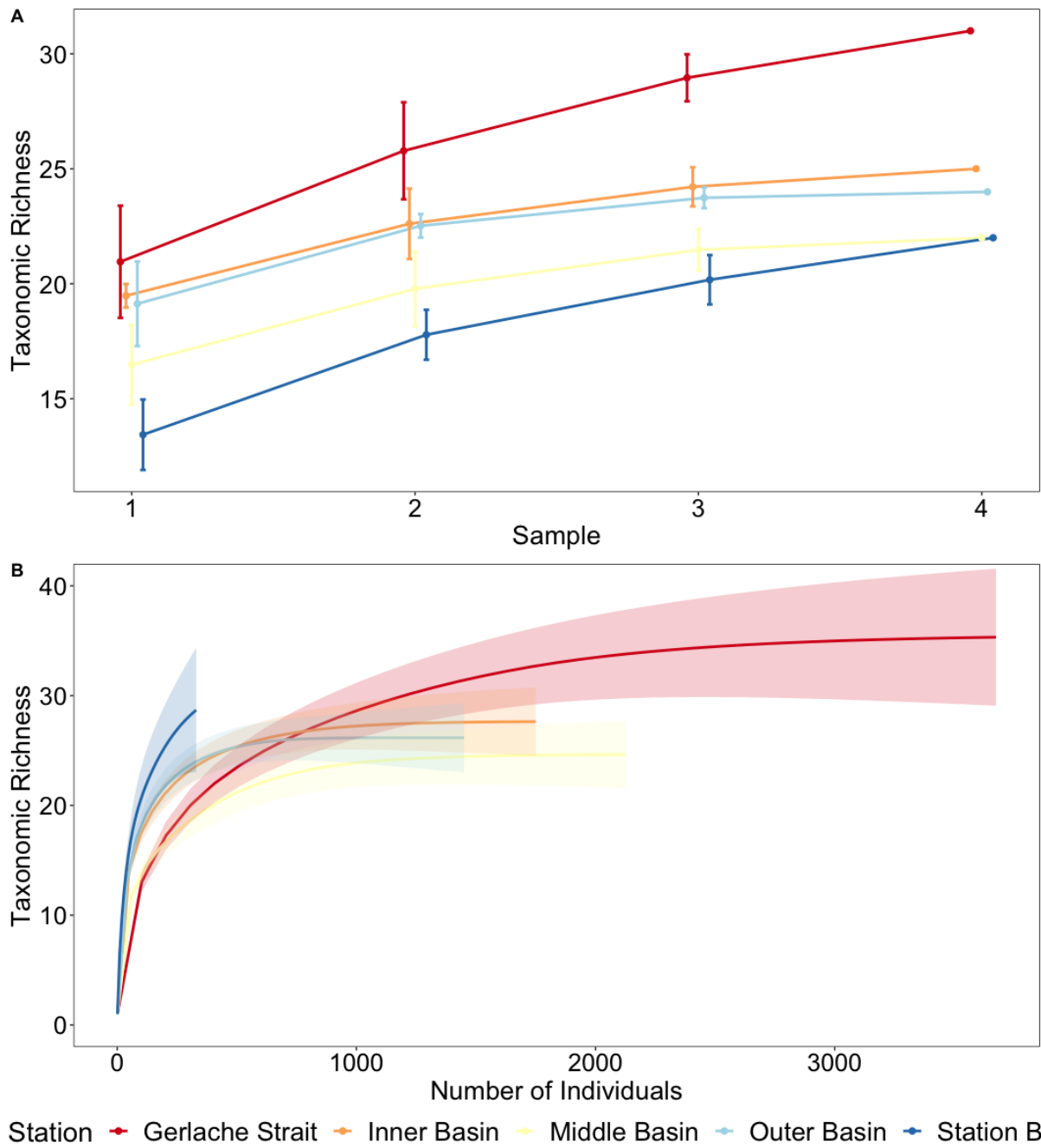
Figure 26: (A) Taxa accumulation curves (S observed) for the different sites on the WAP. Data are mean ± SD. (B) Rarefaction curves for the different sites on the WAP as means ± 95% confidence intervals.

When Nematoda were excluded, the Polychaeta were the most abundant taxon at all stations. If we included nematodes, the Nematoda dominated the community at Gerlache Strait accounting for 53% of the total macrofaunal abundance, followed by Polychaeta (24%), and all the other taxa (Fig. 27). When Nematoda were excluded, Crustacea was the second most

abundant taxon in Andvord Bay accounting for 19%, 18% and 8% of the total community in the Inner, Middle and Outer Basin, respectively. Here, Nematoda accounted for 18%, 18% and 8% of the total community in the Inner, Middle and Outer Basin of the fjord, respectively. Infaunal taxonomic richness was greater in the Inner fjord location with 10 taxonomic groups relative to 8, 9, 8 and 9 groups in the Middle and Outer Basins, Gerlache Strait and Station B, respectively (Fig. 27).
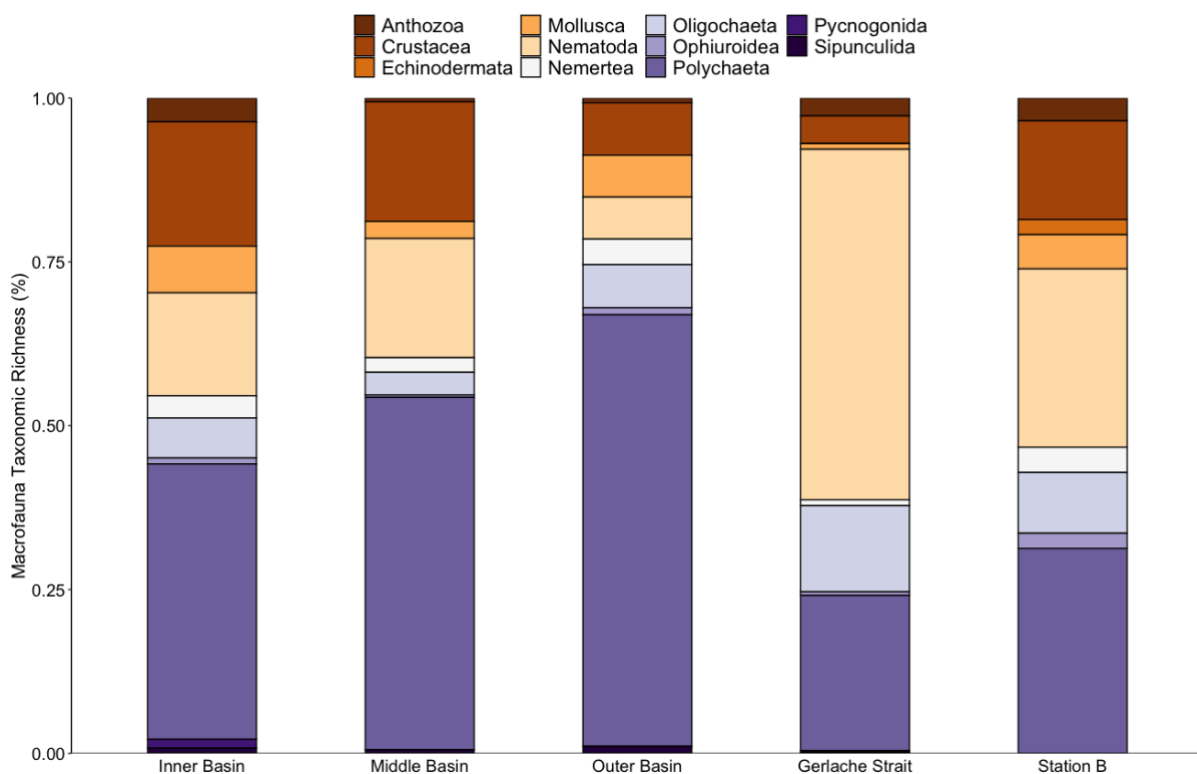
Figure 27: Taxonomic richness of macrofauna collected in the Inner, Middle and Outer Basins of Andvord Bay, Gerlache Strait and Station B.

A nMDS using untransformed macrofauna abundance data showed clear clustering of benthic communities among Andvord Bay, Gerlache Strait and Station B (Fig. 28). Macrofaunal communities found in Andvord Bay and Gerlache Strait were significantly different (R =1.0, p = 0.003; ANOSIM) to the benthic community on the continental shelf at Station B showing an average dissimilarity >75% (SIMPER). Macrofaunal communities in the fjord were clustered closer together showing an average dissimilarity of 48% between fjord stations (SIMPER) and

while the Inner and Middle Basin had a R value of 0.52 ($p = 0.003$; ANOSIM), the Outer Basin showed more differences compared to the other fjord stations (Inner: R = 1.0, $p = 0.003$; Middle: R = 0.98, $p = 0.003$; ANOSIM). The benthic community at Gerlache Strait was both significantly different (60% dissimilarity [SIMPER]) to the sites in the fjord (R = 1.0, $p = 0.003$; ANOSIM) and the continental shelf (R = 1.0, $p = 0.003$; ANOSIM). The taxonomic groups that contributed most to separating the different sites from the continental shelf were Tanaidacea (18.04%) for the Inner Basin, Cirratulidae (26.63%) for the Middle Basin, Paraonidae (43.82%) for the Outer Basin, and Nematoda (52.21%) for Gerlache Strait. SIMPER analysis showed that overall average similarity within the different sites was 76.37% for the Inner Basin, 67.34% for the Middle Basin, 78% for the Outer Basin, 73.89% at Gerlache Strait and 66.84% at Station B. The highest contributions to the similarity matrix in the Inner Basin were from the Tanaidacea (19.34%), Nematoda (15.79%) and Lumbrineridae (14.80%). Similarly, Nematoda, Cirratulidae and Tanaidacea contributed to the highest similarity in the Middle Basin cores (22.78% and 20.72% and 18.12% respectively) while Paraonidae (52.27%), Nematoda (7.22%) and Cirratulidae (6.65%) contributed to the similarities in the Outer Basin. Nematoda was responsible for more than 50% similarity at Gerlache Strait while Paraonidae and Oligochaeta contributed to less than 15%. Nematoda (31.34%), Spionidae (23.18%) and Oligochaeta (12.44%) were responsible for most of the similarity amongst samples at Station B.
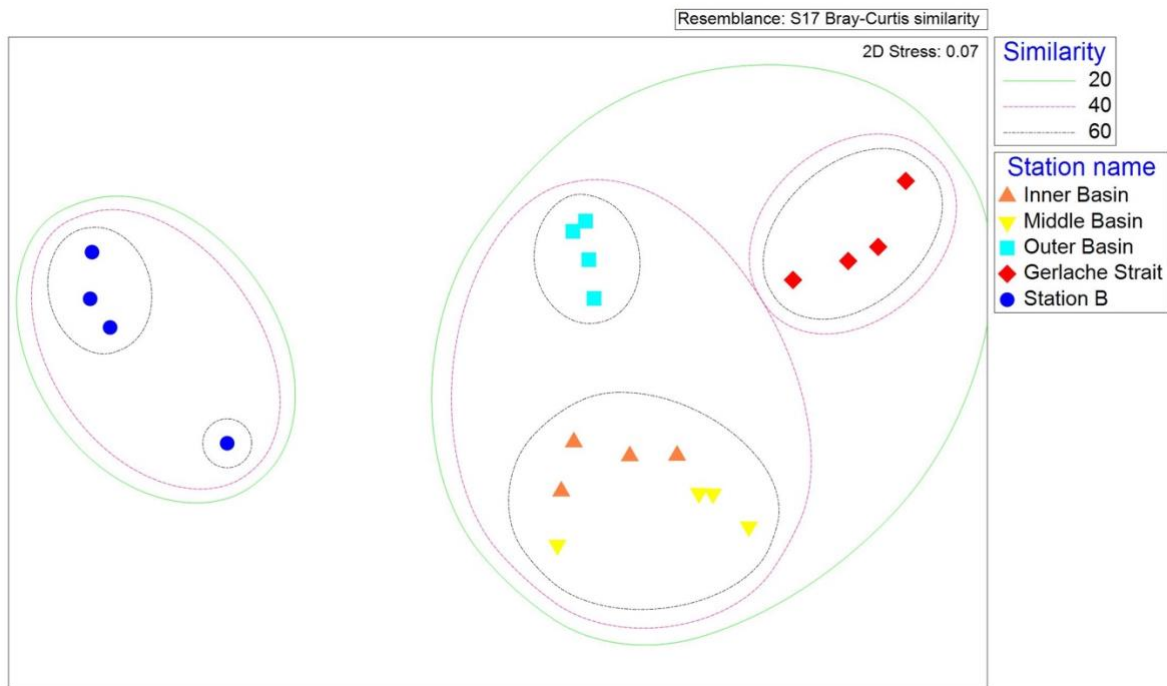
Figure 28: Macrofauna community and abundance non-metric multidimensional scaling plot by site generated by a Bray-Curtis resemblance matrix. Similarity lines show less than 20%, 40% and 60% and similarity between site illustrating community separation (ANOSIM, R = 0.95, $p < 0.001$, $n = 5$). Data are not transformed.

Crustacea taxonomic richness was similar between the Inner and the Middle Basin with similar abundances of tanaids (85% and 88%, respectively), ostracods (5% and 4%, respectively), copepods (6%) and amphipods (2%) (Fig. 29). Copepods were most abundant in the Outer Basin (48%) followed by ostracods (24%), tanaids (21%) and amphipods (6%). Gerlache Strait and Station B had the highest Crustacea diversity with 6 orders represented where copepods remained among the most abundant order (41% and 22%, respectively) (Fig. 29).
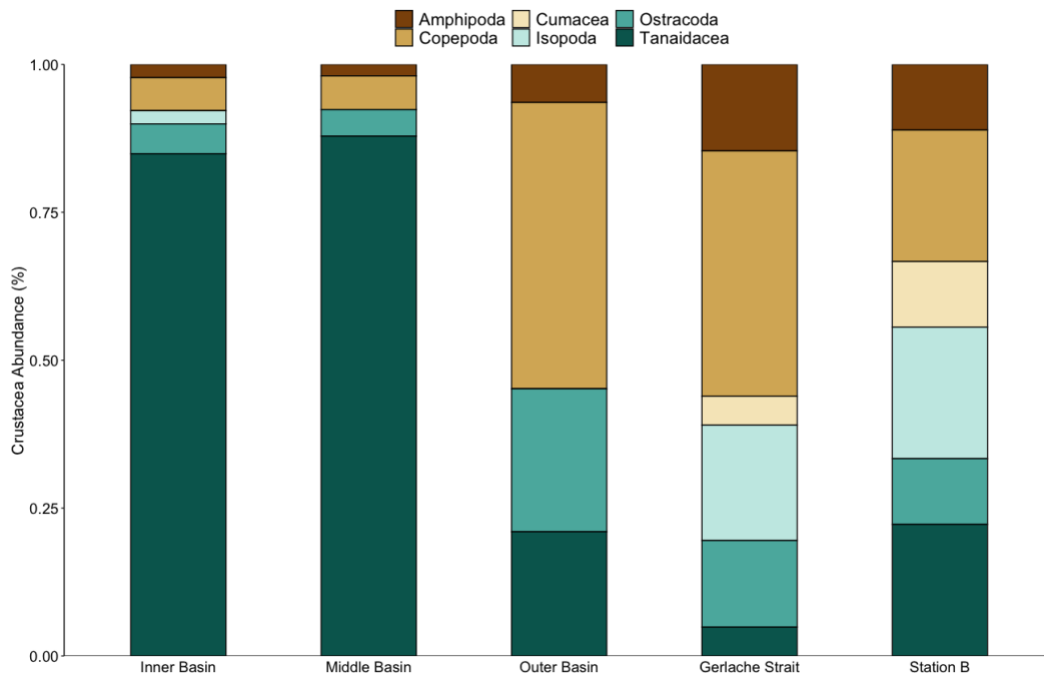
Figure 29: Taxonomic richness of Crustacea collected in the Inner, Middle and Outer Basins of Andvord Bay, Gerlache Strait and Station B.

Polychaeta family richness varied among stations (Fig. 30) with Gerlache Strait having the highest number of families (17) followed by the sites in the fjord (Outer Basin, 14; Inner Basin, 13; Middle Basin, 12) and Station B (11). Paraonids and cirratulids heavily dominated the Inner, Middle and Outer Basins in terms of the polychaete assemblage with lumbrinerids also contributing 27% of the polychaete fauna in the Inner basin. Paraonidae and Cirratulidae also dominated the Gerlache Strait polychaete community as well as Sternapsidae (22%) (Fig. 30). The polychaete assemblage at Station B was characterized by greater evenness with spionids, lumbrinerids and ampharetids contributing the most to polychaete densities (Fig. 30). These differences were also reflected in polychaeta feeding guilds richness at the different locations where the fjord and Gerlache Strait were characterized by a more dominant surface deposit feeder and carnivore assemblage, while Station B was characterized more by suspension / surface deposit feeders, such as Spionidae (Fig. 31).

Figure 30: Polychaeta family richness in the Inner, Middle and Outer Basins of Andvord Bay, Gerlache Strait and Station B.

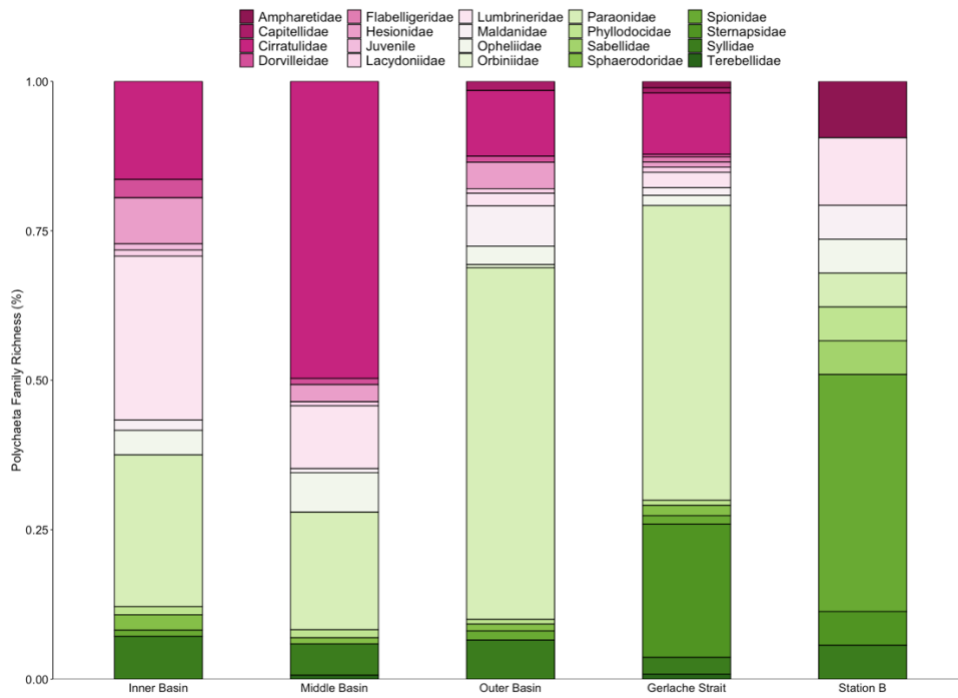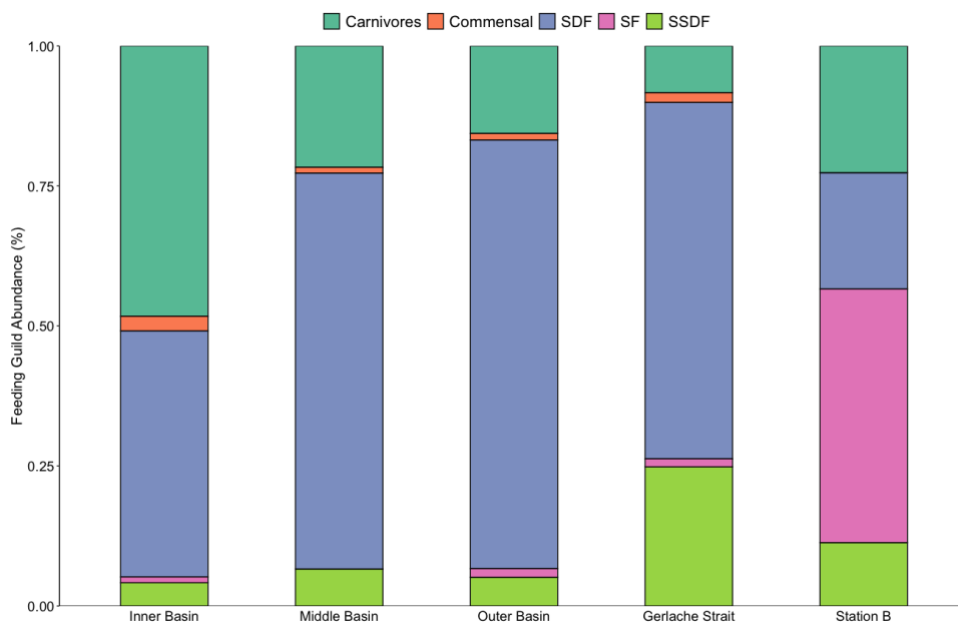Figure 31: Polychaeta feeding guild richness in the Inner, Middle and Outer Basin of Andvord Bay, Gerlache Strait and Station B. Polychaeta feeding guilds found included carnivores, suspension feeders as ("SF"), subsurface deposit feeders as ("SSDF"), surface deposit feeders ("SDF") and commensal feeders.

In terms of macrofaunal biomass (nematodes included), mean biomass was measured from samples collected from the inner location (10.00 ± 3.33 g C m^{-2} [$n = 4$, SD]) and middle section of the fjord (10.72 ± 8.11 g C m^{-2} [$n = 4$, SD]). Macrofaunal biomass was 0.36 ± 0.15 g C m^{-2} ($n = 3$, SD) in the Outer Basins, and this increased to 5.27 ± 1.48 g C m^{-2} [$n = 4$, SD]) in Gerlache Strait before dropping to 0.59 ± 0.64 g C m^{-2} ($n = 4$, SD) at Station B (Fig. 32). Even though statistical analysis showed that C biomass was significantly different between stations (p < 0.001, One-Way ANOVA, Fig. 32), no clear clustering of stations was seen in the nMDS using untransformed macrofaunal carbon biomass data (Fig. 33) with weak interactions among different locations (R = 0.341, $p = 0.001$; ANOSIM). Here, SIMPER analysis showed that the overall average similarity within the different stations was 56.32% for the Inner Basin, 56.43% for the Middle Basin, 52.45% for the Outer Basin, 41.88% for Gerlache Strait and 3.36% for Station B. The locations in the fjords and Gerlache Strait were > 90% dissimilar compared to Station B with Nemertea (Inner Basin: 16.84%; SIMPER), Cirratulidae (Middle Basin: 29.25%; Outer Basin: 14.76%, SIMPER), and Sternapsidae (Gerlache Strait: 17.78%, SIMPER) driving most of the differences. The stations in the fjord and Gerlache Strait were >70% dissimilar to one another with Lumbrineridae in the Inner Basin (13.47%; SIMPER), Cirratulidae in the Middle Basin (19.93%; SIMPER) and Maldanidae in the Outer Basin (11.82%; SIMPER) contributing to the most dissimilarity to Gerlache Strait.
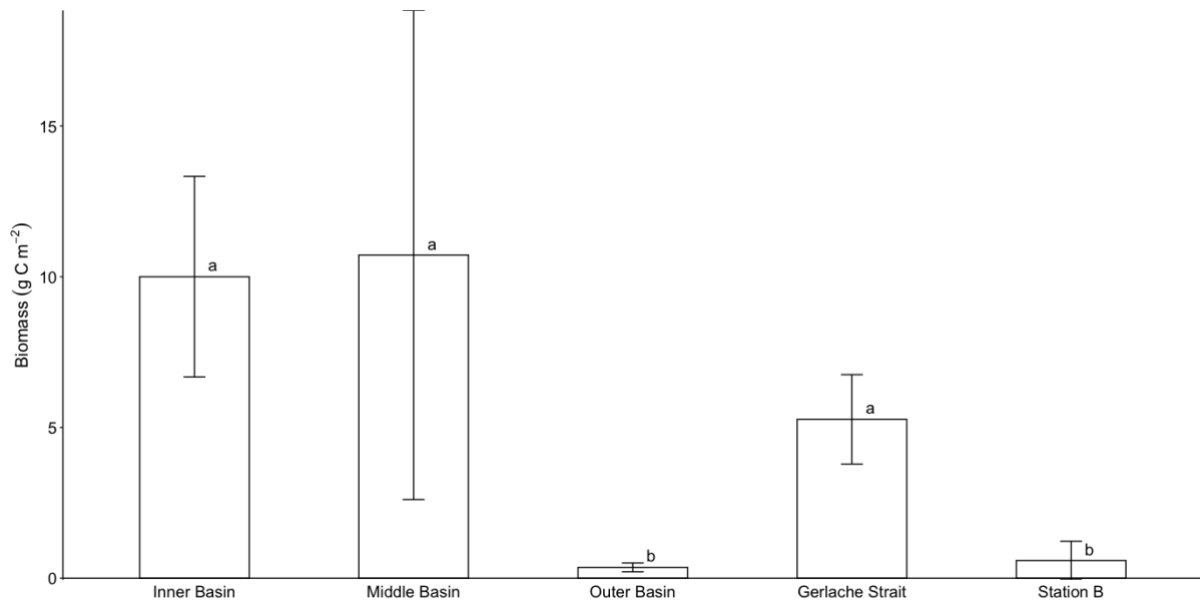
Figure 32: Mean macrofaunal biomass across Andvord Bay, Gerlache Strait and at Station B. Significant differences ($p < 0.05$) between stations are designated by different letters. Error bars denote ± SD.
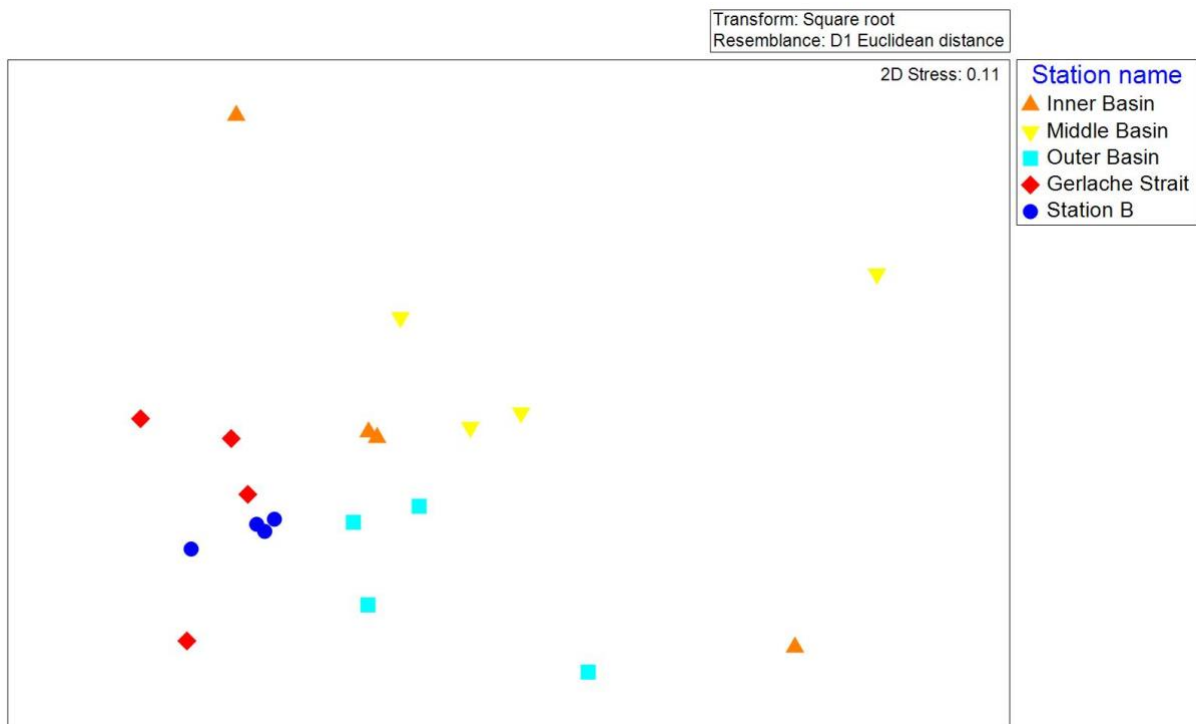
Figure 33: Macrofauna biomass non-metric multidimensional scaling plot by site generated by a Euclidean distance resemblance matrix. Data are square root transformed.

Polychaeta contributed most of the macrofaunal carbon biomass both in Andvord Bay (Inner Basin: 59%; Middle Basin: 78%; Outer Basin: 94%), and Gerlache Strait (74%), while it only

contributed to 26% at Station B (nematodes included). Here on the continental shelf, Crustacea was the dominant taxa, responsible for 66% of the total macrofaunal carbon biomass (Fig. 34). The Polychaeta families that contributed most to polychaete C biomass were different across the various sites with maldanids contributing to 66% of the total polychaete biomass in the Inner Basin, cirratulids accounting for 52% in the Middle Basin, capitellids (23%) and opheliids (31%) accounting for the highest polychaete biomass in the Outer Basin and Gerlache Strait, respectively, and lumbrinerids accounting for 48% of the total polychaete C biomass at Station B (Fig. 35).
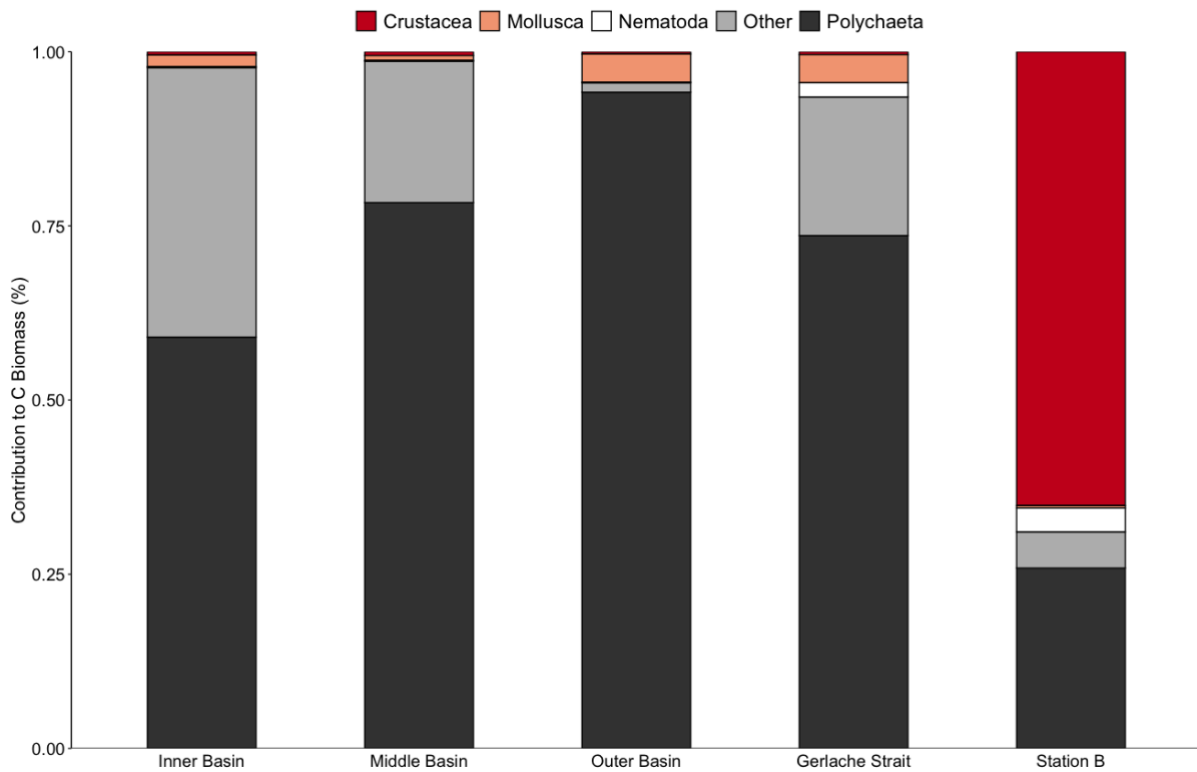
Figure 34: Taxonomic contribution to macrofaunal C biomass in Andvord Bay, Gerlache Strait and Station B.
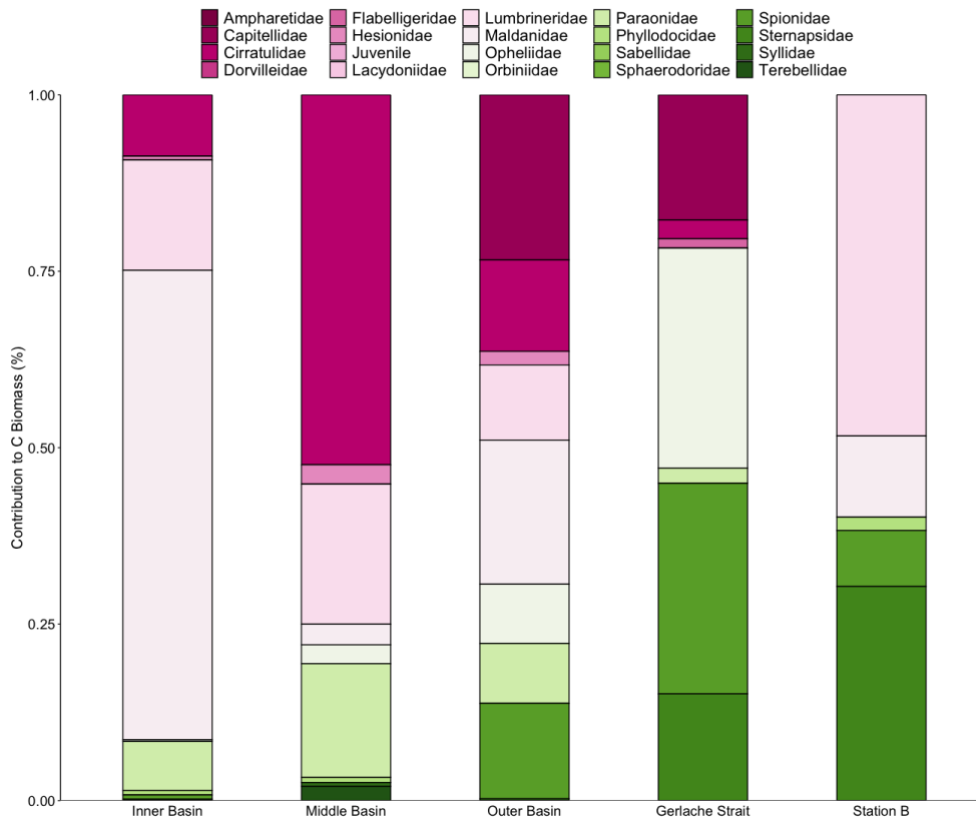
Figure 35: Polychaeta family contribution to C biomass in Andvord Bay, Gerlache Strait and Station B.

3.2 *^{13}C labelling experiments*

Mean total macrofaunal C-uptake was significantly higher ($p < 0.001$, One-Way ANOVA) in the Inner (9.55 ± 4.87 mg C m^{-2} d^{-1}[$n = 4$, SD]) and Middle Basins of the fjord (12.76 ± 2.74 mg C m^{-2} d^{-1} [$n = 4$, SD]) compared to the other stations. In the Outer Basin, macrofaunal C-uptake was 0.24 ± 0.11 mg C m^{-2} d^{-1} ($n = 3$, SD). Among the lowest C-uptake rates measured, Gerlache Strait was 0.37 ± 0.37 mg C m^{-2} d^{-1} ($n = 4$, SD) while rates at Station B were higher (0.56 ± 0.86 mg C m^{-2} d^{-1} [$n = 4$, SD]) were comparatively similar to the Outer Basin (Fig. 36). No significant difference was observed in total macrofaunal C-uptake between the Outer Basin, Gerlache Strait and Station B (Fig. 36). No clear clustering among different sites was seen in a nMDS using untransformed macrofaunal C-uptake rate data (R = 0.393, $p = 0.001$; ANOSIM) (Fig. 37). SIMPER analysis showed that overall average squared distance was 17.76% in the Inner Basin, 18% in the Middle Basin, 12.16% in the Outer Basin, 0.03% at Gerlache Strait

and 0% at Station B. The highest average squared distance was between the Inner and the Middle Basins (80.80%) followed by the Inner and the Outer Basins (63.17%) and the Middle Basin and Station B (55.33%). Here, the groups that contributed the most to the different distances were Cirratulidae (50.59%) in differentiating the Inner and the Middle Basin, Lumbrineridae (73.30%) in differentiating between the Inner and the Outer Basin, and again the Cirratulidae (86.49%) in differentiating between the Middle Basin and Station B.
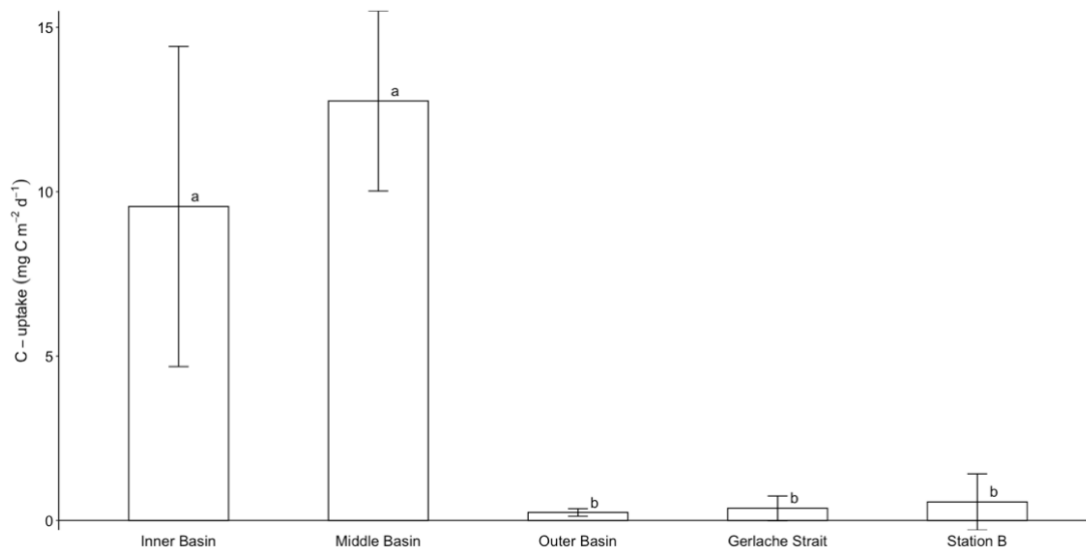
Figure 36: Mean macrofaunal C-uptake observed across Andvord Bay, Gerlache Strait and Station B. Significant differences ($p < 0.05$) between sites are designated by different letters. Error bars denote $\pm$ SD.
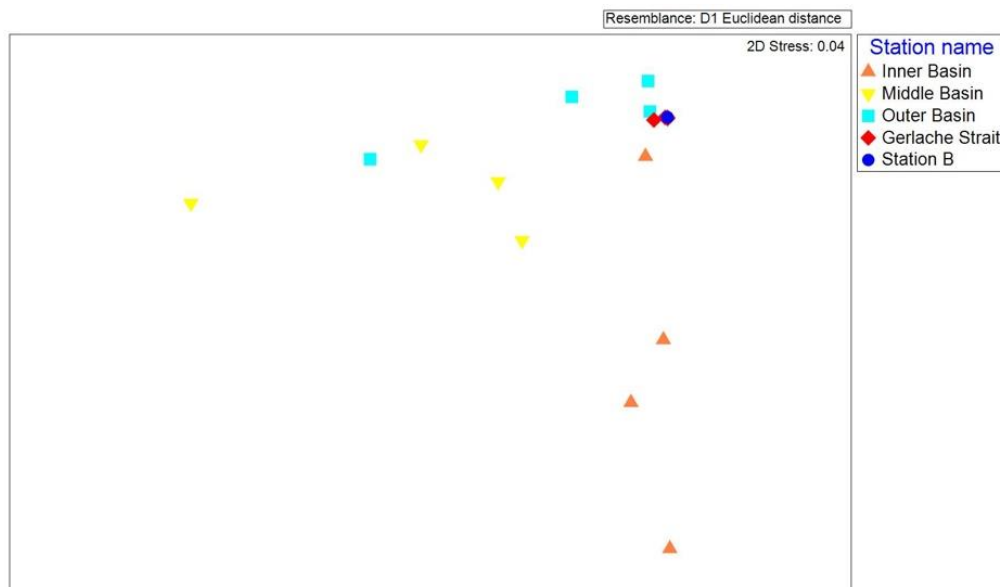
Figure 37: Macrofaunal C-uptake non-metric multidimensional scaling plot by site generated by a Euclidean distance resemblance matrix. Data are square root transformed.

The Polychaeta contributed most to macrofaunal C-uptake rate in the fjord (Inner Basin: 88%; Middle Basin: 98%; Outer Basin: 99%) and in Gerlache Strait (62%) while this group accounted only for 25% of the total C-uptake at Station B (Fig. 38). Crustacea was the group that contributed to the highest amount of C-uptake (75%) at Station B while it contributed less than 1% to uptake in Andvord Bay and Gerlache Strait (Fig. 38). In terms of C-uptake as a function of polychaete family, lumbrinerids (6.02 ± 3.93 mg C m^{-2} d^{-1} [$n = 4$, SD]) in the Inner Basin and cirratulids in the Middle (6.22 ± 3.49 mg C m^{-2} d^{-1} [$n = 4$, SD]) and Outer Basins (2.39 ± 3.06 mg C m^{-2} d^{-1} [$n = 3$, SD]) and Gerlache Strait (0.11 ± 0.16 mg C m^{-2} d^{-1} [$n = 4$, SD]) contributed the most to polychaete C-uptake, while the Maldanidae (0.04 mg C m^{-2} d^{-1} [$n = 1$]) contributed the most to polychaete C-uptake out Station B. The Nematoda showed no uptake at all in this study (Fig. 39).
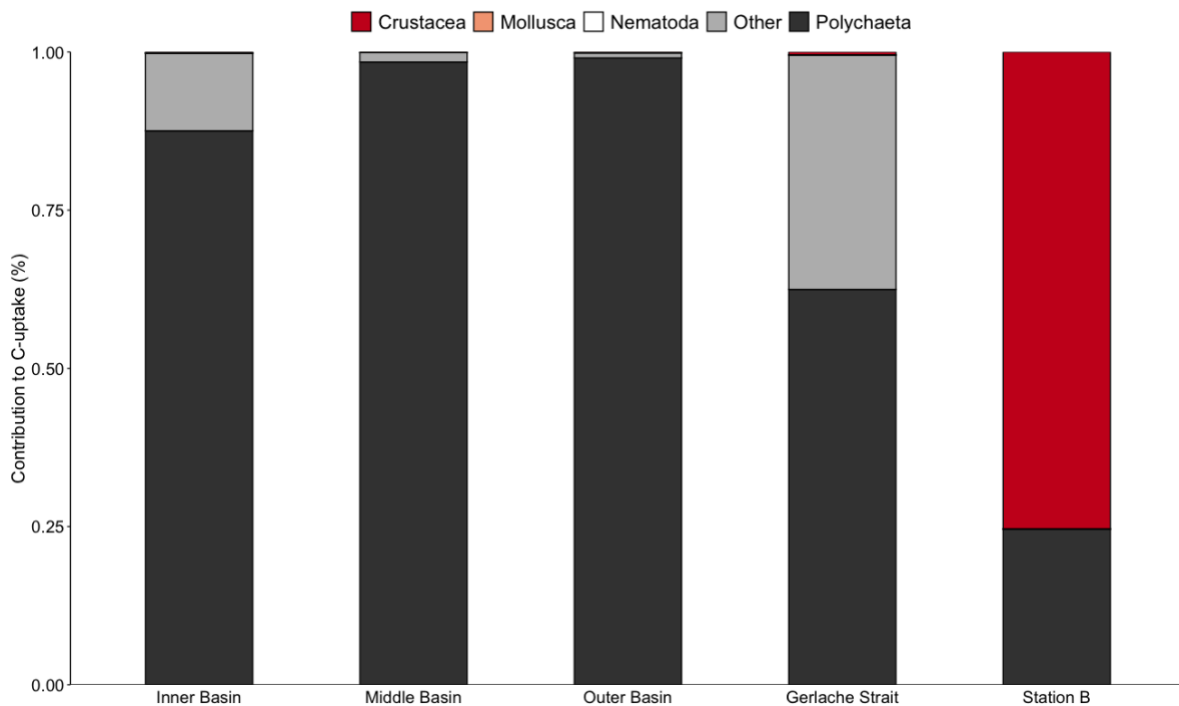
Figure 38: Taxa contribution to macrofaunal C-uptake rates in Andvord Bay, Gerlache Strait and Station B.
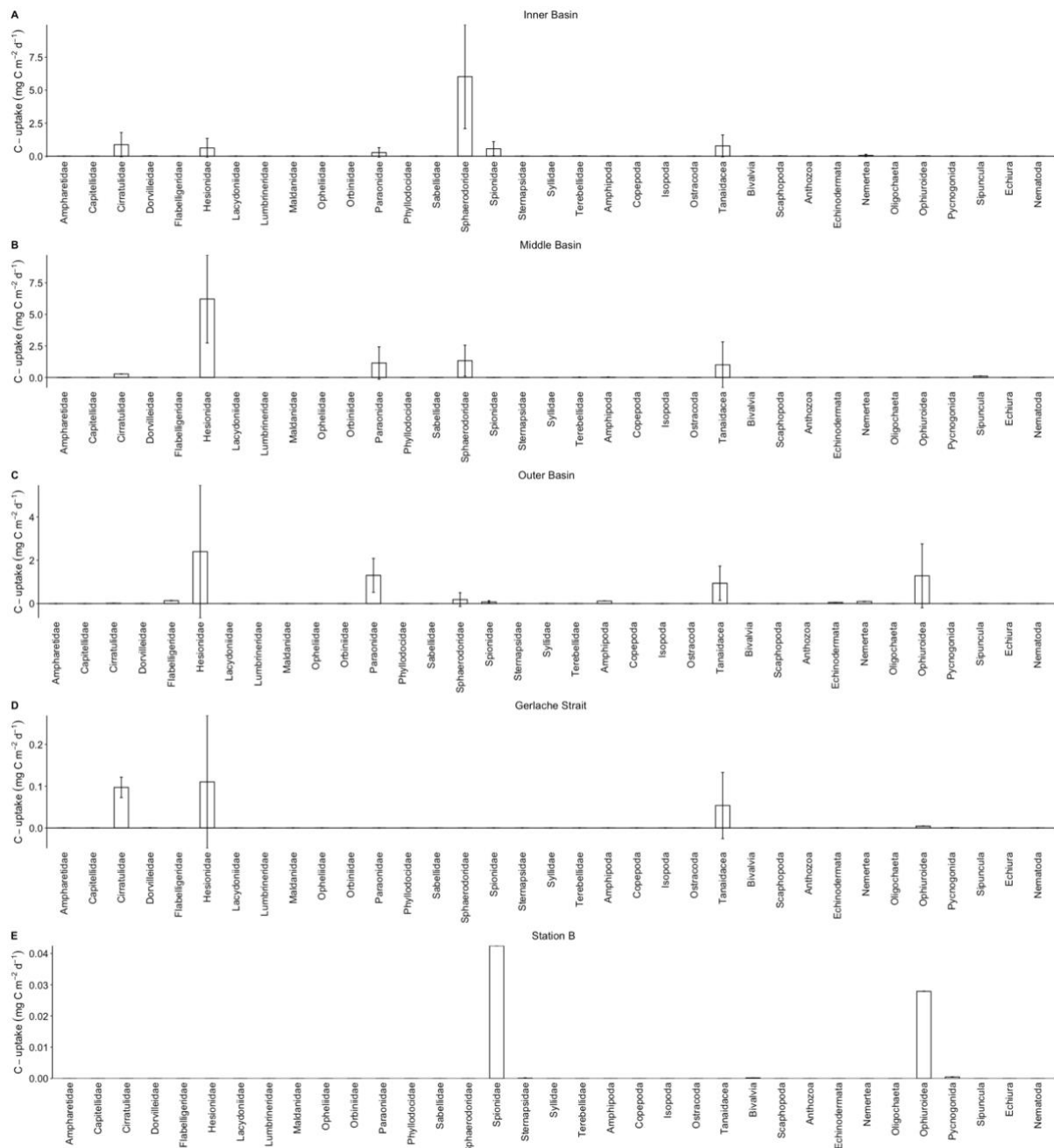
Figure 39: Total C-uptake by polychaete family and orders for the different sites studied. Error bars denote ± SD.

There was no significant difference between the C-uptake rates for the different polychaete feeding guilds for the different locations ($p = 0.45$, SRH) (Fig. 40). Carnivores contributed to the highest C-uptake in the Inner Basin (6.32 ± 4.11 mg C m^{-2} d^{-1} [$n = 4$, SD]), surface deposit feeders were responsible for the highest uptake in the Middle Basin (6.24 ± 3.45 mg C m^{-2} d^{-1} [$n = 4$, SD]), Outer Basin (3.41 ± 3.47 mg C m^{-2} d^{-1} [$n = 3$, SD]) and Gerlache Strait ($0.20 \pm$

103

0.33 mg C m^{-2} d^{-1} [n = 4, SD]) while subsurface deposit feeders accounted for the highest rates at Station B (0.13 ± 0.06 mg C m^{-2} d^{-1} [n = 4, SD]) (Fig. 40). It is important to note the contribution of suspension feeders to C-uptake in the Outer Basin (1.28 ± 1.48 mg C m^{-2} d^{-1} [n = 3, SD]) as in the other locations was negligeable or absent.
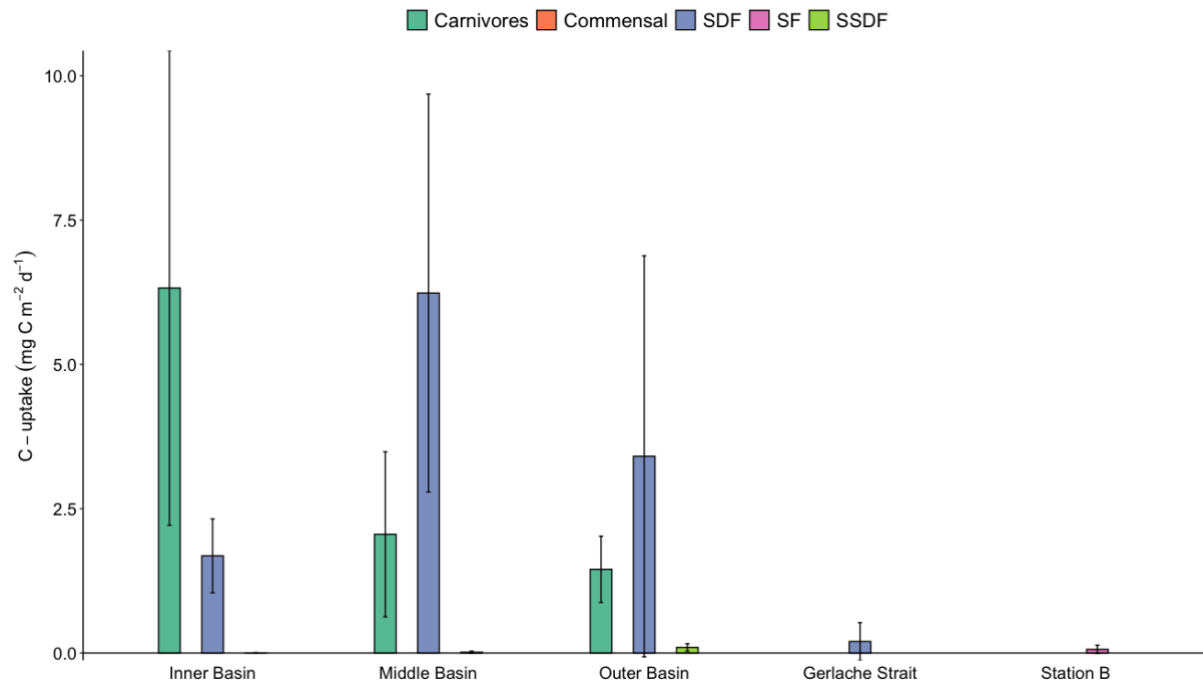
Figure 40: Mean C-uptake by different polychaeta feeding guilds in the different sites along Andvord Bay, Gerlache Strait and Station B. Polychaeta feeding guilds were carnivores, suspension feeders ("SF"), subsurface deposit feeders ("SSDF"), surface deposit feeders ("SDF") and commensal feeders. Error bars denote ± SD.

4   Discussion

This study sampled seafloor sediments and undertook pulse-chase experiments from multiple locations down a glaciomarine fjord and out on the continental shelf of the WAP to assess and explore benthic macrofaunal function and structure. We found significant differences in benthic macrofaunal abundance, biomass and C-uptake among the different study sites. Station B had the lowest benthic macrofaunal abundance (4,659 ± 407 ind. m^{-2}) and the resemblance matrix analysis (Fig. 28) illustrated a different macrofaunal community on the WAP

continental shelf compared to Andvord Bay. The inner and middle fjord basins were characterized by the highest macrofaunal biomass and C-uptake rates compared to the fjord mouth and Stations B. Macrofaunal C-uptake rates were also higher in the Inner and Middle Basins compared to Gerlache strait, which collectively point to the inner and middle fjord basins being hotspots of macrobenthic secondary production and function. We also found that surface feeding macrofauna took up more C in the fjord locations compared to Station B. As such our hypothesis that the fjord would have higher macrofauna abundance, biomass and C-uptake rates than the adjacent continental slope is supported. This study thus highlights the importance of glaciomarine fjords along the WAP and indicates that glacial melting may have significant impacts on benthic macrofaunal structure and function in fjord ecosystems situated along the WAP if global warming progresses.

4.1 Benthic community and biomass

Macrofaunal abundances measured at Station B in previous studies such as the FOODBANCS program (13,844 ± 1,974 ind. m^{-2}, Glover et al. 2008) were much higher than in this study (4,659 ± 407 ind. m^{-2}, Fig. 25) probably due to seasonality as samples collection for the FOODBANCS program occurred both in the fall and in the spring. Although no Copepoda or Ostracoda were reported during the FOODBANCS program, similarly to our study, Tanaidacea was the most common crustacean order found during the study accounting for 62% of the total crustacea found at Station B followed by Amphipoda (19%), Isopoda (18%) and Cumacea (1%) (Glover et al. 2008). Polychaeta were the major contributors to taxonomic composition in both the Glover et al. (2008) study and at Station B in this investigation (nematodes excluded), and Spionidae were the most abundant polychaete family at Station B (Glover et al. 2008), which was also consistent with this study (Fig. 30). Polychaeta was also the dominant taxon in Andvord Bay (nematodes excluded) and surface deposit feeders represented the majority of

polychaetes in Andvord Bay and Gerlache Strait in contrast to Station B. The greater availability of primary production and phytodetritus flux in the fjord (Ziegler et al. 2020) could be one of the drivers for this macrobenthic community difference between the fjord and adjacent shelf as has already been observed for megafaunal communities in the abyssal Pacific and Atlantic Oceans (Smith Jr. et al. 1994; Billett et al. 2001). Indeed, high abundances of subsurface deposit feeders taxa such as Maldanidae and Sternapsidae have been associated with enhanced productivity and food availability in sediments (Neal et al. 2014; Drennan et al. 2021), which would indicate high POC fluxes in Inner and Outer Basin, consistent with relatively high maldanid biomasses (Fig. 35). Investigations into variations in faunal composition in the Prince Gustav Channel (Drennan et al. 2021), the East Antarctic Shelf (Post et al. 2017), the Ross Sea (Cummings et al. 2006), the South Orkney Island (Brasier et al. 2018) and King George Island (Quartino et al. 2001) observed that fine-scale habitat heterogeneity, such as substrate type and composition (e.g., presence and absence of dropostones) can be a major driver leading to different macrofaunal communities being found in different areas. Ziegler et al. (2017) documented higher abundances of drop stones in the inner parts of WAP fjords.

Benthic macrofaunal abundances and biomasses in the inner and middle basins of Andvord Bay were significantly higher (Fig. 32 and 36) compared to the continental shelf at Station B. In fact, mean macrofaunal abundance at sites along the fjord (Inner Basin: $30,155 \pm 4,794$ ind. m^{-2}; Middle Basin: $34,133 \pm 7,685$ ind. m^{-2}; Outer Basin: $26,905 \pm 4,691$ ind. m^{-2}) and Gerlache Strait ($32,615 \pm 7,874$ ind. m^{-2}) were 6 to 7 times greater than the continental shelf. This pattern has also been found in the benthic megafauna from Andvord Bay and Flandres Bay (situated immediately south of Andvord Bay) where megafaunal abundances were 3 to 38- fold greater than at stations on the adjacent continental shelf (Grange and Smith 2013). Elevated levels of POC flux to the seafloor in Andvord Bay, previously measured to be 17-24 g C m^{-2} yr^{-1} (Eidam

et al. 2019; Ziegler et al. 2020) likely lead to higher faunal abundances and biomasses, which have knock on effects on faunal feeding activities in Andvord Bay compared to Station B. Elevated primary productivity in the fjord basins of Andvord Bay and eventual export out of the bay could have also led to the higher benthic macrofaunal abundance and biomass at Gerlache Strait (Fig. 32 and 36). Studies have shown that particles captured in sediment traps can originate several kilometers away from traps (Siegel et al. 2008), so sinking POC produced in Andvord Bay could have been settling to the seafloor of Gerlache Strait enhancing macrobenthic abundance and biomass.

Previous studies in the Arctic (e.g., in Svalbard) have repeatedly shown lower benthic macrofaunal and megafaunal abundances in inner and middle fjord basins compared to the outer sections of fjords and the adjacent continental slope (Wlodarska-Kowalczuk et al. 2005; Wesławski et al. 2011; Meyer et al. 2015). Moreover, macrobenthic species richness in Arctic fjords decreases from outer reaches of fjords to the inner fjord locations as a result from chronic physical disturbance and burial stress related to deglaciation and meltwater runoff (Wlodarska-Kowalczuk et al. 2005). As time and deglaciation progresses in the Arctic, predictions suggest that the chronic environmental disturbance that fjord basins are exposed to will lessen and they will become refugia as the cold and very saline water pockets provide ideal habitats for cold-water species (Wesławski et al. 2011). In contrast to the Arctic, the inner and middle basins of WAP fjords are exposed to less meltwater runoff effects because the glaciers are at an earlier stage of warming (Grange and Smith 2013). This leads to enhanced light penetration and primary productivity, and elevated food-supply to the seafloor and limited burial disturbance (Grange and Smith 2013; Grange et al. 2017; Ziegler et al. 2017, Lundesgaard et al. 2020, Ziegler et al. 2020). It is these more favourable conditions that likely led to the inner and middle basins of Andvord Bay being hotspots of macrobenthic abundance and biomass reletive to fjords that have been studied extensively in the Arctic (e.g., Kongsfjorden).

4.2 Benthos response to the addition of labelled material

Concomitant with the elevated macrobenthic abundance and biomass in the fjord relative to Station B, macrofaunal C-uptake rates were significantly greater in the inner and middle basins compared to the 3 remaining stations. This gradient in macrofaunal C-uptake as well as biomass and abundance agrees with the data from Grange and Smith (2013), and again suggests that inner and middle basins in fjords along the WAP are hotspots of benthic ecosystem function in contrast to the adjacent shelf and their Arctic counterparts due to less sedimentation and burial disturbance, high levels of overlying surface primary production and POC flux to the seafloor (Wlodarska-Kowalczuk et al. 2005; Wesławski et al. 2011; Grange and Smith 2013; Ziegler et al. 2020). Although the higher macrofaunal C-uptake was partially driven by the higher benthic biomass in the inner and middle stations relative to Station B, the high rates recorded in the inner and middle basin were very likely also related to macrobenthic community composition. Macrofaunal taxonomic composition in Andvord Bay was mainly comprised of polychaetes (nematodes excluded) and within this taxon, paraonids and cirratulids were highly abundant in the Inner and Middle Basin. Their presence has been shown to enhance C-cycling activity compared to communities dominated by other polychaete taxa (Wlodarska-Kowalczuk et al. 2005; Sweetman and Witte 2008; Sweetman et al. 2010, 2014). Interesting, the lumbrinerids contributed the most to macrofaunal C-uptake in the Inner Basin as has also been observed in other studies (Sweetman and Witte 2008b), even though carnivores dominate this family. The high level of feeding activity by this particular taxon in the Inner Basin suggests that they were either feeding on fauna that had previously ingested the labelled material or that Lumbrineridae are capable of carnivory as well as feeding on other food sources such as the enriched diatoms. Isotopic signatures of deposit feeding and carnivorous polychaetes have been found to be similar in some instances (e.g., the deep Pacific Ocean at Station M, Sweetman and Witte 2008) and polychaetes that usually are considered carnivores such as syllids ingest highly refractory

detritus. In a previous study on the effects of jelly-falls on the benthos in an Arctic Fjord (Fanafjorden), Spionidae contributed the most to macrobenthic biomass and displayed the highest C-uptake rates among the polychaeta families (Sweetman et al. 2016). However, in our study, this family was only relevant in terms of C-uptake in the Inner Basin, Outer Basin and at Station B (Fig. 39), where total C-uptake rates and biomass were significantly lower than the inner locations of Andvord Bay.

The C-uptake rates seen in the Inner and Middle Basin stations were similar to macrofaunal C-uptake rates measured in pulse-chase experiments conducted using sediments from Fanafjorden in Norway (Sweetman et al. 2016), and the similarity between the WAP and a boreal fjord in western Norway are surprising given that the WAP experiments were undertaken at -1°C and the Fanafjorden study was conducted at 7-8°C. Given a similar temperature in the WAP to the Arctic fjord, the different sites would have higher C-uptake rates, in particular the rates in the Inner and the Middle Basin would range between 89.02 and 111.46 mg C m^{-2} d^{-1}, respectively, while the Outer Basin, Gerlache Strait and Station B would show lower rates ranging from 10.13 mg C m^{-2} d^{-1} to 5.10 mg C m^{-2} d^{-1}. Furthermore, algal turnover rates in Arctic fjords (~0.04-0.1 d^{-1}, Sweetman et al. 2014, 2016) compare well with rates measured in the Outer Basin, Gerlache Strait and Station B (0.03-0.07 d^{-1}) while the 1-2 orders of magnitude higher rates in the Inner and Middle Basins (1.14-1.52 d^{-1}) suggest that labile detritus is consumed much faster and benthic biogeochemical cycling capacity is higher in the inner parts of WAP glaciomarine fjords compared to sites on the continental shelf.

Macrofaunal abundance, biomass and C-uptake rates between the inner and middle fjord locations were not significantly different, however, these metrics were slightly higher in the middle fjord location. Previous studies have shown that a high flux of organic matter can significantly affect the benthic environment (e.g., Pearson and Rosenberg 1978; Sweetman et al. 2010, 2014; Bannister et al. 2014). Therefore, it is possible that intense pulses of organic

material to the seabed in the innermost parts of the fjord (Ziegler et al. 2020) could be negatively impacting the benthic environment right next to the glacier and creating a gradient of organic enrichment (Pearson and Rosenberg 1978) where the inner basin is slightly more organically enriched leading to slightly lower macrofaunal abundance and biomass next to the glacier and lower C-uptake compared to the middle station, which was characterized by biomass and C-uptake maxima. Further experiments are needed to confirm this.

5 Conclusions

This study assessed macrofauna abundance, biomass and composition in a glaciomarine fjord on the WAP and compared these characteristics to Gerlache Strait and Station B on the continental shelf. Furthermore, pulse-chase experiments were undertaken to document the benthic macrofaunal response to a phytodetrital input event at each site. Contrary to the Arctic, our data showed higher macrofaunal abundance and biomass in the inner and middle parts of the fjord compared to the fjord's mouth and the adjacent continental shelf. Similar patterns were seen in terms of macrofaunal C-uptake, which collectively highlight that inner and middle fjord basins are likely 'hotspots' of macrobenthic abundance, biomass and C-cycling activity relative to the adjacent shelf. These conditions are likely to change as climate warming and glacial retreat in the Antarctic progresses and highlights the urgent need to better understand climate sensitivity of the fjords along the WAP and their resilience to significant environmental changes.

CHAPTER 5

CONCLUSIONS AND FUTURE RESEARCH

The deep sea is the largest ecosystem on Earth and remains mostly unknown and undiscovered (Ramirez-Llodra et al. 2011). It is often seen as a vast, dark and inhospitable environment and yet it provides us with many ecosystem services and functions that contribute to support our way of life (Thurber et al. 2014). In the last decades, the deep sea has had to face increasing challenges in relation to anthropogenic impacts that will continue to significantly change this environment (Ramirez-Llodra et al. 2011). For example, rising concerns about the depletion of land-based high grade mineral ores and the increasing demand for minerals for renewable energy has turned our attention to deep-sea mining, such as polymetallic nodules on abyssal plains (Levin et al. 2020a). In particular, the polymetallic nodules deposits in the Clarion-Clipperton Zone (CCZ) have shown great potential for supporting future supplies of high grade mineral ores (Levin et al. 2020a) and are now being targeted for deep-sea mining. Even though, the ISA has established nine no-mining areas (APEIs) to protect regional biodiversity, data about the representativeness of APEIs to license mining areas is still scarce (Simon-Lledó et al. 2019).

Furthermore, climate change is increasingly impacting the marine environment where polar regions are among the fastest warming areas of the planet (Kerr et al. 2018) and while the Arctic ecosystems already indicate advanced stages of climate change (Wlodarska-Kowalczuk et al. 2005), the Antarctic margins have started showing significant impacts in the last two decades and are only now rapidly changing (Grange and Smith 2013; Kerr et al. 2018). Baseline environmental studies, before a disturbance takes place, are an important action that allows us to better understand how ecosystem services and functions will change over time that can help manage different environmental impacts (Thurber et al. 2014).

This project used pulse-chase experiments to investigate benthic ecosystem functioning across different deep-sea habitats such as abyssal plains and bathyal glaciomarine fjords, regions that are likely to be impacted by deep-sea mining and already indicate impacts of climate change.

Overall, my results collectively highlight the importance of POC flux in driving ecosystem dynamics at the abyssal plain of the CCZ and at bathyal depths on the West Antarctic Peninsula. This study supports the widespread view that Antarctic fjords are hotspots of biodiversity and ecosystem functions as I found significantly higher benthic metabolism and C-cycling activity in the inner basins of the fjords, which was in stark contrast to the responses often seen in inner basins of Arctic fjords. The macrofaunal community illustrates further differences between the WAP shelf and fjords, noting clear contrasts between fjord, strait and shelf biota. I also found that the macrofaunal community to be the main contributor to short-term C-uptake (~1 d) in the fjord settings, while bacteria were the key player in short-term C-cycling (1.5 d) on the abyssal plain of the equatorial Pacific Ocean, a finding consistent with numerous other studies that have shown that bacteria are key players in the short-term degradation of detritus at abyssal depths.

However, this research also highlights some key knowledge gaps, which opens the opportunity to propose new studies to improve our understanding of benthic ecosystem functioning in deep-sea environments. This study surveyed, for the first time, benthic ecosystem functioning in the western APEIs of the CCZ and compared these areas to other areas in the CCZ investigated in other studies (De Smet et al. 2017; Wilson 2017; Sweetman et al. 2019) to better assess how processes vary across the different POC flux regimes that characterize the region (McQuaid et al. 2020). However, my dataset shed little information on the effectiveness of the APEIs to preserve and safeguard benthic diversity as no other similar studies from license areas located close to the studied APEIs was available for comparison. Also, the concentration of polymetallic nodules in mine claim areas can be as high as 10-15 kg m^{-2}, and yet, my survey was conducted on soft sediment with little to no nodules present. The APEIs surveyed were situated along a POC flux gradient, from the more eutrophic APEI in the south (#7, ~2 g C_{org} m^{-2} yr^{-1}) to the more oligotrophic APEI in the north (#1, ~1 g C_{org} m^{-2} yr^{-1}) (Lutz et al. 2007;

McQuaid et al. 2020), but a more complete and richer dataset would allow us to better understand the implications of using POC flux in future marine spatial planning studies and management plans. Furthermore, the role of bacteria in the short-term C-cycling in abyssal plains requires further investigation. Bacteria play a key role in the initial degradation of fresh phytodetritus in abyssal plains (e.g., Lochte and Turley 1988; Sweetman et al. 2019), and further research revealed that DIC fixation can provide an additional source of C to the benthic communities in the eastern CCZ (Sweetman et al. 2019).

This study also explored benthic ecosystem functioning in a bathyal fjord, Andvord Bay, and the bathyal continental shelf of the WAP offering baseline information on benthic ecosystem processes in an Antarctic fjord. Seasonal ice cover along the fjord is an important driver of benthic ecosystem functioning (e.g., Braeckman et al. 2021) and given the seasonal changes in sea ice dynamics along Andvord Bay (Lundesgaard et al. 2020), exploring how benthic ecosystem functioning changes in different seasons under different sea ice cover can improve our understating of the region. For example, research in Potter Cove demonstrated shifts in benthic community metabolism from autotrophy to heterotrophy following glacial melt disturbance due to El Niño-La Niña alternations (Braeckman et al. 2021). Furthermore, more glaciomarine fjords in the WAP and more sites along the continental shelf should be investigated to confirm our findings. Megafaunal community surveys in three subpolar glaciomarine fjords (Andvord, Flandres and Barilari Bays) and along the open shelf of the WAP identified these fjords as important biodiversity hotspots (Grange and Smith 2013), able to provide important habitats and foraging areas for Antarctic krill and baleen whales (Nowacek et al. 2011). As we study the benthic ecosystem functioning of more Antarctic fjords, we will be able to provide important information on the structure and dynamics of the fjords along the WAP and verify if, similarly to the megafaunal benthic community, benthic ecosystem functioning is commonly higher within the Antarctic basins or if the hydrography,

dynamics and energetics of Andvord Bay are the key environmental characteristics that make this fjord a greater "hotspot" for benthic metabolism and ecosystem functioning. Given the changes expected on the environment and ecosystem dynamics in the Antarctic peninsula due to climate warming (Kerr et al. 2018), meltwater and sediment inputs will likely become increasingly deleterious for the environment as seen in the Arctic (Wlodarska-Kowalczuk et al. 2005; Barnes et al. 2018).

The benthic macrofaunal community along the Antarctic fjord and the continental shelf of the WAP and its response to phytodetritus was explored in Chapter 3 where I showed differences in macrofaunal abundance, biomass and C-uptake rates between the fjord and the continental shelf of the WAP. Andvord Bay is characterized by different benthic macrofaunal communities than Station B on the continental shelf and, within the same fjord, there are significant differences in the macrofaunal C-cycling activity between the inner and outer fjord basins. Once again, Polychaeta contributed the most to macrofaunal composition both in the fjord and on the continental shelf with distinct differences in Polychaeta family diversity between the different stations and if the inner basins of the fjord showed a predominance of tanaids, other groups of crustaceans were more evenly represented in the other stations. Differences between Andvord Bay and continental shelf macrofaunal communities were also reflected in Polychaeta feeding guilds as surface deposit feeder and carnivore assemblages dominated the fjord while suspension/surface deposit feeders dominated the continental shelf. However, the most distinctive difference was in macrofaunal C-cycling activity within Andvord Bay. The inner basins of the fjord (Inner and Middle Basin stations) sustained significantly higher C-uptake rates than the outer stations. Macrofaunal C-cycling activity in Andvord Bay and Gerlache Strait were dominated by polychaetes whereas macrofaunal C-cycling at Station B was dominated by crustaceans. Further studies are needed to address knowledge gaps in terms of the functioning of other benthic community components such as the role of meiofaunal and

foraminiferal communities in fjord carbon cycling. In Korsfjorden, a deep Norwegian fjord, C-uptake rates of large-size foraminifera (>250 μm) were very slow following a simulated phytodetritus sedimentation event with evidence that the delayed response was likely driven by differences in community composition and structure (Sweetman et al. 2009). An assessment of foraminifera carbon cycling would be interesting to address in Antarctic fjords to compare if the response seen in the macrofauna is also detected in the foraminifera community. Two recent studies looked at the megafaunal community in WAP subpolar fjords that compare results to the continental shelf using photographic surveys (Grange and Smith 2013; Ziegler et al. 2020) providing extensive insights on megafaunal composition, abundance and trophic structure in the area (Grange and Smith 2013) and demonstrating seasonal coupling and decoupling of detritivore activity in the fjord (Ziegler et al. 2020). Further studies on megafaunal feeding activity could also improve our understanding of the role of megafauna in processing labile organic carbon in Antarctic fjord ecosystems.

Benthic ecosystem functioning on the abyssal plain of the western CCZ and in a bathyal fjord and continental shelf of the WAP have been investigated in light of the anthropogenic impacts that are and will soon impact these areas. Marine protected areas are key to safeguard these unique environments, and thus baseline studies on APEIs in the CCZ are fundamental to improve our understanding of their effectiveness in protecting the unique ecosystem attributes of the CCZ. Polar environments are perhaps the most affected regions of our planet by climate change, and, with time, current climate warming impacts will become even more severe. Therefore, there is an urgent need to address these aforementioned issues, which will improve our understanding of the implications of deep-sea mining and climate change in deep-sea ecosystems.

References

Aberle, N., and U. Witte. 2003. Deep-sea macrofauna exposed to a simulated sedimentation event in the abyssal NE Atlantic: in situ pulse-chase experiments using ^{13}C-labelled phytodetritus. Mar. Ecol. Prog. Ser. **251**: 37–47. doi:10.3354/meps251037

Al-Habahbeh, A. K., S. Kortsch, B. A. Bluhm, F. Beuchel, B. Gulliksen, C. Ballantine, D. Cristini, and R. Primicerio. 2020. Arctic coastal benthos long-term responses to perturbations under climate warming: climate change impact on Arctic benthos. Philos. Trans. R. Soc. A Math. Phys. Eng. Sci. **378**. doi:10.1098/rsta.2019.0355

Amesbury, M. J., T. P. Roland, J. Royles, D. A. Hodgson, P. Convey, H. Griffiths, and D. J. Charman. 2017. Widespread biological response to rapid warming on the Antarctic Peninsula. Curr. Biol. **27**: 1616-1622.e2. doi:10.1016/j.cub.2017.04.034

Amon, D. J., A. Hilario, P. M. Arbizu, and C. R. Smith. 2017. Observations of organic falls from the abyssal Clarion-Clipperton Zone in the tropical eastern Pacific Ocean. Mar. Biodivers. **47**: 311–321. doi:10.1007/s12526-016-0572-4

Anderson, T. R., and T. Rice. 2006. Deserts on the sea floor: Edward Forbes and his azoic hypothesis for a lifeless deep ocean. Endeavour **30**: 131–137. doi:10.1016/j.endeavour.2006.10.003

Archer, D., and E. Maier-Reimer. 1994. Effect of deep-sea sedimentary calcite preservation on atmospheric CO_2 concentration. Nature **367**: 260–263. doi:10.1038/367260a0

Ardron, J. A., E. Simon-Lledó, D. O. B. Jones, and H. A. Ruhl. 2019. Detecting the effects of deep-seabed nodule mining: simulations using megafaunal data from the Clarion-Clipperton Zone. Front. Mar. Sci. **6**: 1–13. doi:10.3389/fmars.2019.00604

Aspetsberger, F., M. Zabel, T. Ferdelman, U. Struck, A. Mackensen, A. Ahke, and U. Witte. 2007. Instantaneous benthic response to different organic matter quality: in situ experiments in the Benguela Upwelling System. Mar. Biol. Res. **3**: 342–356.

doi:10.1080/17451000701632885

Bannister, R. J., T. Valdemarsen, P. K. Hansen, M. Holmer, and A. Ervik. 2014. Changes in benthic sediment conditions under an Atlantic salmon farm at a deep, well-flushed coastal site. Aquac. Environ. Interact. **5**: 29–47. doi:10.3354/aei00092

Barnes, D. K. A. 2017. Polar zoobenthos blue carbon storage increases with sea ice losses, because across-shelf growth gains from longer algal blooms outweigh ice scour mortality in the shallows. Glob. Chang. Biol. **23**: 5083–5091. doi:10.1111/gcb.13772

Barnes, D. K. A., A. Fleming, C. J. Sands, M. L. Quartino, and D. Deregibus. 2018. Icebergs, sea ice, blue carbon and Antarctic climate feedbacks. Philos. Trans. R. Soc. A Math. Phys. Eng. Sci. **376**. doi:10.1098/rsta.2017.0176

Barnes, D. K. A., and G. A. Tarling. 2017. Polar oceans in a changing climate. Curr. Biol. **27**: R454–R460. doi:10.1016/j.cub.2017.01.045

Becker, H. J., B. Grupe, H. U. Oebius, and F. Liu. 2001. The behaviour of deep-sea sediments under the impact of nodule mining processes. Deep. Res. Part II **48**: 3609–3627. doi:10.1016/S0967-0645(01)00059-5

Berelson, W. M., R. F. Anderson, J. Dymond, and others. 1997. Biogenic budgets of particle rain, benthic remineralization and sediment accumulation in the equatorial Pacific. Deep. Res. Part II **44**: 2251–2282. doi:10.1016/S0967-0645(97)00030-1

Billett, D. S. M., B. J. Bett, A. L. Rice, M. H. Thurston, J. Galéron, M. Sibuet, and G. A. Wolff. 2001. Long-term change in the megabenthos of the Porcupine Abyssal Plain (NE Atlantic). Prog. Oceanogr. **50**: 325–348. doi:10.1016/S0079-6611(01)00060-X

Boetius, A., and K. Lochte. 1996. Effect of organic enrichments on hydrolytic potentials and growth of bacteria in deep-sea sediments. Mar. Ecol. Prog. Ser. **140**: 239–250. doi:10.3354/meps140239

Bonifácio, P., P. Martínez Arbizu, and L. Menot. 2020. Alpha and beta diversity patterns of

polychaete assemblages across the nodule province of the eastern Clarion-Clipperton

Fracture Zone (equatorial Pacific). Biogeosciences **17**: 865–886. doi:10.5194/bg-17-

865-2020

Bopp, L., L. Resplandy, J. C. Orr, and others. 2013. Multiple stressors of ocean ecosystems in

the 21st century: projections with CMIP5 models. Biogeosciences **10**: 6225–6245.

doi:10.5194/bg-10-6225-2013

Borowski, C., and H. Thiel. 1998. Deep-sea macrofaunal impacts of a large-scale physical

disturbance experiment in the Southeast Pacific. Deep. Res. Part II **45**: 55–81.

doi:10.1016/S0967-0645(97)00073-8

Boyd, P. W., and T. W. Trull. 2007. Understanding the export of biogenic particles in oceanic

waters: is there consensus? Prog. Oceanogr. **72**: 276–312.

doi:10.1016/j.pocean.2006.10.007

Braeckman, U., F. Pasotti, R. Hoffmann, and others. 2021. Glacial melt disturbance shifts

community metabolism of an Antarctic seafloor ecosystem from net autotrophy to

heterotrophy. Commun. Biol. **4**: 1–11. doi:10.1038/s42003-021-01673-6

Brasier, M. J., S. M. Grant, P. N. Trathan, and others. 2018. Benthic biodiversity in the South

Orkney Islands Southern Shelf Marine Protected Area. Biodiversity **19**: 5–19.

doi:10.1080/14888386.2018.1468821

Brinch-Iversen, J., and G. M. King. 1990. Effects of substrate concentration, growth state,

and oxygen availability on relationships among bacterial carbon, nitrogen and

phospholipid phosphorus content. FEMS Microbiol. Lett. **74**: 345–355.

doi:10.1111/j.1574-6968.1990.tb04081.x

Buesseler, K. O., C. H. Lamborg, P. W. Boyd, and others. 2007. Revisiting carbon flux

through the ocean's twilight zone. Science **316**: 567–570. doi:10.1126/science.1137959

Bühring, S. I., S. Ehrenhauss, A. Kamp, L. Moodley, and U. Witte. 2006a. Enhanced benthic

activity in sandy sublittoral sediments: Evidence from ^{13}C tracer experiments. Mar. Biol. Res. **2**: 120–129. doi:10.1080/17451000600678773

Bühring, S. I., N. Lampadariou, L. Moodley, A. Tselepides, and U. Witte. 2006b. Benthic microbial and whole-community responses to different amounts of ^{13}C-enriched algae: in situ experiments in the deep Cretan Sea (Eastern Mediterranean). Limnol. Oceanogr. **51**: 157–165. doi:10.4319/lo.2006.51.1.0157

Byrne, R. H., S. Mecking, R. A. Feely, and X. Liu. 2010. Direct observations of basin-wide acidification of the North Pacific Ocean. Geophys. Res. Lett. **37**: 1–5. doi:10.1029/2009GL040999

Campanyà-Llovet, N., P. V. R. Snelgrove, and C. C. Parrish. 2017. Rethinking the importance of food quality in marine benthic food webs. Prog. Oceanogr. **156**: 240–251. doi:10.1016/j.pocean.2017.07.006

Cannariato, K. G., and J. P. Kennett. 1999. Climatically related millennial-scale fluctuations in strength of California margin oxygen-minimum zone during the past 60 k.y. Geology **27**: 975–978. doi:10.1130/0091-7613(1999)027<0975:CRMSFI>2.3.CO;2

Convey, P., and L. S. Peck. 2019. Antarctic environmental change and biological responses. Sci. Adv. **5**. doi:10.1126/sciadv.aaz0888

Cook, A., A. J. Fox, D. G. Vaughan, and J. G. Ferrigno. 2005. Retreating glacier fronts on the Antarctic Peninsula over the past half-century. Science **308**: 541–544. doi:10.1126/science.1104235

Cook, A. J., P. R. Holland, M. P. Meredith, T. Murray, A. Luckman, and D. G. Vaughan. 2016. Ocean forcing of glacier retreat in the western Antarctic Peninsula. Science **353**: 283–286. doi:10.1126/science.aae0017

Cosson, N., M. Sibuet, and J. Galeron. 1997. Community structure and spatial heterogeneity of the deep-sea macrofauna at three contrasting stations in the tropical northeast

Atlantic. Deep. Res. Part I **44**: 247–269.

Cottier, F. R., F. Nilsen, R. Skogseth, V. Tverberg, J. Skardhamar, and H. Svendsen. 2010. Arctic fjords: a review of the oceanographic environment and dominant physical processes. Geol. Soc. Spec. Publ. **344**: 35–50. doi:10.1144/SP344.4

Cronin, T. M., and M. E. Raymo. 1997. Orbital forcing of deep-sea benthic species diversity. Nature **385**: 624–627. doi:10.1038/385624a0

Cummings, V., S. Thrush, A. Norkko, N. Andrew, J. Hewitt, G. Funnell, and A. M. Schwarz. 2006. Accounting for local scale variability in benthos: implications for future assessments of latitudinal trends in the coastal Ross Sea. Antarct. Sci. **18**: 633–644. doi:10.1017/S0954102006000666

Cuvelier, D., P. A. Ribeiro, S. P. Ramalho, D. Kersken, P. Martinez Arbizu, and A. Colaço. 2020. Are seamounts refuge areas for fauna from polymetallic nodule fields? Biogeosciences **17**: 2657–2680. doi:10.5194/bg-17-2657-2020

D'Hondt, S., A. J. Spivack, R. Pockalny, and others. 2009. Subseafloor sedimentary life in the South Pacific Gyre. Proc. Natl. Acad. Sci. U. S. A. **106**: 11651–11656. doi:10.1073/pnas.0811793106

Danovaro, R. 2017. Global change impact on deep-sea ecosystems. GLIDES **1**: 1–7.

Danovaro, R., J. B. Company, C. Corinaldesi, and others. 2010. Deep-sea biodiversity in the Mediterranean Sea: the known, the unknown, and the unknowable. PLoS One **5**. doi:10.1371/journal.pone.0011832

Danovaro, R., C. Corinaldesi, E. Rastelli, and A. Dell'Anno. 2015. Towards a better quantitative assessment of the relevance of deep-sea viruses, bacteria and Archaea in the functioning of the ocean seafloor. Aquat. Microb. Ecol. **75**: 81–90. doi:10.3354/ame01747

Danovaro, R., C. Gambi, A. Dell'Anno, C. Corinaldesi, S. Fraschetti, A. Vanreusel, M.

Vincx, and A. J. Gooday. 2008. Exponential decline of deep-sea ecosystem functioning linked to benthic biodiversity loss. Curr. Biol. **18**: 1–8. doi:10.1016/j.cub.2007.11.056

Drazen, J. C., R. J. Baldwin, and K. L. Smith. 1998. Sediment community response to a temporally varying food supply at an abyssal station in the NE Pacific. Deep. Res. Part II **45**: 893–913. doi:10.1016/S0967-0645(98)00007-1

Drazen, J. C., A. B. Leitner, S. Morningstar, Y. Marcon, J. Greinert, and A. Purser. 2019. Observations of deep-sea fishes and mobile scavengers from the abyssal DISCOL experimental mining area. Biogeosciences **16**: 3133–3146. doi:10.5194/bg-16-3133-2019

Drazen, J. C., C. R. Smith, K. M. Gjerde, and others. 2020. Midwater ecosystems must be considered when evaluating environmental risks of deep-sea mining. Proc. Natl. Acad. Sci. U. S. A. **117**: 17455–17460. doi:10.1073/pnas.2011914117

Drennan, R., T. G. Dahlgren, K. Linse, and A. G. Glover. 2021. Annelid fauna of the Prince Gustav Channel, a previously ice-covered seaway on the Northeastern Antarctic Peninsula. Front. Mar. Sci. **7**: 595303. doi:10.3389/fmars.2020.595303

Ducklow, H. W., M. R. Stukel, R. Eveleth, and others. 2018. Spring-summer net community production, new production, particle export and related water column biogeochemical processes in the marginal sea ice zone of the Western Antarctic Peninsula 2012-2014. Philos. Trans. R. Soc. A Math. Phys. Eng. Sci. **376**: 20170177. doi:10.1098/rsta.2017.0177

Dunlop, K. M., D. van Oevelen, H. A. Ruhl, C. L. Huffard, L. A. Kuhnz, and K. L. Smith. 2016. Carbon cycling in the deep eastern North Pacific benthic food web: investigating the effect of organic carbon input. Limnol. Oceanogr. **61**: 1956–1968. doi:10.1002/lno.10345

Dunn, D. C., C. L. Van Dover, R. J. Etter, and others. 2018. A strategy for the conservation

of biodiversity on mid-ocean ridges from deep-sea mining. Sci. Adv. **4**: 1–16. doi:10.1126/sciadv.aar4313

Durden, J. M., M. Putts, S. Bingo, and others. 2021. Megafaunal ecology of the Western Clarion Clipperton Zone. Front. Mar. Sci. **8**: 1–22. doi:10.3389/fmars.2021.671062

Eidam, E. F., C. A. Nittrouer, Lundesgaard, K. K. Homolka, and C. R. Smith. 2019. Variability of sediment accumulation rates in an Antarctic fjord. Geophys. Res. Lett. **46**: 13271–13280. doi:10.1029/2019GL084499

Epply, R. W., and B. J. Peterson. 1979. Particulate organic matter flux and planktonic new production in the deep ocean. Nature **282**: 677–680.

Fukuda, R., H. Ogawa, T. Nagata, and I. Koike. 1998. Direct determination of carbon and nitrogen contents of natural bacterial assemblages in marine environments. Appl. Environ. Microbiol. **64**: 3352–3358. doi:10.1128/AEM.64.9.3352-3358.1998

Gilly, W. F., J. M. Beman, S. Y. Litvin, and B. H. Robison. 2013. Oceanographic and biological effects of shoaling of the oxygen minimum zone. Ann. Rev. Mar. Sci. **5**: 393–420. doi:10.1146/annurev-marine-120710-100849

Glover, A. G., C. R. Smith, S. L. Mincks, P. Y. G. Sumida, and A. R. Thurber. 2008. Macrofaunal abundance and composition on the West Antarctic Peninsula continental shelf: evidence for a sediment "food bank" and similarities to deep-sea habitats. Deep. Res. Part II **55**: 2491–2501. doi:10.1016/j.dsr2.2008.06.008

Goineau, A., and A. J. Gooday. 2017. Novel benthic foraminifera are abundant and diverse in an area of the abyssal equatorial Pacific licensed for polymetallic nodule exploration. Sci. Rep. **7**: 1–15. doi:doi: 10.1038/srep45288

Gontikaki, E., D. van Oevelen, K. Soetaert, and U. Witte. 2011. Food web flows through a sub-arctic deep-sea benthic community. Prog. Oceanogr. **91**: 245–259. doi:10.1016/j.pocean.2010.12.014

Gooday, A. J., A. Goineau, and I. Voltski. 2015. Abyssal foraminifera attached to polymetallic nodules from the eastern Clarion Clipperton Fracture Zone: a preliminary description and comparison with North Atlantic dropstone assemblages. Mar. Biodivers. **45**: 391–412. doi:10.1007/s12526-014-0301-9

Gooday, A. J., M. Holzmann, C. Caulle, A. Goineau, O. Kamenskaya, A. A. T. Weber, and J. Pawlowski. 2017. Giant protists (xenophyophores, Foraminifera) are exceptionally diverse in parts of the abyssal eastern Pacific licensed for polymetallic nodule exploration. Biol. Conserv. **207**: 106–116. doi:10.1016/j.biocon.2017.01.006

Grange, L. J., and C. R. Smith. 2013. Megafaunal communities in rapidly warming fjords along the West Antarctic Peninsula: hotspots of abundance and beta diversity. PLoS One **8**: e77917. doi:10.1371/journal.pone.0077917

Grange, L. J., C. R. Smith, D. J. Lindsay, B. Bentlage, and M. J. Youngbluth. 2017. High abundance of the epibenthic trachymedusa Ptychogastria polaris Allman, 1878 (Hydrozoa, Trachylina) in subpolar fjords along the West Antarctic Peninsula. PLoS One **12**: 1–21. doi:10.1371/journal.pone.0168648

Grasshoff, K., K. Kremling, and M. Ehrhardt. 1999. Methods of seawater analysis, 3rd ed. K. Grasshoff and L. Anderson [eds.]. Wiley-VCH.

Griffith, T. W., and J. B. Anderson. 1989. Climatic control of sedimentation in bays and fjords of the northern Antarctic Peninsula. Mar. Geol. **85**: 181–204. doi:10.1016/0025-3227(89)90153-9

Gutt, J., E. Isla, J. C. Xavier, and others. 2020. Antarctic ecosystems in transition – life between stresses and opportunities. Biol. Rev. 000-000 doi:10.1111/brv.12679

Halfar, J., and R. M. Fujita. 2002. Precautionary management of deep-sea mining. Mar. Policy **26**: 103–106. doi:10.1016/S0308-597X(01)00041-0

Hammond, D. E., J. Mcmanus, W. M. Berelson, T. E. Kilgore, and R. H. Pope. 1996. Early

diagenesis of organic material in equatorial Pacific sediments: stoichiometry and kinetics. Deep. Res. Part II **43**: 1365–1412.

Hartnett, H., S. Boehme, C. Thomas, D. DeMaster, and C. Smith. 2008. Benthic oxygen fluxes and denitrification rates from high-resolution porewater profiles from the Western Antarctic Peninsula continental shelf. Deep. Res. Part II **55**: 2415–2424. doi:10.1016/j.dsr2.2008.06.002

Hawkings, J. R., J. L. Wadham, L. G. Benning, K. R. Hendry, M. Tranter, A. Tedstone, P. Nienow, and R. Raiswell. 2017. Ice sheets as a missing source of silica to the polar oceans. Nat. Commun. **8**:14198. doi:10.1038/ncomms14198

Hein, J. R., K. Mizell, A. Koschinsky, and T. A. Conrad. 2013. Deep-ocean mineral deposits as a source of critical metals for high- and green-technology applications: comparison with land-based resources. Ore Geol. Rev. **51**: 1–14. doi:10.1016/j.oregeorev.2012.12.001

Helly, J. J., and L. A. Levin. 2004. Global distribution of naturally occurring marine hypoxia on continental margins. Deep. Res. Part I **51**: 1159–1168. doi:10.1016/j.dsr.2004.03.009

Hendry, K. R., M. P. Meredith, and H. W. Ducklow. 2018. The marine system of the West Antarctic Peninsula: status and strategy for progress. Philos. Trans. R. Soc. A **376**: 1–6. doi:10.1098/rsta.2017.0179

Henley, S. F., O. M. Schofield, K. R. Hendry, and others. 2019. Variability and change in the west Antarctic Peninsula marine system: research priorities and opportunities. Prog. Oceanogr. **173**: 208–237. doi:10.1016/j.pocean.2019.03.003

Higgs, N. D., and M. J. Attrill. 2015. Biases in biodiversity: wide-ranging species are discovered first in the deep sea. Front. Mar. Sci. **2**: 1–8. doi:10.3389/fmars.2015.00061

Hoffmann, K., C. Hassenrück, V. Salman-Carvalho, M. Holtappels, and C. Bienhold. 2017. Response of bacterial communities to different detritus compositions in arctic deep-sea

sediments. Front. Microbiol. **8**: 1–18. doi:10.3389/fmicb.2017.00266

Honjo, S., T. Eglinton, C. Taylor, and others. 2014. Understanding the role of the biological pump in the global carbon cycle: an imperative for ocean science. Oceanography **27**: 10–16. doi:10.5670/oceanog.2014.78

Hop, H., T. Pearson, E. N. Hegseth, and others. 2002. The marine ecosystem of Kongsfjorden, Svalbard. Polar Res. **21**: 167–208. doi:10.1111/j.1751-8369.2002.tb00073.x

Howe, J. A., W. E. N. Austin, M. Forwick, M. Paetzel, R. Harland, and A. G. Cage. 2010. Fjord systems and archives: a review. Geol. Soc. Spec. Publ. 344. doi:10.1144/SP344.2

Ingels, J., R. B. Aronson, C. R. Smith, and others. 2021. Antarctic ecosystem responses following ice-shelf collapse and iceberg calving: science review and future research. Wiley Interdiscip. Rev. Clim. Chang. **12**: 1–28. doi:10.1002/wcc.682

International Seabed Authority [ISA]. 2010. A geological model of polymetallic nodule deposits in the Clarion Clipperton Fracture Zone. ISA Tech. Study No. 6 1–105. doi:10.1007/s13398-014-0173-7.2

International Seabed Authority [ISA]. 2020. Deep CCZ Biodiversity Synthesis Workshop Report. 1–4.

International Seabed Authority [ISA]. 2021. Decision of the Council of the International Seabed Authority relating to the review of the environmental management plan for the Clarion-Clipperton Zone.

Johnson, N. A., J. W. Campbell, T. S. Moore, M. A. Rex, R. J. Etter, C. R. McClain, and M. D. Dowell. 2007. The relationship between the standing stock of deep-sea macrobenthos and surface production in the western North Atlantic. Deep. Res. Part I **54**: 1350–1360. doi:10.1016/j.dsr.2007.04.011

Jones, D. O. B., S. Kaiser, A. K. Sweetman, and others. 2017. Biological responses to

disturbance from simulated deep-sea polymetallic nodule mining. PLoS One **12**. doi:10.1371/journal.pone.0171750

Jones, D. O. B., A. Yool, C. L. Wei, S. A. Henson, H. A. Ruhl, R. A. Watson, and M. Gehlen. 2014. Global reductions in seafloor biomass in response to climate change. Glob. Chang. Biol. **20**: 1861–1872. doi:10.1111/gcb.12480

de Jonge, D. S. W., T. Stratmann, L. Lins, and others. 2020. Abyssal food-web model indicates faunal carbon flow recovery and impaired microbial loop 26 years after a sediment disturbance experiment. Prog. Oceanogr. **189**: 102446. doi:10.1016/j.pocean.2020.102446

Jørgensen, B. B., K. Laufer, A. B. Michaud, and L. M. Wehrmann. 2021. Biogeochemistry and microbiology of high Arctic marine sediment ecosystems–Case study of Svalbard fjords. Limnol. Oceanogr. **66**: S273–S292. doi:10.1002/lno.11551

Kaehler, S., E. A. Pakhomov, and C. D. McQuaid. 2000. Trophic structure of the marine food web at the Prince Edward Islands (Southern Ocean) determined by $\delta^{13}C$ and $\delta^{15}N$ analysis. Mar. Ecol. Prog. Ser. **208**: 13–20. doi:10.3354/meps208013

Kaiser, S., C. R. Smith, and P. M. Arbizu. 2017. Editorial: Biodiversity of the Clarion Clipperton Fracture Zone. Mar. Biodivers. **47**: 259–264. doi:10.1007/s12526-017-0733-0

Kanzog, C., A. Ramette, N. V. Quéric, and M. Klages. 2009. Response of benthic microbial communities to chitin enrichment: an in situ study in the deep Arctic Ocean. Polar Biol. **32**: 105–112. doi:10.1007/s00300-008-0510-4

Kedra, M., M. Włodarska-Kowalczuk, and J. M. Wesławski. 2010. Decadal change in macrobenthic soft-bottom community structure in a high Arctic fjord (Kongsfjorden, Svalbard). Polar Biol. **33**: 1–11. doi:10.1007/s00300-009-0679-1

Keeling, R. E., A. Körtzinger, and N. Gruber. 2010. Ocean deoxygenation in a warming

world. Ann. Rev. Mar. Sci. **2**: 199–229. doi:10.1146/annurev.marine.010908.163855

Kerr, R. A. 1984. Manganese nodules grow by rain from above. Science **223**: 576–577.

Kerr, R., M. M. Mata, C. R. B. Mendes, and E. R. Secchi. 2018. Northern Antarctic Peninsula: a marine climate hotspot of rapid changes on ecosystems and ocean dynamics. Deep. Res. Part II **149**: 4–9. doi:10.1016/j.dsr2.2018.05.006

Kersten, O., C. R. Smith, and E. W. Vetter. 2017. Abyssal near-bottom dispersal stages of benthic invertebrates in the Clarion-Clipperton polymetallic nodule province. Deep Sea Res. Part I **127**: 31-40. doi:10.1016/j.dsr.2017.07.001

Khripounoff, A., J.-C. Caprais, P. Crassous, and J. Etoubleau. 2006. Geochemical and biological recovery of the disturbed seafloor in polymetallic nodule fields of the Clipperton-Clarion Fracture Zone (CCFZ) at 5,000-m depth. Limnol. Oceanogr. **51**: 2033–2041. doi:10.4319/lo.2006.51.5.2033

Kim, D. U., J. S. Khim, and I. Y. Ahn. 2021. Patterns, drivers and implications of ascidian distributions in a rapidly deglaciating fjord, King George Island, West Antarctic Peninsula. Ecol. Indic. **125**: 107467. doi:10.1016/j.ecolind.2021.107467

Kuhn, T., A. Wegorzewski, C. Rühlemann, and A. Vink. 2017. Composition, Formation, and Occurrence of Polymetallic Nodules, p. 23–63. *In* R. Sharma [ed.], Deep-Sea Mining: Resource Potential, Technical and Environmental Considerations. Springer International Publishing.

Lee, C., S. Wakeham, and C. Arnosti. 2004. Particulate organic matter in the sea: the composition conundrum. Ambio **33**: 565–575. doi:10.1579/0044-7447-33.8.565

Leitner, A. B., A. B. Neuheimer, E. Donlon, C. R. Smith, and J. C. Drazen. 2017. Environmental and bathymetric influences on abyssal bait-attending communities of the Clarion Clipperton Zone. Deep. Res. Part I **125**: 65–80. doi:10.1016/j.dsr.2017.04.017

Levin, L. 2003. Oxygen minimum zone benthos: adaptation and community response to

hypoxia. Oceanogr. Mar. Biol. an Annu. Rev. **41**: 1–45.

Levin, L. A., D. J. Amon, and H. Lily. 2020a. Challenges to the sustainability of deep-seabed mining. Nat. Sustain. **3**: 784–794. doi:10.1038/s41893-020-0558-x

Levin, L. A., and N. Le Bris. 2015. The deep ocean under climate change. Science **350**: 766–8. doi:10.1126/science.aad0126

Levin, L. A., K. Mengerink, K. M. Gjerde, and others. 2016. Defining "serious harm" to the marine environment in the context of deep-seabed mining. Mar. Policy **74**: 245–259. doi:10.1016/j.marpol.2016.09.032

Levin, L. A., C. L. Wei, D. C. Dunn, and others. 2020b. Climate change considerations are fundamental to management of deep-sea resource extraction. Glob. Chang. Biol. **26**: 4664–4678. doi:10.1111/gcb.15223

Lochte, K., and C. M. Turley. 1988. Bacteria and cyanobacteria associated with phytodetritus in the deep sea. Nature **333**: 67–69. doi:10.1038/333067a0

Lundesgaard, Ø., P. Winsor, M. Truffer, M. Merrifield, B. Powell, H. Statscewich, E. Eidam, and C. R. Smith. 2020. Hydrography and energetics of a cold subpolar fjord: Andvord Bay, western Antarctic Peninsula. Prog. Oceanogr. **181**: 102224. doi:10.1016/j.pocean.2019.102224

Lutz, M. J., K. Caldeira, R. B. Dunbar, and M. J. Behrenfeld. 2007. Seasonal rhythms of net primary production and particulate organic carbon flux to depth describe the efficiency of biological pump in the global ocean. J. Geophys. Res. Ocean. **112**: C10011. doi:10.1029/2006JC003706

Maier, S. R., T. Kutti, R. J. Bannister, P. van Breugel, P. van Rijswijk, and D. van Oevelen. 2019. Survival under conditions of variable food availability: resource utilization and storage in the cold-water coral *Lophelia pertusa*. Limnol. Oceanogr. **64**: 1651–1671. doi:10.1002/lno.11142

Martino, A. De, A. Meichenin, J. Shi, K. Pan, and C. Bowler. 2007. Genetic and phenotypic characterization of *Phaeodactylum tricornutum* (Bacillariophyceae) accessions. J. Phycol. **43**: 992–1009. doi:10.1111/j.1529-8817.2007.00384.x

Mayor, D. J., B. Thornton, S. Hay, A. F. Zuur, G. W. Nicol, J. M. McWilliam, and U. F. M. Witte. 2012. Resource quality affects carbon cycling in deep-sea sediments. ISME J. **6**: 1740–1748. doi:10.1038/ismej.2012.14

McClain, C. R., A. P. Allen, D. P. Tittensor, and M. A. Rex. 2012. Energetics of life on the deep seafloor. Proc. Natl. Acad. Sci. U. S. A. **109**: 15366–15371. doi:10.1073/pnas.1208976109

McQuaid, K. A., M. J. Attrill, M. R. Clark, A. Cobley, A. G. Glover, C. R. Smith, and K. L. Howell. 2020. Using habitat classification to assess representativity of a protected srea network in a large, data-poor area targeted for deep-sea mining. Front. Mar. Sci. **7**: 1–21. doi:10.3389/fmars.2020.558860

Mengerink, K. J., C. L. Van Dover, J. Ardron, and others. 2014. A call for deep-ocean stweardship. Science **344**: 8–10.

Meredith, M. P., and J. C. King. 2005. Rapid climate change in the ocean west of the Antarctic Peninsula during the second half of the 20th century. Geophys. Res. Lett. **32**: 1–5. doi:10.1029/2005GL024042

Middelburg, J. J., C. M. Duarte, and J.-P. Gattuso. 2005. Respiration in coastal benthic communities, p. 206–224. *In* Respiration in Aquatic Ecosystems. Oxford University Press.

Miljutin, D. M., M. A. Miljutina, P. M. Arbizu, and J. Galéron. 2011. Deep-sea nematode assemblage has not recovered 26 years after experimental mining of polymetallic nodules (Clarion-Clipperton Fracture Zone, Tropical Eastern Pacific). Deep. Res. Part I **58**: 885–897. doi:10.1016/j.dsr.2011.06.003

Miljutina, M. A., D. M. Miljutin, R. Mahatma, and J. Galéron. 2010. Deep-sea nematode assemblages of the Clarion-Clipperton Nodule Province (Tropical North-Eastern Pacific). Mar. Biodivers. **40**: 1–15. doi:10.1007/s12526-009-0029-0

Mincks, S. L., C. R. Smith, and D. J. DeMaster. 2005. Persistence of labile organic matter and microbial biomass in Antarctic shelf sediments: evidence of a sediment "food bank". Mar. Ecol. Prog. Ser. **300**: 3–19. doi:10.3354/meps300003

Moffitt, S. E., T. M. Hill, P. D. Roopnarine, and J. P. Kennett. 2015. Response of seafloor ecosystems to abrupt global climate change. Proc. Natl. Acad. Sci. U. S. A. **112**: 4684–4689. doi:10.1073/pnas.1417130112

Molari, M., E. Manini, and A. Dell'Anno. 2013. Dark inorganic carbon fixation sustains the functioning of benthic deep-sea ecosystems. Global Biogeochem. Cycles **27**: 212–221. doi:10.1002/gbc.20030

Moodley, L., J. J. Middelburg, H. T. S. Boschker, G. C. A. Duineveld, R. Pel, P. M. J. Herman, and C. H. R. Heip. 2002. Bacteria and foraminifera: key players in a short-term deep-sea benthic response to phytodetritus. Mar. Ecol. Prog. Ser. **236**: 23–29. doi:10.3354/meps236023

Morata, N., E. Michaud, M. A. Poullaouec, J. Devesa, M. Le Goff, R. Corvaisier, and P. E. Renaud. 2020. Climate change and diminishing seasonality in Arctic benthic processes: benthic processes in an Arctic fjord. Philos. Trans. R. Soc. A Math. Phys. Eng. Sci. **378**. doi:10.1098/rsta.2019.0369

Mullineaux, L. S., A. Metaxas, S. E. Beaulieu, and others. 2018. Exploring the ecology of deep-sea hydrothermal vents in a metacommunity framework. Front. Mar. Sci. **5**. doi:10.3389/fmars.2018.00049

Neal, L., H. Wiklund, A. I. Muir, K. Linse, and A. G. Glover. 2014. The identity of juvenile Polynoidae (Annelida) in the Southern Ocean revealed by DNA taxonomy, with notes

on the status of *Herdmanella gracilis* Ehlers s*ensu* Augener. Mem. Museum Victoria **71**: 203–216. doi:10.24199/j.mmv.2014.71.16

Niner, H. J., J. A. Ardron, E. G. Escobar, and others. 2018. Deep-sea mining with no net loss of biodiversity—An impossible aim. Front. Mar. Sci. **5**: 53. doi:10.3389/fmars.2018.00053

Norling, K., R. Rosenberg, S. Hulth, A. Grémare, and E. Bonsdorff. 2007. Importance of functional biodiversity and species-specific traits of benthic fauna for ecosystem functions in marine sediment. **332**: 11–23.

Nowacek, D. P., A. S. Friedlaender, P. N. Halpin, and others. 2011. Super-aggregations of krill and humpback whales in Wilhelmina bay, Antarctic Peninsula. PLoS One **6**: 2–6. doi:10.1371/journal.pone.0019173

Nozawa, F., H. Kitazato, M. Tsuchiya, and A. J. Gooday. 2006. "Live" benthic foraminifera at an abyssal site in the equatorial Pacific nodule province: Abundance, diversity and taxonomic composition. Deep. Res. Part I **53**: 1406–1422. doi:10.1016/j.dsr.2006.06.001

van Nugteren, P., P. M. J. Herman, L. Moodley, J. J. Middelburg, M. Vos, and C. H. R. Heip. 2009. Spatial distribution of detrital resources determines the outcome of competition between bacteria and a facultative detritivorous worm. Limnol. Oceanogr. **54**: 1413–1419. doi:10.4319/lo.2009.54.5.1413

O'Daly, S. H., S. L. Danielson, S. M. Hardy, R. R. Hopcroft, C. Lalande, D. A. Stockwell, and A. M. P. McDonnell. 2020. Extraordinary carbon fluxes on the shallow Pacific Arctic Shelf during a remarkably warm and low sea ice period. Front. Mar. Sci. **7**: 1–17. doi:10.3389/fmars.2020.548931

van Oevelen, D., M. Bergmann, K. Soetaert, and others. 2011. Carbon flows in the benthic food web at the deep-sea observatory HAUSGARTEN (Fram Strait). Deep. Res. Part I **58**: 1069–1083. doi:10.1016/j.dsr.2011.08.002

van Oevelen, D., K. Soetaert, and C. Heip. 2012. Carbon flows in the benthic food web of the Porcupine Abyssal Plain: the (un)importance of labile detritus in supporting microbial and faunal carbon demands. Limnol. Oceanogr. **57**: 645–664. doi:10.4319/lo.2012.57.2.0645

Pape, E., T. N. Bezerra, F. Hauquier, and A. Vanreusel. 2017. Limited Spatial and Temporal Variability in Meiofauna and Nematode Communities at Distant but Environmentally Similar Sites in an Area of Interest for Deep-Sea Mining. Front. Mar. Sci. **4**: 205. doi:10.3389/fmars.2017.00205

Parkinson, C. L., and D. J. Cavalieri. 2012. Antarctic sea ice variability and trends, 1979-2010. Cryosphere **6**: 871–880. doi:10.5194/tc-6-871-2012

Pasotti, F., L. A. Saravia, M. De Troch, M. S. Tarantelli, R. Sahade, and A. Vanreusel. 2015. Benthic trophic interactions in an Antarctic shallow water ecosystem affected by recent glacier retreat. PLoS One **10**: 1–26. doi:10.1371/journal.pone.0141742

Paulikas, D., S. Katona, E. Ilves, and S. H. Ali. 2022. Deep-sea nodules versus land ores: a comparative systems analysis of mining and processing wastes for battery-metal supply chains. J. Ind. Ecol. 1–24. doi:10.1111/jiec.13225

Paulus, E. 2021. Shedding light on deep-sea biodiversity—A highly vulnerable habitat in the face of anthropogenic change. Front. Mar. Sci. **8**: 1–15. doi:10.3389/fmars.2021.667048

Pearson, T. H., and R. Rosenberg. 1978. Macrobenthic succession in relation to organic enrichment and pollution of the marine environment E. Harold Barnes [ed.]. Oceanogr. Mar. Biol. An Annu. Rev. **16**: 229–311.

Post, A. L., C. Lavoie, E. W. Domack, A. Leventer, A. Shevenell, and A. D. Fraser. 2017. Environmental drivers of benthic communities and habitat heterogeneity on an East Antarctic shelf. Antarct. Sci. **29**: 17–32. doi:DOI: 10.1017/S0954102016000468

Powell, R., and G. W. Domack. 2002. Modern glaciomarine environments, p. 361–389. *In*

J.B.T.-M. and P.G.E. Menzies [ed.], Modern and Past Glacial Environments. Butterworth-Heinemann.

Quartino, M. L., H. Klöser, I. R. Schloss, and C. Wiencke. 2001. Biomass and associations of benthic marine macroalgae from the inner Potter Cove (King George Island, Antarctica) related to depth and substrate. Polar Biol. **24**: 349–355. doi:10.1007/s003000000218

Radziejewska, T. 2002. Responses of deep-sea meiobenthic communities to sediment disturbance simulating effects of polymetallic nodule mining. Int. Rev. Hydrobiol. **87**: 457–477. doi:10.1002/1522-2632(200207)87:4<457::AID-IROH457>3.0.CO;2-3

Rahmstorf, S. 2002. Ocean circulation and climate during the past 120,000 years. Nature **419**: 207–214. doi:10.1038/nature01090

Rajendran, N., O. Matsuda, Y. Urushigawa, and U. Simidu. 1994. Characterization of microbial community structure in the surface sediment of Osaka Bay, Japan, by phospholipid fatty acid analysis. Appl. Environ. Microbiol. **60**: 248–257.

Rajendran, N., Y. Suwa, and Y. Urushigawa. 1993. Distribution of phospholipid ester-linked fatty acid biomarkers for bacteria in the sediment of Ise Bay, Japan. Mar. Chem. **42**: 39–56. doi:10.1016/0304-4203(93)90248-M

Ramirez-Llodra, E., A. Brandt, R. Danovaro, and others. 2010. Deep, diverse and definitely different: unique attributes of the world's largest ecosystem. Biogeosciences **7**: 2851–2899. doi:10.5194/bg-7-2851-2010

Ramirez-Llodra, E., P. A. Tyler, M. C. Baker, and others. 2011. Man and the last great wilderness: human impact on the deep sea. PLoS One **6**. doi:10.1371/journal.pone.0022588

Renaud, P. E., M. Włodarska-Kowalczuk, H. Trannum, B. Holte, J. M. Węsławski, S. Cochrane, S. Dahle, and B. Gulliksen. 2007. Multidecadal stability of benthic community structure in a high-Arctic glacial fjord (van Mijenfjord, Spitsbergen). Polar

Biol. **30**: 295–305. doi:10.1007/s00300-006-0183-9

Rex, M. A., R. J. Etter, J. S. Morris, and others. 2006. Global bathymetric patterns of standing stock and body size in the deep-sea benthos. Mar. Ecol. Prog. Ser. **317**: 1–8. doi:10.3354/meps317001

Rex, M. a, and R. J. Etter. 2010. Deep-sea biodiversity: pattern and scale. Zoology **61**: 354. doi: 10.1525/bio.2011.61.4.17

Rowe, G. T., and J. W. Deming. 1985. The role of bacteria in the turnover of organic carbon in deep-sea sediments. Ocean. Mar. Biol. Annu. Rev **43**: 925–950.

Ruhl, H. A. 2004. Shifts in Deep-Sea Community Structure Linked to Climate and Food Supply. Science **305**: 513–515. doi:10.1126/science.1099759

Ruhl, H. A., B. J. Bett, S. J. M. M. Hughes, and others. 2014. Links between deep-sea respiration and community dynamics. Ecology **95**: 1651–1662. doi:10.1890/13-0675.1

Schmittner, A., E. D. Galbraith, S. W. Hostetler, T. F. Pedersen, and R. Zhang. 2007. Large fluctuations of dissolved oxygen in the Indian and Pacific oceans during Dansgaard-Oeschger oscillations caused by variations of North Atlantic Deep Water subduction. Paleoceanography **22**. doi:10.1029/2006PA001384

Shahbaz, M., T. Kätterer, B. Thornton, and G. Börjesson. 2020. Dynamics of fungal and bacterial groups and their carbon sources during the growing season of maize in a long-term experiment. Biol. Fertil. Soils **56**: 759–770. doi:10.1007/s00374-020-01454-z

Shulse, C. N., B. Maillot, C. R. Smith, and M. J. Church. 2017. Polymetallic nodules, sediments, and deep waters in the equatorial North Pacific exhibit highly diverse and distinct bacterial, archaeal, and microeukaryotic communities. Microbiologyopen **6**: 1–16. doi:10.1002/mbo3.428

Siegel, D. A., E. Fields, and K. O. Buesseler. 2008. A bottom-up view of the biological pump: Modeling source funnels above ocean sediment traps. Deep Sea Res. Part I **55**:

108–127. doi:https://doi.org/10.1016/j.dsr.2007.10.006

Sigman, D. M., and E. A. Boyle. 2000. Glacial/Interglacial variations in atmospheric carbon dioxide. Nature **407**: 859–869. doi:10.1038/35038000

Simon-Lledó, E., B. J. Bett, V. A. I. Huvenne, K. Köser, T. Schoening, J. Greinert, and D. O. B. Jones. 2019. Biological effects 26 years after simulated deep-sea mining. Sci. Rep. **9**: 1–13. doi:10.1038/s41598-019-44492-w

Sinniger, F., J. Pawlowski, S. Harii, and others. 2016. Worldwide analysis of sedimentary DNA reveals major gaps in taxonomic knowledge of deep-sea benthos. Front. Mar. Sci. **3**: 1–14. doi:10.3389/fmars.2016.00092

De Smet, B., E. Pape, T. Riehl, P. Bonifácio, L. Colson, and A. Vanreusel. 2017. The community structure of deep-sea macrofauna associated with polymetallic nodules in the eastern part of the Clarion-Clipperton Fracture Zone. Front. Mar. Sci. **4**: 1–14. doi:10.3389/fmars.2017.00103

Smith, C. R., W. Berelson, D. J. Demaster, F. C. Dobbs, D. Hammond, D. J. Hoover, R. H. Pope, and M. Stephens. 1997. Latitudinal variations in benthic processes in the abyssal equatorial Pacific: Control by biogenic particle flux. Deep. Res. Part II **44**: 2295–2317. doi:10.1016/S0967-0645(97)00022-2

Smith, C. R., and A. W. J. Demopoulos. 2003. The deep Pacific Ocean floor. Ecosyst. World, Vol. 28 Ecosyst. Deep Ocean. 179–218.

Smith, C. R., D. J. Hoover, S. E. Doan, R. H. Pope, D. J. Demaster, F. C. Dobbs, and M. A. Altabet. 1996. Phytodetritus at the abyssal seafloor across 10° of latitude in the central equatorial Pacific. Deep Sea Res. Part II **43**: 1309–1338. doi:10.1016/0967-0645(96)00015-X

Smith, C. R., F. C. De Leo, A. F. Bernardino, A. K. Sweetman, and P. M. Arbizu. 2008a. Abyssal food limitation, ecosystem structure and climate change. Trends Ecol. Evol. **23**:

518–528. doi:10.1016/j.tree.2008.05.002

Smith, C. R., D. J. De Master, C. Thomas, P. Sršen, L. Grange, V. Evrard, and F. DeLeo. 2012. Pelagic-benthic coupling, food banks, and climate change on the west Antarctic Peninsula shelf. Oceanography **25**: 189–201. doi:10.5670/oceanog.2012.94

Smith, C. R., S. Mincks, and D. J. DeMaster. 2008b. The FOODBANCS project: Introduction and sinking fluxes of organic carbon, chlorophyll-a and phytodetritus on the western Antarctic Peninsula continental shelf. Deep. Res. Part II **55**: 2404–2414. doi:10.1016/j.dsr2.2008.06.001

Smith, C. R., and C. Rabouille. 2002. What controls the mixed-layer depth in deep-sea sediments? The importance of POC flux. Limnol. Oceanogr. **47**: 418–426. doi:10.4319/lo.2002.47.2.0418

Smith, C. R., V. Tunnicliffe, A. Colaço, and others. 2020. Deep-sea misconceptions cause underestimation of seabed-mining impacts. Trends Ecol. Evol. **35**: 853–857. doi:10.1016/j.tree.2020.07.002

Smith Jr., K. L., R. S. Kaufmann, and R. J. Baldwin. 1994. Coupling of near-bottom pelagic and benthic processes at abyssal depths in the eastern North Pacific Ocean. Limnol. Oceanogr. **39**: 1101–1118. doi:https://doi.org/10.4319/lo.1994.39.5.1101

Smith, K. L., R. S. Kaufmann, R. J. Baldwin, and A. F. Carlucci. 2001. Pelagic-benthic coupling in the abyssal eastern North Pacific: an 8-year time-series study of food supply and demand. Limnol. Oceanogr. **46**: 543–556. doi:10.4319/lo.2001.46.3.0543

Smith, K. L., H. A. Ruhl, C. L. Huffard, M. Messié, and M. Kahru. 2018. Episodic organic carbon fluxes from surface ocean to abyssal depths during long-term monitoring in NE Pacific. Proc. Natl. Acad. Sci. U. S. A. **115**: 12235–12240. doi:10.1073/pnas.1814559115

Snelgrove, P., and C. R. Smith. 2002. A riot of species in an environmental calm: the paradox

of the species-rich deep-sea floor. Oceanogr. Mar. Biol. An Annu. Rev. 311–342. doi:10.1201/9780203180594.ch6

Snelgrove, P. V. R., K. Soetaert, M. Solan, and others. 2018. Global carbon cycling on a heterogeneous seafloor. Trends Ecol. Evol. **33**: 96–105. doi:10.1016/j.tree.2017.11.004

Solan, M., B. J. Cardinale, A. L. Downing, K. A. M. Engelhardt, J. L. Ruesink, and D. S. Srivastava. 2004. Extinction and ecosystem function in the marine benthos. Science **306**: 1177–1180. doi:10.1126/science.1103960

Sparenberg, O. 2019. A historical perspective on deep-sea mining for manganese nodules, 1965–2019. Extr. Ind. Soc. **6**: 842–854. doi:10.1016/j.exis.2019.04.001

Stramma, L., G. C. Johnson, J. Sprintall, and V. Mohrholz. 2008. Expanding oxygen-minimum zones in the tropical oceans. Science **320**: 655–658. doi:10.1126/science.1153847

Stramma, L., S. Schmidtko, L. A. Levin, and G. C. Johnson. 2010. Ocean oxygen minima expansions and their biological impacts. Deep. Res. Part I **57**: 587–595. doi:10.1016/j.dsr.2010.01.005

Stratmann, T., L. Lins, A. Purser, and others. 2018a. Abyssal plain faunal carbon flows remain depressed 26 years after a simulated deep-sea mining disturbance. Biogeosciences **15**: 4131–4145. doi:10.5194/bg-15-4131-2018

Stratmann, T., L. Mevenkamp, A. K. Sweetman, A. Vanreusel, and D. van Oevelen. 2018b. Has phytodetritus processing by an abyssal soft-sediment community recovered 26 years after an experimental disturbance? Front. Mar. Sci. **4**: 1–13. doi:10.3389/fmars.2018.00059

Stratmann, T., K. Soetaert, C. L. Wei, Y. S. Lin, and D. van Oevelen. 2019. The SCOC database, a large, open, and global database with sediment community oxygen consumption rates. Sci. Data **6**: 10–15. doi:10.1038/s41597-019-0259-3

Stratmann, T., I. Voorsmit, A. Gebruk, and others. 2018c. Recovery of Holothuroidea

    population density, community composition, and respiration activity after a deep-sea

    disturbance experiment. Limnol. Oceanogr. **63**: 2140–2153. doi:10.1002/lno.10929

Suhr, S. B., D. W. Pond, A. J. Gooday, and C. R. Smith. 2002. Selective feeding by benthic

    foraminifera on labile phytodetritus on the western Antarctic Peninsula shelf (500 m

    water depth): evidence from fatty acid biomarker analysis. Mar. Ecol. Prog. Ser. **262**:

    153–162. doi:10.3354/meps262153

Sweetman, A. K., A. Chelsky, K. A. Pitt, H. Andrade, D. van Oevelen, and P. E. Renaud.

    2016. Jellyfish decomposition at the seafloor rapidly alters biogeochemical cycling and

    carbon flow through benthic food-webs. Limnol. Oceanogr. **61**: 1449–1461.

    doi:10.1002/lno.10310

Sweetman, A. K., J. J. Middelburg, A. M. Berle, A. F. Bernardino, C. Schander, A. W. J.

    Demopoulos, and C. R. Smith. 2010. Impacts of exotic mangrove forests and mangrove

    deforestation on carbon remineralization and ecosystem functioning in marine

    sediments. Biogeosciences **7**: 2129–2145. doi:10.5194/bg-7-2129-2010

Sweetman, A. K., K. Norling, C. Gunderstad, B. T. Haugland, and T. Dale. 2014. Benthic

    ecosystem functioning beneath fish farms in different hydrodynamic environments.

    Limnol. Oceanogr. **59**: 1139–1151. doi:10.4319/lo.2014.59.4.1139

Sweetman, A. K., C. R. Smith, C. N. Shulse, and others. 2019. Key role of bacteria in the

    short-term cycling of carbon at the abyssal seafloor in a low particulate organic carbon

    flux region of the eastern Pacific Ocean. Limnol. Oceanogr. **64**: 694–713.

    doi:10.1002/lno.11069

Sweetman, A. K., S. Sommer, O. Pfannkuche, and U. Witte. 2009. Retarded response by

    macrofauna-size foraminifera to ohytodetritus in a deep Norwegian fjord. J. Foraminifer.

    Res. **39**: 15–22. doi:10.2113/gsjfr.39.1.15

Sweetman, A. K., A. R. Thurber, C. R. Smith, and others. 2017. Major impacts of climate change on deep-sea benthic ecosystems. Elem Sci Anth. **5**: 4. doi:10.1525/elementa.203

Sweetman, A. K., and U. Witte. 2008. Response of an abyssal macrofaunal community to a phytodetrital pulse. Mar. Ecol. Prog. Ser. **355**: 73-84. doi: 10.3354/meps07240

Syvitski, J., D. C. Burrel, and J. M. Skei. 1987. Fjords: processes and products, Springer-Verlag.

Thiel, H. 2001. Evaluation of the environmental consequences of polymetallic nodule mining based on the results of the TUSCH Research Association. Deep. Res. Part II **48**: 3433–3452. doi:10.1016/S0967-0645(01)00051-0

Thornton, B., Z. Zhang, R. W. Mayes, M. N. Högberg, and A. J. Midwood. 2011. Can gas chromatography combustion isotope ratio mass spectrometry be used to quantify organic compound abundance? Rapid Commun. Mass Spectrom. **25**: 2433–2438. doi:10.1002/rcm.5148

Thurber, A. R., A. K. Sweetman, B. E. Narayanaswamy, D. O. B. Jones, J. Ingels, and R. L. Hansman. 2014. Ecosystem function and services provided by the deep sea. Biogeosciences **11**: 3941–3963. doi:10.5194/bg-11-3941-2014

Vanreusel, A., A. Hilario, P. a. Ribeiro, L. Menot, and P. M. Arbizu. 2016. Threatened by mining, polymetallic nodules are required to preserve abyssal epifauna. Sci. Rep. **6**: 26808. doi:10.1038/srep26808

Vaughan, D. G., G. J. Marshall, W. M. Connolley, J. C. King, and R. Mulvaney. 2001. Devil in the detail. Science **293**: 1777–1779. doi:10.1126/science.1065116

Volz, J. B., J. M. Mogollón, W. Geibert, P. M. Arbizu, A. Koschinsky, and S. Kasten. 2018. Natural spatial variability of depositional conditions, biogeochemical processes and element fluxes in sediments of the eastern Clarion-Clipperton Zone, Pacific Ocean. Deep. Res. Part I **140**: 159–172. doi:10.1016/j.dsr.2018.08.006

Vonnahme, T. R., M. Molari, F. Janssen, F. Wenzhöfer, M. Haeckel, J. Titschack, and A. Boetius. 2020. Effects of a deep-sea mining experiment on seafloor microbial communities and functions after 26 years. Sci. Adv. **6**: eaaz5922. doi:10.1126/sciadv.aaz5922

Washburn, T. W., D. O. B. Jones, C.-L. Wei, and C. R. Smith. 2021a. Environmental heterogeneity throughout the Clarion-Clipperton Zone and the potential representativity of the APEI network. Front. Mar. Sci. **8**: 1–17. doi:10.3389/fmars.2021.661685

Washburn, T. W., L. Menot, P. Bonifácio, and others. 2021b. Patterns of macrofaunal biodiversity across the Clarion-Clipperton Zone: an area targeted for seabed mining. Front. Mar. Sci. **8**: 1–22. doi:10.3389/fmars.2021.626571

Wear, E. K., M. J. Church, B. N. Orcutt, C. N. Shulse, M. V. Lindh, and C. R. Smith. 2021. Bacterial and Archaeal communities in polymetallic nodules, sediments, and bottom waters of the abyssal Clarion-Clipperton Zone: emerging patterns and future monitoring considerations. Front. Mar. Sci. **8**: 1–16. doi:10.3389/fmars.2021.634803

Wedding, L. M., A. M. Friedlander, J. N. Kittinger, L. Watling, S. D. Gaines, M. Bennett, S. M. Hardy, and C. R. Smith. 2013. From principles to practice: a spatial approach to systematic conservation planning in the deep sea. Proc. R. Soc. B Biol. Sci. **280**: 20131684. doi:10.1098/rspb.2013.1684

Wedding, L. M., S. M. Reiter, C. R. Smith, and others. 2015. Managing mining of the deep seabed. Science **349**: 144–145. doi:10.1126/science.aac6647

Wei, C.-L., G. T. Rowe, E. Escobar-Briones, and others. 2010. Global patterns and predictions of seafloor biomass using random forests. PLoS One **5**: e15323. doi:10.1371/journal.pone.0015323

Weikard, H.-P. 2002. Diversity functions and the value of biodiversity. Land Econ. **78**: 20–27. doi:10.2307/3146920

Wenzhoefer, F., M. Adler, O. Kohls, C. Hensen, B. Strotmann, S. Boehme, H. D. Schulz, and Anonymous. 2001. Calcite dissolution driven by benthic mineralization in the deep-sea; in situ measurements of Ca^{2+}, pH, pCO_2 and O_2. Geochim. Cosmochim. Acta **65**: 2677–2690.

Wesławski, J. M., M. A. Kendall, M. Włodarska-Kowalczuk, K. Iken, M. Kedra, J. Legezynska, and M. K. Sejr. 2011. Climate change effects on Arctic fjord and coastal macrobenthic diversity-observations and predictions. Mar. Biodivers. **41**: 71–85. doi:10.1007/s12526-010-0073-9

Wieking, G., and I. Kröncke. 2003. Macrofauna cummunities of the Dogger Bank (central North Sea) in the late 1990s: Spatial distribution, species composition and trophic structure. Helgol. Mar. Res. **57**: 34–46. doi:10.1007/s10152-002-0130-2

Wiklund, H., L. Neal, A. G. Glover, R. Drennan, M. Rabone, and T. G. Dahlgren. 2019. Abyssal fauna of polymetallic nodule exploration areas, eastern Clarion-Clipperton Zone, central Pacific Ocean: Annelida: Capitellidae, Opheliidae, Scalibregmatidae, and Travisiidae. Zookeys **2019**: 1–82. doi:10.3897/zookeys.883.36193

Wilkins, D., S. Yau, T. J. Williams, M. A. Allen, M. V. Brown, M. Z. Demaere, F. M. Lauro, and R. Cavicchioli. 2013. Key microbial drivers in Antarctic aquatic environments. FEMS Microbiol. Rev. **37**: 303–335. doi:10.1111/1574-6976.12007

Willers, C., P. J. Jansen van Rensburg, and S. Claassens. 2015. Phospholipid fatty acid profiling of microbial communities-a review of interpretations and recent applications. J. Appl. Microbiol. **119**: 1207–1218. doi:10.1111/jam.12902

Wilson, G. D. F. 2017. Macrofauna abundance, species diversity and turnover at three sites in the Clipperton-Clarion Fracture Zone. Mar. Biodivers. **47**: 323–347. doi:10.1007/s12526-016-0609-8

Witte, U., N. Aberle, M. Sand, and F. Wenzhöfer. 2003a. Rapid response of a deep-sea

benthic community to POM enrichment: an in situ experimental study. Mar. Ecol. Prog. Ser. **251**: 27–36. doi:10.3354/meps251027

Witte, U., F. Wenzhöfer, S. Sommer, and others. 2003b. In situ experimental evidence of the fate of a phytodetritus pulse at the abyssal sea floor. Nature **424**: 763–766. doi:10.1038/nature01799

Wlodarska-Kowalczuk, M., T. H. Pearson, and M. A. Kendall. 2005. Benthic response to chronic natural physical disturbance by glacial sedimentation in an Arctic fjord. Mar. Ecol. Prog. Ser. **303**: 31–41. doi:10.3354/meps303031

Woulds, C., J. H. Andersson, G. L. Cowie, J. J. Middelburg, and L. A. Levin. 2009. The short-term fate of organic carbon in marine sediments: comparing the Pakistan margin to other regions. Deep. Res. Part II **56**: 393–402. doi:10.1016/j.dsr2.2008.10.008

Ziegler, A. F., M. Cape, Lundesgaard, and C. R. Smith. 2020. Intense deposition and rapid processing of seafloor phytodetritus in a glaciomarine fjord, Andvord Bay (Antarctica). Prog. Oceanogr. **187**: 102413. doi:10.1016/j.pocean.2020.102413

Ziegler, A. F., C. R. Smith, K. F. Edwards, and M. Vernet. 2017. Glacial dropstones: Islands enhancing seafloor species richness of benthic megafauna in West Antarctic Peninsula fjords. Mar. Ecol. Prog. Ser. **583**: 1–14. doi:10.3354/meps12363

Supplementary Information

SI1: Number of macrofauna individuals collected at each site in the CCZ.

		Crustacea						Hydrozoa	Nematoda	Nemertea	Mollusca		Polychaeta
		Amphipoda	Copepoda	Cumacea	Isopoda	Ostracoda	Tanaidacea	Hydrozoa	Nematoda	Nemertea	Bivalvia	Gastropoda	Cirratulidae
APEI 1													
AKS# 261		0	6	0	0	0	0	0	6	0	1	0	0
APEI 4													
AKS# 257		0	6	0	0	0	0	0	11	0	0	0	0
AKS# 259		2	14	0	3	3	2	0	11	0	1	0	0
APEI 7													
AKS# 252		0	13	0	3	2	5	0	26	1	2	1	1
AKS# 254		1	7	1	5	4	7	2	30	0	3	1	1

Glyceridae	Lacydoniidae	Lumbrineridae	Maldanidae	Opheliidae	Paraonidae	Spionidae	Syllidae	Terebellidae	Sipuncula	Total	No nematoda	No meiofauna
1	0	0	1	0	0	0	0	1	0	16	10	4
0	0	1	0	0	0	0	0	0	0	18	7	1
0	0	0	0	0	0	0	1	0	0	37	23	9
1	0	0	1	2	11	0	0	0	0	69	41	28
2	3	0	0	0	1	1	1	0	1	71	33	26